Renewable Hybrid Polygeneration System from Various Unconventional Feedstock

SHAHID HUSSAIN ANSARI

submitted in accordance with the requirements for

the degree of

DOCTOR OF PHILOSOPHY

in the subject

Science, Engineering and Technology

at the

University of South Africa

Supervisor: Prof. Xinying Liu

Co-Supervisor: Prof. Diane Hildebrandt

(Submitted: February 2021)

DECLARATION

Name: SHAHID HUSSAIN ANSARI

Student number: 57669708

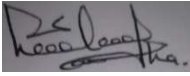Degree: PHD Science, Engineering and Technology----Exact

wording of the title of the thesis appearing on the electronic copy submitted for

examination for the degree of PHD:

"Renewable Hybrid Polygeneration System from Various Unconventional Feedstock"

I declare that the above thesis is my own work and that all the sources that I have used or quoted have been indicated and acknowledged by means of complete references.

I further declare that I submitted the thesis to originality checking software and that it falls within the accepted requirements for originality.

I further declare that I have not previously submitted this work, or part of it, for examination at Unisa for another qualification or at any other higher education institution.

Signature: Date: 25 February 2021

(Submitted: February 2021)

Title of Thesis: Renewable Hybrid Polygeneration System from Various Unconventional Feedstock

Central Summary

The production of low-carbon energy products from biomass gasification is encouraged, in order to expand our sources of energy and to mitigate the harmful impact of the pollutants on the climate and the environment. The benefits of a renewable hybrid polygeneration system that uses various types of unconventional feedstock in the energy mix are extraordinary. However, the location, logistics issues, availability and meteorological conditions of a plant can play a crucial role in order to investigate the full potential of these unconventional resources. In this study, the systematic issues regarding hybridization of CSP (concentrated solar power) with biomass gasification without energy storage to produce energy, liquid fuel and other chemicals is considered as an alternative process. The main goal was to develop a design guideline and recommendations for utilizing the CSP thermal energy as a heat source for the gasification process. This study also explored the role of CSP in the gasification process to balance the heat load requirement. The overall study was carried out by investigating various cases for the biomass gasification process with CSP and without CSP with target analysis via process synthesis and attainable region principles and the development of a simple simulation model using Aspen Plus®. The results were validated by comparing with already-available experimental data for biomass gasification in the literature.

Systematic issues relating to the renewable hybrid polygeneration system were evaluated by conducting various case studies using target analysis and process simulation. From a material balance point of view, producing a specific molar ratio of hydrogen (H_2) and carbon monoxide (CO) can be achieved by varying the steam to biomass ratio and the CSP heat injection. The target analysis of various types of biomass to dimethyl ether shows that co-feeding biomass with methane can improve the performance of the process significantly, in terms of material, energy and work balance. The case study to produce ethanol from biomass then ethanol reforming to produce hydrogen, proves that 100% hydrogen efficiency can be

achieved. However, the process releases a significant amount of energy and work potential, which might not be recovered economically, especially with small scale applications. Co-feeding of water in ethanol reforming to produce more H_2 is applied to recover this extra energy. If a low-cost heat source is available, such as solar heat or waste heat from other processes, then maximum of 187% selectivity of H_2 based on ethanol can be achieved.

The case study on solid waste to hydrogen shows that H_2 production efficiency with CSP is about 12.5 kmol/MW_{th} when using pinewood sawdust as a feedstock and 13.2 kmol/MW_{th} in the case of municipal solid waste. Adding CSP to the system can boost H_2 production to 50% - 146 g/kg when using wet pinewood sawdust (PW) as a feedstock, and 61% - 224 g/kg when using MSW. A case study of the biomass gasification using various gasifying agents to produce methane (CH_4) rich syngas to be used in a normal gas turbine. The set target for this case study was 40% CH_4 mole concentration. This case study proves that this target can be achieved by utilizing the heat generated from methanation to the gasifier. Applying CSP to the gasification process will also help to boost the CH_4 produced after methanation by about 20%. The case study on solar energy to H_2 concluded that with CSP, for steam gasification case, it is 117 g/kg of wet biomass and for CO_2-gasification, it is 119 g/kg of wet biomass. For both cases, H_2 production efficiency is 14-15 kmol per MW_{th}. This case study provides a parametric analysis to transform biomass, solar and CO_2 into valuable and carbon-neutral alternative fuels.

The case study on the biomass integrated gasification combined cycle (IGCC) shows a higher net electricity output per unit of crop residue feed with solar-assisted IGCC and that it achieves a net thermal efficiency of about 53%. The investigation of a hybrid process proves that 0.55 MW of electricity can be produced per unit of solar-thermal energy input to the gasifier; having solar to electricity efficiency of approximately 55%. The case study on the hybrid CSP CO_2-IGCC process shows that the peak net efficiency is 46%, which is slightly higher than seen with the steam-IGCC process (45%). A solar thermal to power efficiency rate of 55% is achieved in CSP CO_2-IGCC process, which is less than seen with CSP steam-IGCC process (58%). Case study for sCO_2 Brayton cycle of a CSP-assisted biomass gasification process shows that the net thermal efficiency of about 60% is attainable, which is better than

any existing biomass based IGCC process. Further, it is shown that the performance of the system is superior to that of indirectly heated sCO_2 without solar aid. The injected solar power boosts the power output as high as 52% and its conversion efficiency is about the same value. The peak net efficiency of the hybrid process is 45% and a solar to power efficiency is 58%. In terms of the liquid fuel production option, 17-18 kg of liquid fuel can be produced per GJ of solar energy injected into the process.

In conclusion, the outcomes from case studies by target analysis and simulation model are promising. The case studies show that the renewable hybrid polygeneration system is an attractive option to convert renewables resources (biomass and solar) into clean power, liquid fuel, green H_2 fuel, chemicals, etc. We concluded that the incorporation of CSP-thermal energy into the biomass gasification process with the concept of polygeneration process will provide us opportunities to explore the maximum potential of unconventional feedstock.

Isihloko seThesisisi: Uhlelo Olungavuselelwa lweHybrid Polygeneration kusuka Kokuphakelayo Okuhlukahlukene Okungajwayelekile

Isifinyezo Esimaphakathi

Kukhuthazwa ukukhiqizwa kwemikhiqizo yamandla kagesi aphansi avela biomass gasification, ukuze sandise imithombo yethu yamandla futhi sinciphise umthelela olimazayo wokungcolisa isimo sezulu kanye nemvelo. Izinzuzo zohlelo hybrid polygeneration oluvuselelekayo olusebenzisa izinhlobo ezahlukahlukene zokuphakelayo okungahambelani nokuxubana kwamandla zixakile. Kodwa-ke, indawo, izingqinamba zezinto ezisetshenziswayo, ukutholakala nezimo zezulu zesitshalo kungadlala indima ebaluleke kakhulu ukuphenya amandla aphelele alezi zinsizakusebenza ezingavumelani. Kulolu cwaningo, izingqinamba ezihlelekile maqondana nokuhlanganiswa CSP (amandla elanga agxiliwe) biomass gasification ngaphandle kokugcina amandla ukukhiqiza amandla, uphethiloli wamanzi namanye amakhemikhali kubhekwa njengenye inqubo. Inhloso enkulu bekuwukwakha umhlahlandlela wokuklanywa nezincomo zokusebenzisa amandla CSP afudumele njengomthombo wokushisa wenqubo yokwenza igesi. Lolu cwaningo luphinde lwahlola iqhaza CSP enqubeni gasification ukulinganisela imfuneko yokushisa. Ucwaningo lonke lwenziwa ngokuphenya amacala ahlukahlukene enqubo biomass gasification CSP futhi ngaphandle CSP ngokuhlaziywa okuqondiwe ngenqubo yokuhlanganiswa kanye nemithetho yesifunda efinyelelekayo kanye nokwakhiwa kwemodeli elula yokulingisa kusetshenziswa Aspen Plus®. Imiphumela iqinisekiswe ngokuqhathanisa nedatha yokuhlola esivele ikhona biomass gasification ezincwadini.

Izingqinamba ezihlelekile eziphathelene nohlelo lwe-hybrid polygeneration oluvuselelekayo zahlolwa ngokwenza izifundo ezahlukahlukene zamacala kusetshenziswa ukuhlaziywa kokuqondiwe nenqubo yokulingisa. Ngokombono webhalansi yezinto ezibonakalayo, ukukhiqiza isilinganiso esithile molar hydrogen (H_2) carbon monoxide (CO) kungatholakala ngokushintsha umusi ube biomass ratio kanye nomjovo wokushisa CSP. Ukuhlaziywa okuhlosiwe kwezinhlobo ezahlukahlukene biomass kuya dimethyl ether

kukhombisa ukuthi ukondla biomass methane kungathuthukisa ukusebenza kwenqubo kakhulu, ngokuya ngempahla, amandla kanye nomsebenzi olinganiselayo. Ucwaningo olwenziwe ukukhiqiza ethanol kusuka biomass bese kuguqulwa ethanol ukukhiqiza hydrogen, kufakazela ukuthi ukusebenza kahle hydrogen ngo-100% kungatholakala. Kodwa-ke, le nqubo ikhipha inani elikhulu lamandla nomsebenzi, okungenzeka kungatholakali ngokomnotho, ikakhulukazi ngezicelo ezincane. Ukondliwa kwamanzi ngokubambisana ekuguqulweni ethanol ukukhiqiza H_2 eyengeziwe kuyasetshenziswa ukuthola amandla lawa angeziwe. Uma kutholakala umthombo wokushisa ontengo ephansi, njengokushisa kwelanga noma ukushisa kwemfucumfucu kusuka kwezinye izinqubo, khona-ke ukukhethwa okungu-187% H_2 okususelwa ethanol kungatholakala.

Ucwaningo olwenziwe ngodoti oqinile hydrogen lukhombisa ukuthi ukusebenza kahle kokukhiqizwa H_2 CSP cishe kungu-12.5 kmol / MWth uma usebenzisa pinewood sawdust njenge-feedstock 13.2 kmol / MWth uma kungudoti oqinile kamasipala. Ukungeza CSP ohlelweni kungakhuphula ukukhiqizwa H_2 kuye ku-50% - 146 g / kg uma usebenzisa pinewood sawdust (PW) emanzi njenge-feedstock, 61% - 224 g / kg uma usebenzisa MSW. Ucwaningo lwamacala biomass gasification kusetshenziswa ama-ejenti ahlukahlukene e-gasifying ukukhiqiza syngas acebile methane (CH_4) azosetshenziswa turbine ejwayelekile yegesi. Umgomo obekiwe walolu cwaningo 40% CH_4 yokuhlushwa kwemvukuzane. Lolu cwaningo lwamacala lufakazela ukuthi le nhloso ingafinyelelwa ngokusebenzisa ukushisa okwenziwe kusuka ku-methanation kuye ku-gasifier. Ukufaka CSP kunqubo gasification kuzosiza ukukhulisa CH_4 ekhiqizwa ngemuva kwe-methanation cishe ngama-20%. Ucwaningo olwenziwe ngamandla elanga eya H_2 luphethe ngokuthi CSP, ngecala steam gasification, 117 g / kg ye-biomass emanzi CO_2-gasification, 119 g / kg biomass emanzi. Kuwo womabili amacala, ukusebenza kahle kokukhiqizwa H_2 kungu-14-15 kmol MW_{th} ngayinye. Lolu cwaningo lwamacala luhlinzeka ngokuhlaziywa kwe-parametric ukuguqula biomass, solar CO_2 ibe ngamafutha asemqoka futhi angathathi hlangothi ekhabhoni.

Ucwaningo olwenziwe kumjikelezo ohlangene biomass gasification ohlangene (IGCC) lukhombisa ukukhishwa okuphezulu kukagesi ngamayunithi kokuphakelayo kwezinsalela zezitshalo IGCC esizwa ngelanga nokuthi ifinyelela ukusebenza kahle kwenani lokushisa

okungaba ngama-53%. Ukuphenywa kwenqubo hybrid kufakazela ukuthi 0.55 MW kagesi ungakhiqizwa ngeyunithi ngayinye yokufakwa kwamandla kagesi welanga gasifier; ukuba nelanga kugesi osebenza kahle cishe 55%. Ucwaningo lwamacala ngenqubo ye-hybrid CSP CO_2-IGCC ikhombisa ukuthi ukusebenza kahle kwenetha okungu-46%, okuthe ukuphakama kancane kunokubonwa ngenqubo steam-IGCC (45%). Izinga elishisayo lokushisa ngamandla elisebenza ngamandla 55% liyatholwa kwinqubo CSP CO_2-IGCC, engaphansi kokubonwa ngenqubo CSP steam-IGCC (58%). Ucwaningo olwenziwe ngomjikelezo sCO_2 Brayton wenqubo biomass gasification esizwa CSP ikhombisa ukuthi ukusebenza kahle kwe-thermal okungaba 60% kuyatholakala, okungcono kunanoma iyiphi inqubo ekhona biomass based IGCC. Ngaphezu kwalokho, kukhonjiswa ukuthi ukusebenza kohlelo kuphakeme kunalokho sCO_2 okungaqondile okungaqondile ngaphandle kosizo lwelanga. Amandla elanga ajikiwe akhuphula amandla kagesi afinyelela 52% futhi ukusebenza kwawo ngokuguqulwa kucishe kube nenani elifanayo. Ukusebenza kahle kwenetha kwenqubo hybrid kungama-45% kanti amandla elanga asebenza kahle ngamandla 58%. Ngokuya ngenketho yokukhiqiza uphethiloli ongamanzi, 17-18 kg kaphethiloli ongamanzi ingakhiqizwa GJ ngayinye yamandla elanga afakiwe kule nqubo.

Ekuphetheni, imiphumela evela ocwaningweni lwamacala ngokuhlaziywa kokuhlosiwe nemodeli yokulingisa iyathembisa. Ucwaningo lwamacala lukhombisa ukuthi uhlelo oluvuselelekayo hybrid polygeneration luyindlela ekhangayo yokuguqula izinsizakusebenza ezivuselelekayo (biomass nelanga) zibe ngamandla ahlanzekile, uphethiloli oketshezi, uphethiloli oluhlaza H_2, amakhemikhali, njll. Siphethe ngokuthi ukufakwa kwamandla CSP-thermal Inqubo biomass gasification ngomqondo wenqubo yokuzalwa kabusha izosinikeza amathuba okuhlola amandla amakhulu feedstock engajwayelekile.

Acknowledgements

I would like to express my sincere gratitude to the following people and institutions for assisting me and guiding me to complete the research work done for this study. The accomplishment of this work was done under the guidance of:

➢ My supervisor, Professor Diane Hildebrandt, and co-supervisor, Professor Xinying Liu for their friendship, invaluable support, inspiration, continuous guidance and kind supervision. Both of them are great mentors in my life. Whenever, I was stuck with the research, they always came forward to guide me and discuss in detail to open new opportunities.

➢ Dr Baraka Celestine Sempuga for his co-supervision, assistance, guidance, technical support regarding installation of the software, training sessions to start up thesimulation software, target analysis and process simulation. He always appreciates me every time during these life-changing opportunities to grow and learn more advanced technologies.

➢ Dr Joshua Gorimbo and Mahluli Moyo for their precious time, guidance and support.

➢ Special thanks go to the editor, Mrs Philippa Lange, for being a great friend. She always helped with editing the draft research papers and with the preparation of various Powerpoint presentations to be presented at international conferences.

➢ I would like to acknowledge the academic support received from the Institute for the Development of Energy for African Sustainability (IDEAS), College of Science, Engineering and Technology (CSET) at the University of South Africa.

➢ The financial support received from University of South Africa (UNISA) and National Research Foundation (NRF) (grant numbers 95983 and 113648) is acknowledged with many thanks.

➢ I would also like to thank Genevieve and Alicia for their friendly administrative support at UNISA.

Finally, I would like to express my utmost thanks to my family (my mother, my wife, my sons (Mr Abdul Arham Ansari, Mr Muhammad Hassaan Ansari, Mr Muhammad Safwan Ansari and Mr Muhammad Haddi Ansari), my brothers (Mr Muhammad Zahid and Mr Tahir Shahzad))

for their full support and love during the entire period of PhD study. I would like to extend my thanks to all of them, who supported and helped me in this endeavour.

List of Publications and International and National Conferences Publications

1. Shahid H. Ansari, Ralph Muvhiiwa, Baraka C. Sempuga and Xinying Liu (2021), D**imethyl ether synthesis from biomass gasification: Thermodynamic approach to determine performance limits**, Computer Aided Chemical Engineering (Proceedings of the 31st European Symposium on Computer Aided Process Engineering, 6-9 June 2021, Istanbul, Turkey, Elsevier).

2. Shahid H. Ansari, Baraka C. Sempuga and Xinying Liu (2020), **Ethanol reforming: Setting up performance parget**, Computer Aided Chemical Engineering (Proceedings of the 30th European Symposium on Computer Aided Process Engineering, Elsevier). (https://doi.org/10.1016/B978-0-12-823377-1.50344-X)

3. Ralph Muvhiiwa, Shahid H. Ansari, Baraka Sempuga, Joshua Gorimbo, Xinying Liu, Xiaojun Lu (2021), **Exploring the possibility of using a CH₄ gas turbine for power generation by applying different agents for biomass gasification.** (In preparation.)

4. Shahid H. Ansari, Ashfaq Ahmed, Abdul Razzaq, Diane Hildebrandt, Xinying Liu, Young-Kwon Park, **Incorporation of solar-thermal energy into a gasification process to co-produce bio-fertilizer and power,** International Journal of Environment Pollution (Doi.og/10.1016/j.encpol.2020.115103).

International Conferences

1. Shahid H. Ansari, Baraka C. Sempuga, Diane Hildebrandt and Xinying Liu (2020), **CSP-hybrid staged-gasification of solid waste to produce hydrogen: Aspen Plus simulation**, proceedings of the 12th International Exergy, Energy and Environment Symposium (IEEES-12).

2. Shahid H. Ansari, Jianqi Shen and Xinying Liu (2020), **Using concentrated solar energy in biomass gasification to produce hydrogen**, 26th International Conference on Concentrating Solar Power and Chemical Energy Systems SolarPACES-2020.

3. Shahid H. Ansari and Xinying Liu (2019), **Hybrid CSP biomass CO2-gasification process for power production: Aspen Plus simulation**, 25th International Conference on Concentrating Solar Power and Chemical Energy Systems SolarPACES-2019.

4. Lameck Nkhonjera, Shahid H. Ansari and Xinying Liu (2019), **Development of hybrid CSP biomass gasification process with supercritical carbon dioxide cycle for power generation**, 25th International Conference on Concentrating Solar Power and Chemical Energy Systems SolarPACES-2019.

5. Shahid H. Ansari and Xinying Liu (2018), **Aspen Plus simulation study of concentrated solar power and biomass gasification for co-production of power and liquid fuel**, 24th International Conference on Concentrating Solar Power and Chemical Energy Systems SolarPACES-2018.

6. Shahid H. Ansari, Xinying Liu, Maria Fernandez-Torres (2018), Poster presentation: **Aspen simulation of a hybrid concentrated solar power – biomass integrated gasification combined cycle process,** Africa-EU Renewable Energy Research and Innovation Symposium 2018 (RERIS 2018).

7. Shahid H. Ansari, Diane Hildebrandt and Xinying Liu (2016), **Numerical simulation and mathematical modelling in coordination with experimental investigation of process parameters associated with the Fischer Tropsch fixed bed reactor performance**, Proceedings of AMPE-2016, 239-252.

National Conferences

1. **Catalysis Society of South Africa (CATSA) 2015:** Oral presentation: **Parametric investigation of methane/propane formation via a catalytic dehydrogenation process.**

2. **CATSA 2016:** Poster presentation: **Simulation study of paraffins thermodynamic equilibrium in Fischer Tropsch system.**

3. **CATSA 2017:** Poster presentation: **Parametric investigation of hydrogen and olefins production via a catalytic dehydrogenation process.**

4. **SASEC 2018:** Oral presentation: **Study of an integrated biomass gasification combined cycle process facilitated with concentrated solar power.**

5. **Syngas Convention - Fuels and Chemicals from Synthesis Gas, State of Art 3, 2018:** Poster presentation: **Co-production of bio-char and liquid hydrocarbons assisted by concentrated solar power.**

6. **CATSA 2019:** Poster presentation: **Effects of temperature and feed molar ratio on hydrogen yield in autothermal reforming of ethanol.**

Table of Contents

Chapter 1: Introduction

1.1: Motivation and Rationale for the Study

In the last few decades, there has been a significant increase in the consumption of natural resources - both non-renewables and renewables - to meet the demand for energy [1]–[4]. This increase is attributed to demographic changes, climate change and rapid economic development. Current and future energy demands are dependent on limited, environmentally damaging and potentially unstable non-renewable fossil fuels [5]. In order to address these issues, the production of the energy products (electric power, liquid fuel, hydrogen and other chemicals) from renewable resources like biomass and solar is emerging as the secure energy strategy for the future, as renewable resources never run out. The production of the energy products in this way will ensure low risk investment and secure revenues. It will make a timing balance between energy generation and energy demand based on dispatchability, affordability, security, stability and availability of resources in an environment friendly manner.

Biomass and other renewable resources are contributing commendable share in the global energy mix. Globally, biomass is the fourth in the list of renewable energy resources, contributing about 14% of the global's energy consumption, out of the 18% contribution by renewables to the energy mix [6]. Global warming, energy security, affordability, energy supply and economic impacts are the challenges which motivated the academic researchers to do more. This can be achieved via:

- ➢ cogeneration process (combined heat and power (CHP) system)

- ➢ trigeneration process (combined cooling, heat and power (CCHP) system)

- ➢ polygeneration process (gaseous fuel, liquid fuel, solid fuel, heating, cooling, chemicals and electricity together)

- ➢ renewable hybrid polygeneration system

The renewable hybrid polygeneration system from various types of unconventional feedstock to meet energy demand is an unquestionable solution instead of an individual process. The incorporation of solar/wind/geothermal with the polygeneration process could help to minimize greenhouse gases (GHG). The renewable hybrid polygeneration system will ensure that the overall system reliability, dispatchability, security and stability to produce various chemicals and energy products. This novel concept will reduce the operating and running cost of the gasifier and will enhance energy utilization and operational flexibility of the proposed process. The concept of polygeneration can produce four different products: liquid fuel with heat or electricity; synthetic natural gas with heat or electric power; hydrogen with heat or electricity; other chemicals with heat or power. The renewable hybrid polygeneration system is a combination of different kinds of chemical processes under one platform.

The renewable hybrid polygeneration system is based on thermochemical conversion of solid carbonaceous materials (unconventional feedstock in this study) - such as agricultural residue, biomass, and municipal solid waste (MSW) - into various energy products and hydrocarbons. Generally, thermochemical conversion is classified as pyrolysis and hydrothermal liquefaction (absence of air), gasification (needs partial air) and combustion process (needs excess air) [7]. The energy efficiency of each thermochemical conversion process is dependent on the quality of the unconventional feedstock based on ultimate analysis, proximate analysis and heating value [8].

Biomass gasification is an endothermic chemical conversion process that produces synthetic gas (syngas) - primarily composed of carbon monoxide (CO), hydrogen (H_2), carbon dioxide (CO_2), water (H_2O) and methane (CH_4) - as well as some lighter hydrocarbon compounds in negligible quantity. The produced syngas has an H_2/CO ratio of $1 - 2$, when steam, air, oxygen (O_2) and CO_2 are applied as the gasifying agents [9], [10]. The biomass gasification is operated at a temperature of 600-1200 °C and pressure of 1-30 bar [11]. In the literature, steam has been recognized as a suitable gasifying agent because it favours char gasification, the water gas shift (WGS) reaction and the methane reforming reaction to produce syngas with higher H_2 content and higher heating value [12]. However, for steam gasification, an external heat supply is needed, which can be furnished by: partial biomass combustion in

the gasifier; external combustion of an additional amount of biomass (about 30%); external combustion of a fraction of the syngas produced by gasification. This energy can also be sustainably provided by CSP without any additional external combustion [13]–[15]. The hybridization approach will provide a solution to store energy from low density energy resources into high density energy resources. Solar thermal energy can serve the purpose of an external and unlimited source of energy to improve the operational flexibility of the biomass gasification process and has been recognized as a promising option to convert solar energy in storable form [16].

Solar-assisted gasifiers can be classified as one of two types: contact (indirectly or directly irradiated); the gas-solid contact (fluidized bed, entrained flow or packed bed) [17], [18]. The incorporation of indirect irradiations via concentrated solar power (CSP) to biomass gasification technologies aim to meet required heat load of the gasifier, higher H_2 content, less tar content, higher energy efficiency [19], [20]. Indirect use of CSP to the biomass gasification process also avoids difficulties like scale of operation as compared to direct irradiations solar gasification reactors. The CSP technology allows to deal with the intermittency, dispatchability and continuous operation. But the addition of CSP to the biomass gasification will be commercially viable in the near future.

The main contribution of this study is the use of Aspen Plus® for systematic analysis of the virtual designs for CSP-hybrid biomass gasification using unconventional feedstock with the concept of polygeneration process. The CSP-hybrid biomass gasification process is designed by simulation study and then compared with experimental data to predict performance of the gasifier. This study will take part as a main role in optimizing the operating parameters and operational limits of existing gasification technologies. The systematic analysis helps to understand the important benefits and possibilities of commercialization of CSP to the process of biomass gasification. The modelling and simulation studies related with biomass gasification by using Aspen Plus® is detailed in the literature [21]–[24]. Some simulation studies have assessed the practicability of hybridizing CSP and biomass gasification [25]–[27].

However, the upstream characteristics (like type of biomass and its availability, transportation logistics, the use of CSP as an external source to the gasification system) and

downstream characteristics (like combined cycle, steam reforming of syngas, water gas shift reaction, sub-sequent adjustment of syngas for power generation, liquid fuel, hydrogen, methanol, ethanol, and other chemicals production) has not been achieved extensively with respect to process target analysis and systematic analysis about gasification process. The energy efficiency, conversion of solar to fuel and polygeneration approach to have a promising, environmentally friendly and hybrid process that utilize the maximum energy content available, this remains a main research goal of this study.

This study focused on the simulation of hybrid CSP-biomass gasification with direct use of solar thermal-energy via inert heat transfer material into the gasification system. The study also considered the intermittency of solar with syngas combustion without any syngas storage system or without any solar thermal energy storage. It will enhance the flexibility to run the overall process on continuous basis. The study also evaluated the steam reforming of syngas and WGS reaction of syngas to ease the solar share to the gasifier and to increase the H_2 contents in syngas for further application to produce various chemicals, e.g. FT liquid fuel, H_2 fuel, methanol, ethanol and dimethyl ether. Although, the renewable hybrid polygeneration systems have remarkable advantages but there are some technical challenges to operate the overall system with power reliability and stability.

The findings to study this renewable hybrid polygeneration system will lead to conclusion that solar energy can play a vital role in thermochemical biomass gasification process to explore full potential of unconventional feedstock. Renewable hybrid polygeneration system represent a promising energy efficient solution to meet energy demands with uninterrupted power supply. The hybridization will allow to save the solar thermal-energy as liquid fuel with higher energy capacity, hydrogen or other chemicals. It will promote system stability, reliability and energy security on sustainable basis.

1.2:   Novelty of Renewable Hybrid Polygeneration System

The benefits of a hybrid biomass gasification with polygeneration process are very promising because the process is dependent on the abundantly available biomass, agricultural residue, MSW and solar energy. In a hybrid process, two or more different types of resources

like biomass and CSP thermal energy are combined in order to better explore their individual advantages. In this study, hybridization of CSP with biomass gasification without energy storage system to produce energy, liquid fuel and other chemicals is considered as an alternative process. However, the availability of abovementioned resources is characterized by site-specific and meteorological conditions that can create a problem of supply of these resources on continuous basis. Thus, there is a need to choose a smart hybrid process that can properly utilize these resources.

The novelty of present research work is to study the systematic issues related to the gasification process. This study will provide an optimization approach to address systematic issues in order to deliver a strong theoretical basis for advanced research and development resulted with the process design tools to evaluate the technology dissemination and commercial deployment. This study is intended to develop a scientific link between feedstock availability and demand for final energy products or chemicals. The main focus is to develop a design guidelines and future recommendations to utilize the CSP thermal energy as a heat source for the gasification process to enhance the role of CSP on the system performance.

The systematic issues related to the feasible regions are evaluated by conducting target analysis of the biomass gasification system via process synthesis techniques and attainable region principles. The systematic issues related to actual plant are investigated by process simulation in a process simulator known as Aspen Plus®. By process simulation, the real gasification process with possible polygeneration system can be optimized for various operating conditions. The process simulator will predict that how far the developed model process is placed in order to consider the actual process.

Firstly, process synthesis techniques and attainable region principles were used to determine the target of syngas production from various types of unconventional feedstock then syngas to other energy products. This analysis will lead to a feasible region from which a design target for the process can be set. It is based on three basic tools namely the mass, energy and work (entropy) to identify the major components of the process and ignores the components in smaller quantities and the impurities. This is done to simplify the analysis while extracting the essential information that does not require the details, which will be included at a later stage of

process design. It starts by first identifying the major components of the process and ignores the components in smaller quantities and the impurities. This is done to simplify the analysis while extracting the essential information that does not require the details, which will be included at a later stage of process design. From major components, we can derive the independent material balances with achievable outcomes of the overall process.

The target represents the theoretical performance limits for the gasification process, and the predefined operating conditions are determined to get as close to the set targets as possible. From a material balance point of view, to produce specified mole of hydrogen (H_2) and carbon monoxide (CO) can be achieved under optimum operating conditions. From energy and work (H and G) point of view, in order to achieve these target ratios, the enthalpy change (ΔH) and Gibbs free energy change (ΔG) both will be zero for all the cases. For a fully energy integrated process, at $\Delta G = 0$ the process does not require heat for it to proceed. Therefore, at this point any source of heat at a temperature high enough to enable heat flow at any point in the process will be sufficient to drive the process. We consider this to be the ultimate target for biomass gasification to produce syngas. If ΔH of the process is positive then it will tell us that there is an opportunity to conserve additional external energy in the form of power, liquid fuel, H_2, methanol, ethanol and other chemicals.

Secondly the systematic issues related to process design, Aspen Plus® was used to evaluate mass, energy and workflows for the syngas production from various types of unconventional feedstock. This software is based on proximate and ultimate analysis of the feedstock, type of gasifying agent and operating conditions to predict the syngas composition, syngas yield, energy efficiency and selectivity of syngas. The evaluation of using CSP for biomass gasification and polygeneration is the core theme to save the consumption of unconventional feedstock with less GHG emissions.

Although Aspen Plus® software has been used in the literature to develop simulation models for biomass gasification alone. But in this study, the analysis was carried out by developing a simple simulation model with CSP and without CSP using Aspen Plus®. The simulation results were validated with the output results of process synthesis techniques and

attainable region principles. After validation, the simulation results were also compared with the experimental data in the literature.

The modelling methodology consisted of splitting the CSP-assisted biomass gasification process with polygeneration system into various distinct sections. The detailed modelling of each section was carried in order to determine the specified outcomes for each inter linked operating parameters of various unit processes and unit operations. The simulation results for biomass gasification without CSP has been compared with experimental data. Because no real-life CSP-assisted biomass gasifier is commercially working yet.

The most successful CSP biomass gasification prototype method using sand as a heat transfer medium with better stability and dispatchability of the process. This hybridization approach will eliminate the need to store solar thermal-energy. However, more extensive research work should be done on CSP, biomass gasification and the polygeneration system to explore the full potential of renewables.

1.3:   Aim and Objectives

The present work proposes and simulate renewable hybrid polygeneration system and the easiness to store solar thermal-energy in the form of liquid fuel, H_2 and other hydrocarbon compounds or chemicals. This research intends to provide valuable information about renewable hybrid polygeneration pathways and benefits of incorporation of solar thermal energy. The primary goal is to address systematic issues related to virtual process design, optimization and technology dissemination of renewable hybrid polygeneration system. This study is intended to evaluate operating parameters, the using of CSP thermal energy for biomass gasification to achieve higher energy efficiency and best performance of the gasifier.

In this work, target analysis of the biomass gasification system has been achieved based on the process synthesis techniques and attainable region principles. The ultimate process design targets can be achieved by using three basic tools of material, energy and work balance. These tools have been used to determine feasible regions for syngas production with specified molar ratio of H_2 and CO from various types of unconventional feedstock. The performance of

the gasification system has been investigated through: the net-energy requirement of the system, which is represented by change in enthalpy of the process (ΔH): and the net-work requirement of the process, which is represented by change in Gibbs free energy of the process (ΔG). The feasibility of ultimate process targets was realized and tested by process simulation in Aspen Plus® to conclude that how far from the actual process.

The main research goal is to generate a simulation model to examine the utilization of various types of unconventional feedstock, hybridization of CSP, combined cycle, steam reforming of syngas, water gas shift reaction of syngas, sub-sequent adjustment of syngas to produce power, liquid fuel, hydrogen, methanol, ethanol and other chemicals.

The benchmark objectives of present study were:

➢ To study renewable hybrid polygeneration system that will provide a comprehensive overview in order to address the systematic issues, e.g. dispatchability, intermittency, stability, reliability and technology dissemination.

➢ In order to achieve realistic virtual designs for renewable hybridization system, the process synthesis techniques and attainable region principles have been applied to determine the feasible regions with ultimate process design targets from a material, energy and work balance point of view.

➢ To develop a simple model in Aspen Plus® version 10 and to investigate the case studies for renewable hybrid polygeneration system from various types of unconventional feedstock. The simulation data was prepared according to input conditions established for biomass gasification. The simulation results from the developed model were validated with experimental data and improved to deploy for commercial applications.

➢ To evaluate the benefits of utilizing CSP thermal-energy as an external high temperature heat to the biomass gasification. It will address design guidelines

for maximum share of CSP to biomass gasification to attain optimum system performance.

➢ To control the timing imbalance smartly between peak demand and renewable energy production, which will increase the share of renewables to the grid and to study the effects of applying CSP thermal-energy on the efficiency of the gasification system and yield of syngas.

➢ To evaluate the effect of subsequent adjustment of the syngas produced for further downstream applications (producing power, liquid fuel and other chemicals).

1.4:   Research Methodology

The Aspen Plus® is a powerful simulation tool mostly used in process design to evaluate mass, energy and workflow. This software is used to find out syngas composition, syngas yield, energy efficiency and selectivity of syngas with various gasification agents (steam, air, oxygen and CO_2). A simple simulation model was developed to study the hybrid CSP biomass gasification with the concept of polygeneration to achieve the benchmark objectives described in this work through case studies.

The share of CSP thermal energy was simulated as a process heat equivalent to the gasifier unit. The evaluation of using CSP for biomass gasification and polygeneration is the core theme to save the consumption of biomass. When there was no CSP, combustion of a fraction of produced syngas was introduced to balance the required heat duty of the gasifier. Hence, it was mandatory to enforce certain limits related to the renewable hybrid polygeneration system.

Regarding biomass gasification technologies, the choice was dual fluidized bed gasifier. This is a viable solution with multiple fluidizing reactors in series with heat transfer medium from CSP facility. Solid inert heat transfer material has been considered to transfer solar thermal

energy between CSP and biomass gasification. Practically, there is need to apply advanced technology to store solar thermal-energy. Regarding solar thermal energy technologies, CSP was selected to inject. But the deployment of CSP technology requires huge land, considerable financial investment, well-trained manpower and risk of hybridization of CSP with biomass gasification.

The incorporation of solar thermal energy through CSP technology to the biomass gasification process has been assessed via case studies by using Aspen Plus® process simulator. Figure 1.4(i) described about predefined work plan for this research study.

1.5:   Outline of this Thesis

The thesis consists of nine chapters. Eight chapters are ready for publication or have already been published. There is a certain amount of repetition in the Aspen Plus® simulation assumptions have been applied in the development of a model, given that the entire simulation system is almost the same.

Chapter 1 This chapter includes a summary of the renewable hybrid polygeneration system, the current status of CSP technologies and the current status of biomass gasification technologies. The chapter includes a comprehensive review of CSP and biomass gasification technologies, as well as the state-of-the-art renewable hybrid polygeneration system. It provides a literature review on this subject, including on matters such as: the biomass gasification or pyrolysis-gasification concept; the downstream applications of syngas; the renewable hybrid polygeneration process; the hybridization of CSP biomass gasification; the integrated gasification combined cycle; the modeling and simulation of hybrid CSP-biomass gasification using Aspen Plus®. This chapter also introduces each of the chapters in this report.

Chapter 2 This chapter provides a detailed review of process synthesis techniques and attainable region principles, to determine the specified molar ratio of hydrogen to carbon monoxide from a material, energy and work balance point of view. The chapter starts with the identification of the major components in the process and ignores the components of smaller

quantities and the impurities. This is done to simply the analysis while extracting the essential information that does not require the details, which will be included at a later stage of design to simulate the biomass gasification. The target represents the performance limit for the process. The material, energy and work balance figures are used to determine the attainable region for the biomass gasification process. and we explore the process options with high performance in terms of material, energy and work balances. This chapter includes two publications: Dimethyl ether synthesis from biomass gasification: Thermodynamic approach to determine performance limits (European Symposium on Computer Aided Process Engineering ESCAPE-31); and, Ethanol reforming: Setting up a performance target (European Symposium on Computer Aided Process Engineering ESCAPE-30).

Chapter 3 deals with CSP-hybrid staged-gasification of solid waste to produce hydrogen: Aspen Plus simulation. (This paper has been accepted for IEEES-12 conference and has been published in the abstract booklet of the conference.

Chapter 4 explores the possibility of using a CH_4 gas turbine for power generation by applying different agents for biomass gasification. (The paper is in the writing phase.)

Chapter 5 deals with using concentrated solar energy in biomass gasification to produce hydrogen (SolarPACES-2020 paper).

Chapter 6 deals with the hybrid CSP biomass CO_2-gasification process for power production: Aspen Plus simulation and a comparative study of supercritical carbon dioxide power cycles integrated with solar-assisted biomass gasification (SolarPACES-2019).

Chapter 7 provides the Aspen Plus Simulation Study of Concentrated Solar Power and Biomass Gasification for co-Production of Power and Liquid Fuel (SolarPACES-2018), a study of an integrated biomass gasification combined cycle process facilitated with concentrated solar power (SASEC-2018 paper).

Chapter 8 This chapter concludes on the potential of renewable hybrid polygeneration system from various types of unconventional feedstock. It also concludes that CSP hybrid

biomass gasification will be a landmark technology to meet energy demand. This chapter concludes about the overall system reliability, dispatchability, security and stability to produce many types of hydrocarbons, other chemicals and energy products related to biomass gasification with the concept of polygeneration process. The chapter provides information about renewable hybrid polygeneration pathways and the commercial benefits of incorporating solar thermal-energy into biomass gasification.

Figures
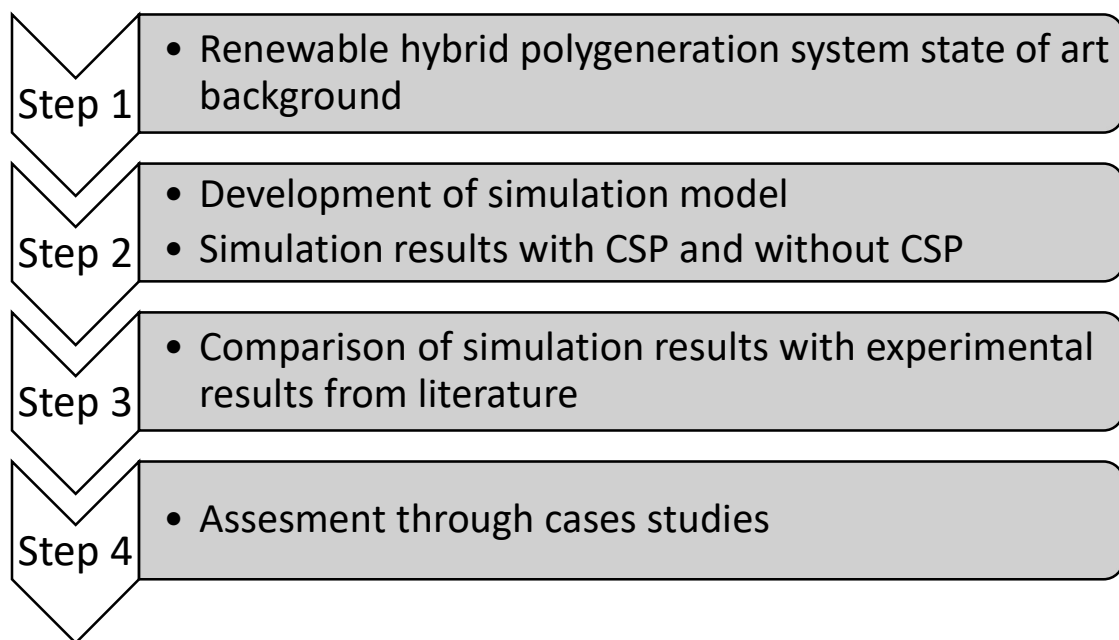
Figure 1.4(i): Predefined basic work plan of renewable hybrid polygeneration system

References

[1]   E. Dogan and F. Seker, "Determinants of CO2 emissions in the European Union: The role of renewable and non-renewable energy," Renew. Energy, vol. 94, pp. 429–439, Aug. 2016

[2]   N. Apergis, M. Ben Jebli, and S. Ben Youssef, "Does renewable energy consumption and health expenditures decrease carbon dioxide emissions? Evidence for sub-Saharan Africa countries," Renew. Energy, vol. 127, pp. 1011–1016, Nov. 2018

[3]   P. A. Østergaard, N. Duic, Y. Noorollahi, H. Mikulcic, and S. Kalogirou, "Sustainable development using

renewable energy technology," Renewable Energy, vol. 146. Elsevier Ltd, pp. 2430–2437, 01-Feb-2020

[4]   M. A. Harclerode, P. Lal, and M. E. Miller, "Quantifying global impacts to society from the consumption of natural resources during environmental remediation activities," J. Ind. Ecol., vol. 20, no. 3, pp. 410–422, Jun. 2016

[5]   I. Dincer, "Renewable energy and sustainable development: A crucial review," Renew. Sustain. energy Rev., vol. 4, no. 2, pp. 157–175, Jun. 2000

[6]   A. K. Shrivastava, S. Yadav, L. S. Yadav, S. Khan, A. R. Khan, and S. Sharma, "Global warming issues—Need for sustainable drainage system in urban sreas—Green construction technologies," Journal, 2018, pp. 15–28

[7]   A. Demirbas, "Thermochemical conversion processes," in Biofuels Securing the Planet's Future Energy Needs, Springer London, 2008, pp. 261–304

[8]   S. Pang, "Advances in thermochemical conversion of woody biomass to energy, fuels and chemicals," Biotechnology Advances, vol. 37, no. 4. Elsevier Inc., pp. 589–597, 01-Jul-2019

[9]   A. AlNouss, G. McKay, and T. Al-Ansari, "A comparison of steam and oxygen fed biomass gasification through a techno-economic-environmental study," Energy Convers. Manag., vol. 208, p. 112612, Mar. 2020

[10]   H. Gu, Y. Tang, J. Yao, and F. Chen, "Study on biomass gasification under various operating conditions," J. Energy Inst., vol. 92, no. 5, pp. 1329–1336, Oct. 2019

[11]   S. K. Sansaniwal, K. Pal, M. A. Rosen, and S. K. Tyagi, "Recent advances in the development of biomass gasification technology: A comprehensive review," Renewable and Sustainable Energy Reviews, vol. 72. Elsevier Ltd, pp. 363–384, 01-May-2017

[12]   R. Tavares, E. Monteiro, F. Tabet, and A. Rouboa, "Numerical investigation of optimum operating conditions for syngas and hydrogen production from biomass gasification using Aspen Plus," Renew. Energy, vol. 146, pp. 1309–1314, Feb. 2020

[13]   R. Milani, A. Szklo, and B. S. Hoffmann, "Hybridization of concentrated solar power with biomass gasification in Brazil's semiarid region," Energy Convers. Manag., vol. 143, pp. 522–537, 2017

[14]   Z. Bai, Q. Liu, J. Lei, H. Hong, and H. Jin, "New solar-biomass power generation system integrated a two-stage gasifier," Appl. Energy, vol. 194, pp. 310–319, May 2017

[15]   E. G. Hertwich and X. Zhang, "Concentrating-solar biomass gasification process for a 3rd generation biofuel," Environ. Sci. Technol., 2009

[16]   M. Suárez-Almeida, A. Gómez-Barea, A. F. Ghoniem, and C. Pfeifer, "Solar gasification of biomass in a dual fluidized bed," Chem. Eng. J., p. 126665, Aug. 2020

[17]   T. Kodama, S. Bellan, N. Gokon, and H. S. Cho, "Particle reactors for solar thermochemical processes," Sol. Energy, vol. 156, pp. 113–132, Nov. 2017

[18]   E. Alonso and M. Romero, "Review of experimental investigation on directly irradiated particles solar reactors," Renewable and Sustainable Energy Reviews, vol. 41. Elsevier Ltd, pp. 53–67, 01-Jan-2015

[19]   V. S. Sikarwar et al., "An overview of advances in biomass gasification," Energy and Environmental Science, vol. 9, no. 10. Royal Society of Chemistry, pp. 2939–2977, 01-Oct-2016

[20]   J. H. Peterseim, S. White, A. Tadros, and U. Hellwig, "Concentrated solar power hybrid plants, which technologies are best suited for hybridisation?," Renew. Energy, vol. 57, pp. 520–532, 2013

[21]   S. A. Mohamed et al., "A review on current status and challenges of inorganic phase change materials for thermal energy storage systems," Renew. Sustain. Energy Rev., vol. 70, pp. 1072–1089, Apr. 2017

[22]   A. M. A. Ahmed, A. Salmiaton, T. S. Y. Choong, and W. A. K. G. Wan Azlina, "Review of kinetic and equilibrium concepts for biomass tar modeling by using Aspen Plus," Renewable and Sustainable Energy Reviews, vol. 52. Elsevier Ltd, pp. 1623–1644, 01-Dec-2015

[23]   S. Rupesh, C. Muraleedharan, and P. Arun, "Aspen plus modelling of air–steam gasification of biomass with sorbent enabled CO2 capture," Resour. Technol., vol. 2, no. 2, pp. 94–103, Jun. 2016

[24]   N. Ramzan, A. Ashraf, S. Naveed, and A. Malik, "Simulation of hybrid biomass gasification using Aspen plus: A comparative performance analysis for food, municipal solid and poultry waste," Biomass and Bioenergy, vol. 35, no. 9, pp. 3962–3969, Oct. 2011

[25]   J. H. Peterseim, A. Tadros, S. White, U. Hellwig, J. Landler, and K. Galang, "Solar tower-biomass hybrid plants – maximizing plant performance," Energy Procedia, vol. 49, pp. 1197–1206, 2014

[26]   N. Piatkowski, C. Wieckert, A. W. Weimer, and A. Steinfeld, "Solar-driven gasification of carbonaceous feedstock - a review," Energy Environ. Sci., vol. 4, no. 73, 2011

[27]   Y. Tanaka, S. Mesfun, K. Umeki, A. Toffolo, Y. Tamaura, and K. Yoshikawa, "Thermodynamic performance of a hybrid power generation system using biomass gasification and concentrated solar thermal processes," Appl. Energy, vol. 160, pp. 664–672, Dec. 2015

Chapter 2: Process Synthesis Techniques and Attainable Region Principles

2.1: Dimethyl Ether Synthesis via Biomass Gasification

The production of dimethyl ether (DME) from biomass has been gaining much attention because of its potential to be used as an alternative high cetane number fuel for diesel engines. In this study, we determine the performance targets to produce DME from biomass by using attainable region principles. The target represents the performance limit for the process. We use the material, energy and work balances to determine the attainable region for the process and we explore the process options with high performance in terms of material, energy and work balance.

The study shows that the performance of biomass to DME process is limited by the availability of external energy. With nearly 66% carbon efficiency if no energy is available and will, only increase marginally to 68% if an external source of energy is available. The study also shows that co-feeding biomass with methane can significantly improve the performance of the process both in terms of material, energy and work balances. In particular, it shows that a 91% carbon efficiency is possible by co-feeding biomass and methane at a ratio of 1:0.83 resulting in no energy cost and zero chemical potential loss. This is the ultimate target for the conversion of biomass to DME. The study also shows that a carbon negative process is possible with more than 100% carbon efficiency, which enable co-feeding CO_2, however this target can lead to significant energy inefficiency due to the large negative ΔH, which will require large amounts of energy to be removed from the process.

2.1.1: Introduction

DME is considered as a cleaner fuel that holds the potential to replace the use of diesel in vehicles due to its high cetane number. In general, DME is produced from syngas derived from natural gas. DME can also be produced from biomass derived syngas. There is a potential

of using biomass waste resources due to their vast availability, which will significantly reduce the production cost and will make it independent from petroleum prices [1]. DME production from biomass derived syngas has been considered as an alternative way to replace fossil fuels [2]. DME production is divided into two methods: direct synthesis and indirect synthesis [3]. In general, methanol is produced from syngas then dehydrated to produce DME [4,5].

Most recently, single step direct DME synthesis (simultaneously methanol synthesis and dehydration process in one reactor) has overcome the equilibrium limitations and has higher carbon conversion efficiency [6-8]. In this study, we explore the limit of performance and performance targets for the production of DME from biomass. We also explore the effect of co-feeding biomass and methane on the process performance from a material, energy and work (chemical potential) perspective. The targets obtained here can be used as a base in the design and optimisation of the gasification section, the single stage DME synthesis from syngas, and the overall process.

2.1.2: Methodology

The scope of our study is setting up the process design targets via three basic tools namely the mass, energy and work (entropy) balance to determine a feasible region for the DME synthesis from biomass. We start by first identifying the major components of the process and ignore the components in smaller quantities and the impurities. This is done to simply the analysis while extracting the essential information that does not require the details, which are subsequently included at a later stage of design. There are three performance targets namely, the material balance, the energy balance, determined by the change in enthalpy across the process (ΔH), and the work (chemical potential) balance given by the change in the Gibbs free energy across the process (ΔG).

The main compounds that were considered were biomass ($CH_{1.5}O_{0.6}$), water (H_2O), oxygen (O_2), carbon dioxide (CO_2), methane (CH_4), hydrogen (H_2), carbon monoxide (CO) and DME (C_2H_6O). A mass independent equation was derived for these major components on the basis of the principles defined by [9-11].

$$CH_{1.5}O_{0.6} + aH_2O + bO_2 + cH_2 + dCO + eCH_4 + fCO_2 + gC_2H_6O = 0 \qquad (1)$$

We derive a set of independent material balances from the over equation (1), which will represent all achievable outcome from the process. Each component can then be written in terms of extent as $N_i = \sum_{i,j} v_{ij} E_j$.

The constraints set by the energy and work balances are also included. These are expressed as follows:

$$\Delta H_p = \sum_i N_i \Delta \hat{H}_i(T_o)$$
$$\Delta G_p = \sum_i N_i \Delta \hat{G}_i(T_o)$$

$$(2)$$

ΔH_p represents the net energy requirement of the process and ΔG_p is the change in the Gibbs free energy and represents the work requirement (or work potential) of the process. In other words, ΔG_p represents the portion of the energy equivalent to mechanical work that must be supplied (positive) or removed (negative) from the process.

The attainable region for the process is obtained by linear programming with specific material, energy and work balance objective functions and constraints. The specific objective functions we look at include energy and work neutral processes while maximizing the production rate of DME per mole of biomass fed. The significance of an energy neutral process is that one is able to identify the material balance for converting biomass to DME at no energy cost or loss, making the process most energy efficient. The significant of a work neutral process is that the energy quality of the feed material is conserved as it is converted to products. A positive value for the work requirement means that the process is work deficient and would need a supply of high-quality energy from an external source. A negative value for the work requirement means that the process will lose some of the work potential (energy quality) making it more inefficient. Therefore, the objective is to conserve as much chemical potential and energy as possible while maximizing the production of DME.

2.1.3: Results and Discussion

Figure 2.1.3(i) shows the material, energy and work targets for the process at varying oxygen feed. The amount of oxygen in the feed is used as a parameter to meet the energy and work targets and does not affect the material balance by much as can be seen in Figure 2.1.3(i). It is also shown that at zero ΔG, ΔH is positive, which means that the process requires energy input if the chemical potential is conserved. On the other at zero ΔH, ΔG is negative, which means that the process will lose some chemical potential even if it is fully energy integrated. Therefore, the process is energy limited since it will require energy in order to conserve the chemical potential. Therefore, if no external energy is available the maximum DME production rate is 0.33mol/mol biomass with a carbon efficiency of 66%. At this point, the process has some chemical potential available, which will be lost if not recovered as useful energy.

If an external source of energy is available, such solar energy or low-grade energy then the production rate can be increased by about 4% to 0.34mol/mol biomass. Although the gain in the production rate is minimal, the reduction in CO_2 emissions, which is about 8%, can be significant on a large scale.

If we consider the carbon to hydrogen ratio (C/H) in biomass (1/1.5) and in DME (1:3) [9-11], we see that biomass is hydrogen deficient in making DME and thus the additional hydrogen required is sourced from water. However, co-feeding biomass with water brings in access oxygen, which is discarded by producing CO_2, which reduces the efficiency of the process.

Figure 2.1.3(ii) shows the exploration of the possibility of co-feeding biomass with CH_4 in order to improve the performance in terms of the material, energy and work balance. CH_4 is an oxygen free source of hydrogen and can assist in correcting the C/H ratio imbalance between biomass and DME and thus can improve the performance of the process. Furthermore, addition of CH_4 provides an extra degree of freedom in the attainable region, which makes possible to set better targets for the process.

For instance, Figure 2.1.3(ii) shows that by co-feeding methane with biomass it is now possible to have a set of material balances with zero ΔG, which means these targets will fully conserve the chemical potential; thus they are ultimately the most efficient targets for the process. It is also possible to target an energy and work neutral process simultaneously when ΔG and ΔH are zero. This target results in a DME production rate of 0.83 mol/mol of biomass with a carbon efficiency of 91% and an improvement of about 25% in carbon efficiency compared to the targets shown in Figure 2.1.3(i) with only biomass in the feed.

Figure 2.1.3(ii) also shows that the process can reach 100% carbon efficiency at zero CO_2 production, and possibly more than 100%, as it can accept CO_2 as the feed to the process. However, with significant energy losses, as ΔH becomes more negative. In principle, since ΔG is zero, the excess energy must be removed from the process at ambient temperature, which may not be practical in real processes. Thus, there is a possible for worse performance than the target for all the targets with negative ΔH in real processes, as a temperature gradient will be required to remove heat from these processes.

Heat removed from the process at a temperature higher than ambient will remove some work potential from the process and result in loss in chemical potential, which will reduce the energy and material efficiency of the process. This observation highlights the fact that a higher carbon efficiency might not necessarily lead to an efficient process as one must consider the energy balance.

2.1.4: Conclusion

An attainable region approach was used to show that the production of DME from biomass: is energy limited and has a maximum carbon efficiency of 66%; has an inherent chemical potential loss due to the imbalance in the C/H ratio between biomass and DME. We have also shown that co-feeding biomass with CH_4 can improve the performance by reducing the C/H imbalance without the additional of excess oxygen, which leads to more CO_2 emission, and thus to highly efficient energy and work processes. Co-feeding CH_4 can increase the carbon

efficiency to 100% with no CO_2 production and ultimately can allow feeding CO_2, which could lead to a carbon negative process.

Note: This paper is published in the proceedings of the 31st European symposium on computer aided process engineering (ESCAPE-31).

2.2: Ethanol Reforming to Hydrogen Production

Process Synthesis techniques and Attainable region principles were used to determine the target of ethanol reforming to hydrogen from a material, energy and work balance point of view. From material balance point of view 100% hydrogen efficiency, defined as the fraction of hydrogen in the feed that is converted into the desired product (H_2), can be achieved by partial oxidation at ration of ethanol to oxygen of 1 : 1.5, producing H_2 and CO_2. However, the process releases a significant amount of energy and work potential, which might not be economically recovered especially for small scale applications. Co-feeding water is one of the ways to recover this energy by producing more H_2. Therefore, we looked at the ultimate energy target for the process, which is considered to be the point at which ΔH is zero across the process. In order to achieve this, water and oxygen must be fed to the process at ratios of 1:1.77 and 1: 0.62 respectively. This increases H_2 production by 59%. However, the process will still have a significant amount of work potential indicated by the negative change in Gibbs free energy across the process.

When work balance target of $\Delta G = 0$ was considered, we can show that the hydrogen production can be increased up to 87%. However, the process will require heat to be supplied. If a low-cost heat source is available, such as solar or waste heat from other processes, then a maximum of 187% selectivity of H_2 based on ethanol can be achieved. For a fully energy integrated process, at $\Delta G = 0$ the process does not require high quality heat for it to proceed. Therefore, at this point, any source of heat at a temperature high enough to enable heat flow at any point in the process will be sufficient to drive the process. The authors consider this to be the ultimate target for ethanol reforming, which enables the chemical potential of ethanol to be

preserved, and provides an opportunity to store additional external energy in the form of H_2. The feasibility of these targets were validated by means of Aspen Plus® simulation.

2.2.1: Background of Hydrogen Production via Ethanol Reforming

Hydrogen fuel cell technologies has big potential to be used in vehicle or portable power plants as a clean energy supply solution. But there are challenges in its implementation. For example, currently, most of the hydrogen is produced from fossil fuel such as natural gas or coal, which is not renewable. Furthermore, the hydrogen produced from water electrolysis by using renewable power is still expensive. Furthermore, if hydrogen is produced from a big hydrogen plant, it still needs to be transported to the user end and stored at the user end, which raised concerns of its safety. Thus, it would be a good option to study the potential of using liquid fuel, which are easy to be stored and transported as a feed stock for on-site hydrogen production in vehicle or hydrogen filling station [12].

Among various ethanol to hydrogen processes studied, ethanol autothermal reforming, which is a combination of the exothermic ethanol partial oxidation process and endothermic ethanol steam reforming process, is most suited for mobile application as it doesn't require external heat load [13]. Furthermore, an ethanol water mixture can be used in the autothermal reforming process, thus the high energy cost paid to remove all water in the ethanol production by distillation and zeolite adsorption can be saved [14].

To achieve thermal neutral, for every mol of ethanol, 1.78 mole of water and 0.61 mole of Oxygen is needed [15], to produce 4.78 mole of hydrogen. But there is still a significant amount of work as indicated by the negative change in the free energy across the process. To utilize this work, a work balanced target at $\Delta G = 0$ was considered and analyzed by targeting techniques.

2.2.2: Methodology to Determine a Feasible Region

The targeting technique employs three basic tools namely the mass, energy and work (entropy) balance to determine a feasible region from which a design target for the process can

be set. It starts by first identifying the major components of the process and ignores the components in smaller quantities and the impurities. This is done to simply the analysis while extracting the essential information that does not require the details, which will be included at a later stage of design. The major components that were considered here are C_2H_6O, H_2, CO_2, H_2O, CO, CH_4, O_2. From these components, we can derive the following independent material balances using the method developed by [Yin, 2010]:

$$C_2H_6O + 0.5O_2 \Rightarrow 3H_2 + 2CO.............E_1$$
$$CO_2 + H_2 \Rightarrow CO + H_2O.......................E_2$$
$$CH_4 + 2O_2 \Rightarrow CO_2 + 2H_2O..................E_3 \quad (1)$$
$$H_2 + 0.5O_2 \Rightarrow H_2O............................E_4$$
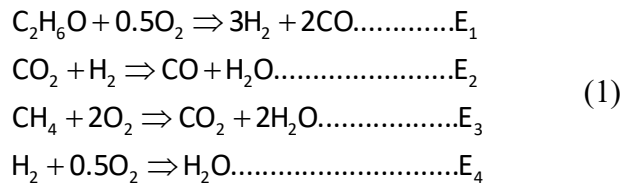
Note that these are not necessarily the actual reactions occurring in the process, they are simply material balance representing all achievable outcome from the process. Each component can then be written in terms of extent as: $N_i = \sum_{i,j} v_{ij} E_j$.

The constraints set by the energy and work balances are also included. These are expressed as follows:

$$\Delta H_P = \sum_i N_i \Delta \hat{H}_i (T_0)$$
$$\Delta G_P = \sum_i N_i \Delta \hat{G}_i (T_0) \quad (2)$$

ΔHp represents the net energy requirement of the process and ΔG_P is the change in the Gibbs free energy and represents the work requirement (or work potential) of the process. In other words, ΔG_P represents the portion of the energy equivalent to mechanical work that must be supplied (positive) or removed (negative) from the process.

2.2.3: Results and Discussion

It can be shown that the process has four degrees of freedom representing four possible targets that can be set simultaneously. In order to explore these targets, we used a linear programming approach to determine the feasible regions. Two cases are considered namely ΔHp

= 0 for an energy neutral process and $\Delta Gp = 0$ for a work neutral process. Figure 2.2.3(i) shows the feasible regions obtained by plotting the oxygen fed to the process versus the hydrogen production at $\Delta Hp = 0$ per mole of ethanol fed. The negative number of moles indicates that the component is a feed while the positive number indicates that the component is a product. The feasible region is considered to be where H_2, CO_2, CO, and CH_4 are products and O_2 is the feed. H_2O is allowed to be either feed or products. It is clear from Figure 2.2.3(i) that the maximum H_2 production occurs at zero CH_4 and CO produced. At this point $\Delta Gp < 0$, this means that the process should proceed with less effort. It also means that the process has the potential to do work, which can be recovered by applying an appropriate process configuration. Therefore, the ultimate H_2 production target for an autothermal ethanol reformer is about 4.77 per mole of ethanol.

$$C_2H_6O + 1.77H_2O + 0.62O_2 \Rightarrow 4.77H_2 + 2CO_2 \quad \Delta G = -195 \text{ kJ}; \Delta H = 0 \text{ kJ} \quad (3)$$

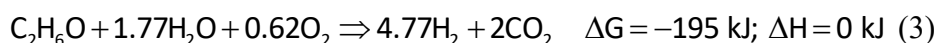Figure 2.2.3(ii) shows the feasible region for a work-neutral process ($\Delta Gp = 0$). The maximum hydrogen production also occurs at zero CH_4 and CO produced. However, at this point $\Delta Hp > 0$. This means that energy in the form of heat must be supplied to the process from an external source. The significance of a work neutral process is that the chemical potential of the feed material is fully conserved when they are converted into products [16]. Consequently, the energy that must be supplied can be in the form of heat and can be at any temperature that enables the flow of energy from an external source to the process. This target represents the limit of performance for any ethanol reforming process contrary to what is considered to be the limit set by an auto thermal reformer [15]. The H_2 production target at this limit is 5.59 per mole of ethanol.

$$C_2H_6O + 2.59H_2O + 0.21O_2 \Rightarrow 5.59H_2 + 2CO_2 \quad \Delta G = 0 \text{ kJ}; \Delta H = 236 \text{ kJ} \quad (4)$$
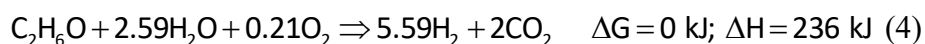
This target provides a means for improving the hydrogen production of an auto thermal reformer by up to 17%, if a source of low-cost energy is available, which is likely the case in the actual application environmental such as in the vehicle. For a fully energy integrated process, at $\Delta G = 0$ the process does not require high quality heat for it to proceed. Therefore, at this point, any source of heat at a temperature high enough to enable heat flow at any point in the process will be sufficient to drive the process. One of the efficient ways of supplying the energy to the process is by generating steam using any heat source at low temperature but high enough to produce the

steam (above 100 °C at 1atm) and feed the steam that carries the required amount of energy into the process.

Simulations in Aspen Plus® were conducted to explore how the targets in (3) and (4) can be achieved, the flow sheets are shown in Figure 2.2.3(iii). The main assumptions taken in the simulation are: 1) the reforming reaction reaches equilibrium and therefore an equilibrium reactor (RGibbs) was used to simulate the reaction. 2) Pure H_2 can be recovered from the product stream at the reactor temperature, therefore, a perfect separator was used to selectively remove H_2 from the other products. The latter assumption is possible in a membrane reactor, which can separate out H_2 during the reaction.

For the $\Delta H = 0$ process, the feed stream containing ethanol and water is pre-heated and fed to membrane reactor. The temperature in the reactor is set to between 500 °C and 1000 °C. The membrane process, which selectively removes H_2 from the reactor, is simulated by multistage equilibrium reactors with hydrogen separation between stages. The energy required in the reformers is supplied by burning the tail gas from the reformer after H_2 has be separated out. For this purpose, a stoichiometric reactor (RStoic) was used. The combustion is assumed to occur at the same temperature as the reactor. Heat integration is done between the feed stream and the product streams from the combustor. A temperature approach of 10 °C is considered in the heat integration process.

The flowsheet of the $\Delta G = 0$ process is the same as that of $\Delta H = 0$ except for the additional steam generated from an external source of energy and fed to the reactor. The stream brings in the additional energy required to reach the target of H_2 at $\Delta G = 0$. In the current simulation approach, it assumed that external heat is available to generate steam and 102 °C and 1bar from a stream of liquid water at 25 °C.

The simulation results show that for the $\Delta H = 0$ process the H_2 production target of 4.77/mole of ethanol at oxygen to ethanol ratio of 0.62/1 can be achieved over the temperature range 500 – 1000 °C. The water to ethanol feed ratio varies depending on the reaction temperature, the minimum feed ratio 4.40/1 occurs at 700 °C. If we consider recycling the water, then the net water to ethanol feed ratio is constant over the temperature range and is 1.77/1; this is the same as the target water feed ratio in (3).

The simulation results for the $\Delta G = 0$ process show that the H_2 production target of 5.59/mole of ethanol at an oxygen to ethanol ratio of 0.21/1 can be achieved in a temperature range of 500 °C to 1000 °C. The water to ethanol feed ratio also varies depending on the reaction temperature, the minimum feed ratio 9.01/1 occurs at 620 °C. If we consider recycling the water, then the net water to ethanol feed ratio is constant over the temperature range and is 2.59/1; this is the same as the target water feed ratio in (4).

2.2.4: Conclusions

By conducting work balance target analysis, we found that hydrogen production of the ethanol to hydrogen process can be increased up to 87% compared to ethanol partial oxidation process and 17% more compared to the target of the ΔH neutral process, with less oxygen required and more water can be tolerated. Although external heat is needed, low cost heat can be utilized in a fully-integrated energy process operated at $\Delta G = 0$. We consider this to be the ultimate target for ethanol reforming, which not only enables to conserve the chemical potential of ethanol but also provides an opportunity to store additional external energy in the form of H_2.

Note: This paper is published in the proceedings of the 30th European symposium on computer aided process engineering (ESCAPE-30).

Figures
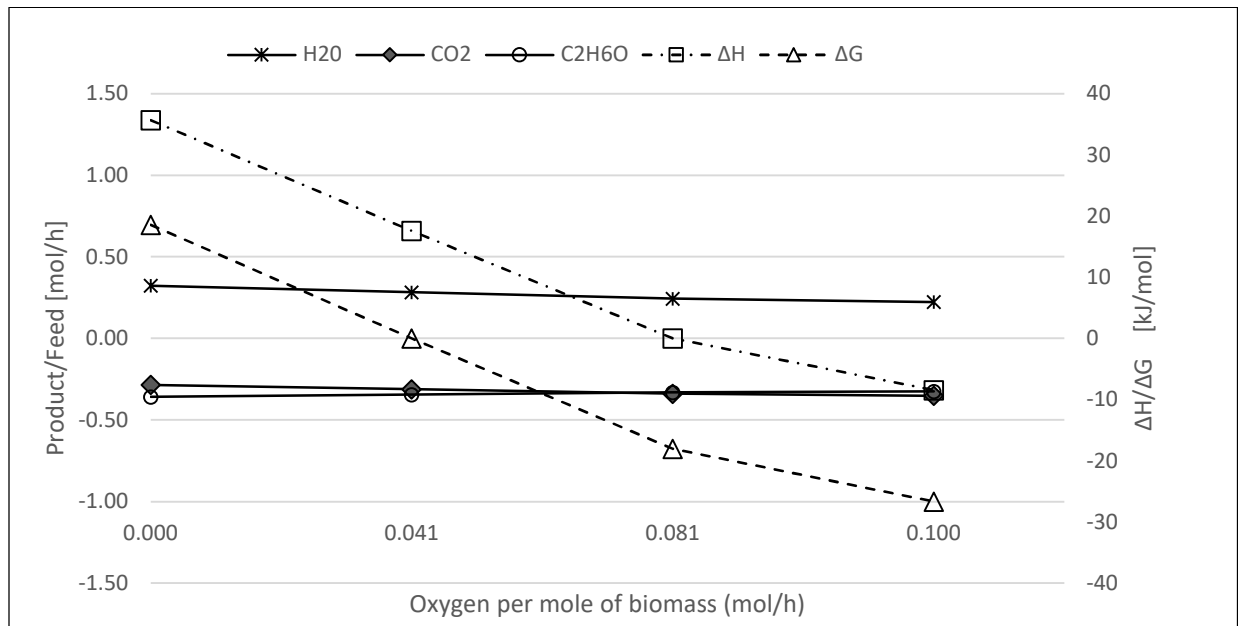
Figure 2.1.3(i): Material, energy and work balance target for DME process per mole of biomass and varying oxygen feed to the gasifier. The maximum DME production rate is about 0.34 mol/mol biomass.
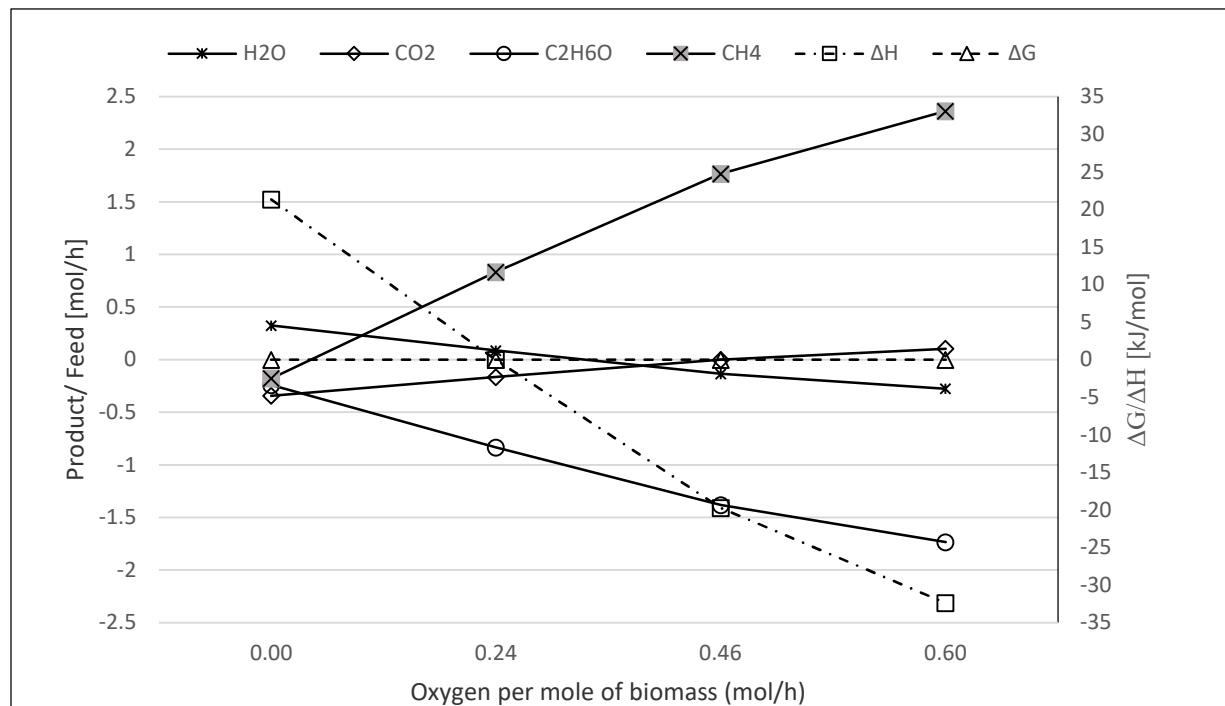
Figure 2.1.3(ii): Co-feeding biomass with CH_4 to produce DME improves the material, energy and work balance performance of the process. The addition of CH_4 eliminates the C/H ratio imbalance between biomass and DME, without the addition of excess oxygen, and provides an extra degree of freedom to improve the performance of the process.
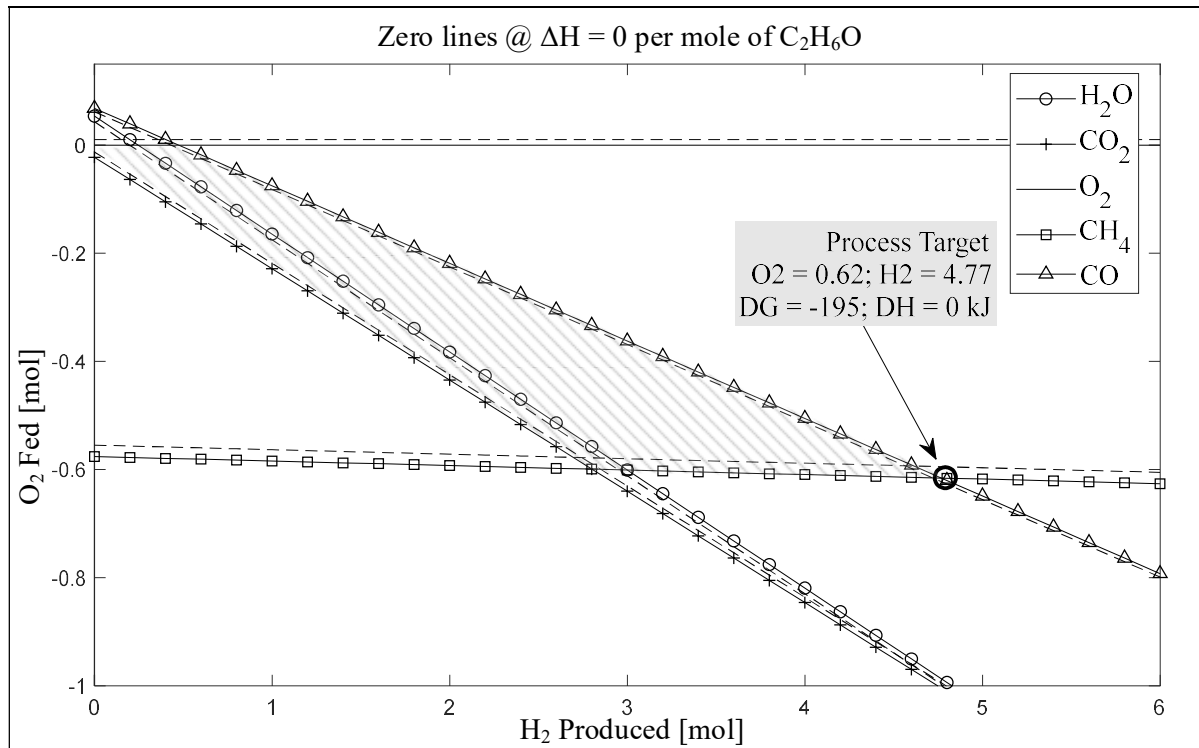
Figure 2.2.3(i): Feasible region for an energy neutral ethanol reforming process. The solid lines are the boundaries that indicate zero moles of the components. The dashed lines indicate the side where the components are net products. The ultimate hydrogen production target is 4.77 moles per mole of C_2H_6O.
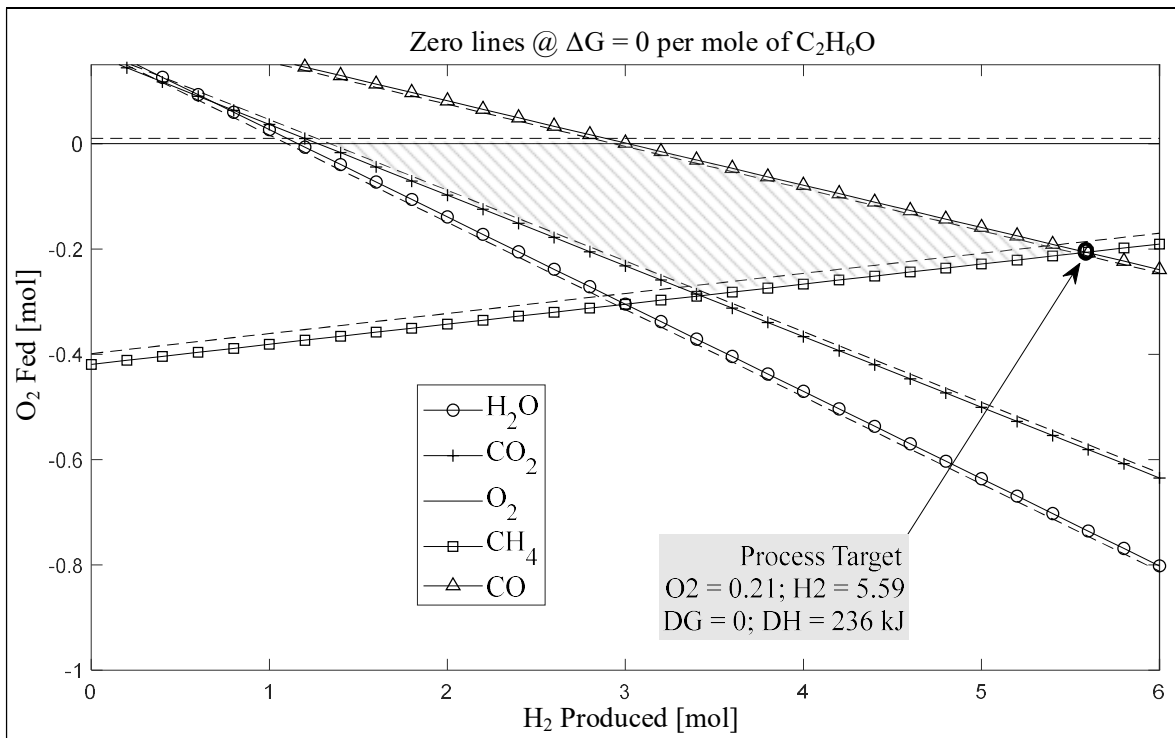
Figure 2.2.3(ii): Feasible region for a work neutral ethanol reforming process. The solid lines are the boundaries that indicate zero moles of the components. The dashed lines indicate the side where the components are net products. The ultimate hydrogen production target is 5.59 moles per mole of C_2H_6O.
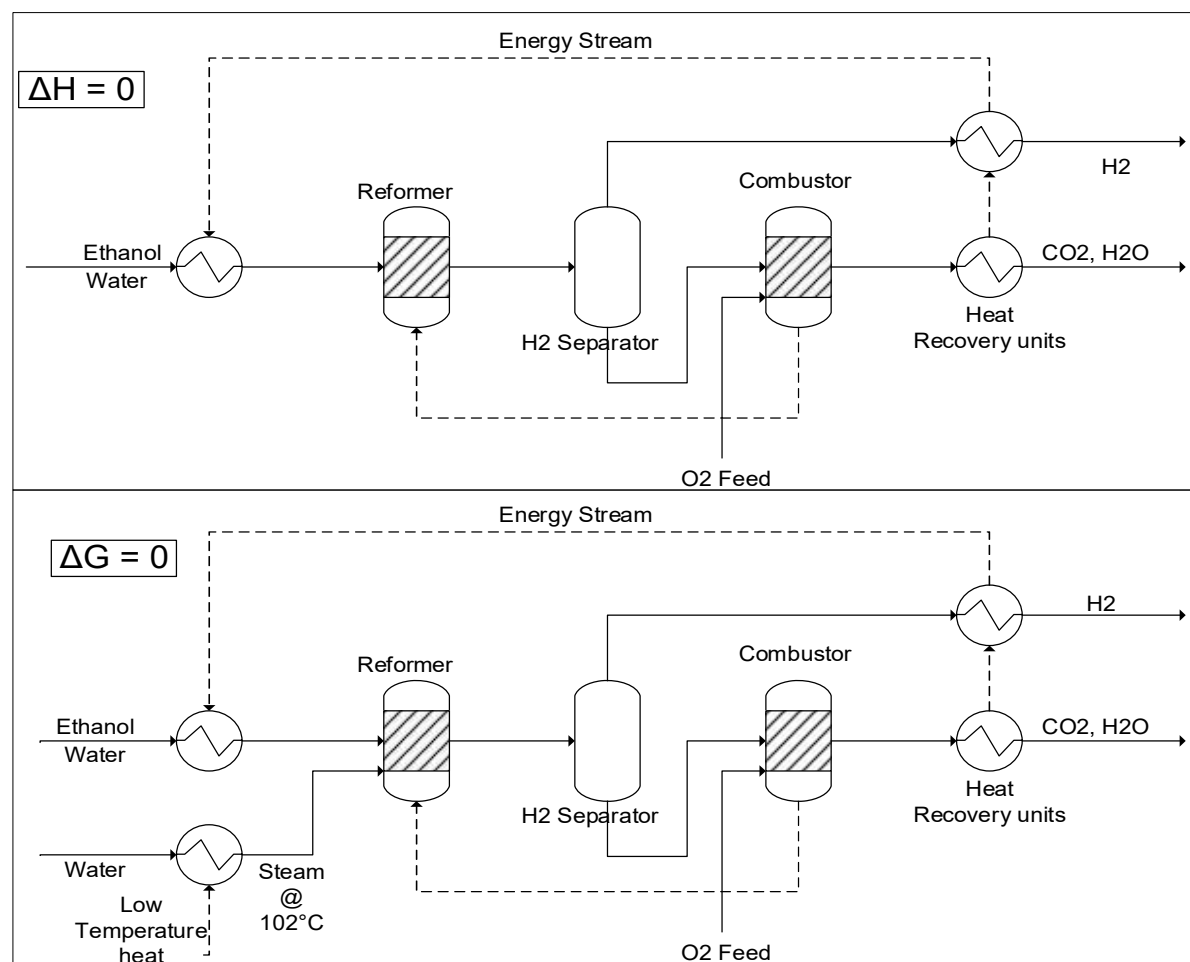
Figure 2.2.3(iii): Flow diagram for the Aspen Plus simulations at $\Delta H = 0$ and $\Delta G = 0$

References

[1]   Sousa-Aguiar, E.F., Appel, L.G., Mota, C., 2005. Natural gas chemical transformations: The path to refining in the future. Catalysis Today. Elsevier, pp. 3–7. https://doi.org/10.1016/j.cattod.2004.12.003

[2]   Azizi, Z., Rezaeimanesh, M., Tohidian, T., Rahimpour, M.R., 2014. Dimethyl ether: A review of technologies and production challenges. Chem. Eng. Process. Process Intensif. https://doi.org/10.1016/j.cep.2014.06.007

[3]   Nakyai, T., Patcharavorachot, Y., Arpornwichanop, A., Saebea, D., 2020. Comparative exergoeconomic analysis of indirect and direct bio-dimethyl ether syntheses based on air-steam biomass gasification with CO2 utilization. Energy 209, 118332. https://doi.org/10.1016/j.energy.2020.118332

[4]   Cho, W., Song, T., Mitsos, A., McKinnon, J.T., Ko, G.H., Tolsma, J.E., Denholm, D., Park, T., 2009. Optimal design and operation of a natural gas tri-reforming reactor for DME synthesis. Catal. Today 139, 261–267. https://doi.org/10.1016/j.cattod.2008.04.051

[5]   Kim, I.H., Kim, S., Cho, W., Yoon, E.S., 2010. Simulation of commercial dimethyl ether production plant. Comput. Aided Chem. Eng. 28, 799–804. https://doi.org/10.1016/S1570-7946(10)28134-8

[6]   Delgado Otalvaro, N., Kaiser, M., Delgado, K.H., Wild, S., Sauer, J., Freund, H., 2020. Optimization of the direct synthesis of dimethyl ether from CO 2 rich synthesis gas: Closing the loop between experimental investigations and model-based reactor design †. https://doi.org/10.1039/d0re00041h

[7]   Marchionna, M., Patrini, R., Sanfilippo, D., Migliavacca, G., 2008. Fundamental investigations on di-methyl ether (DME) as LPG substitute or make-up for domestic uses. Fuel Process. Technol. 89, 1255–1261. https://doi.org/10.1016/j.fuproc.2008.07.013

[8]   Ng, K.L., Chadwick, D., Toseland, B.A., 1999. Kinetics and modelling of dimethyl ether synthesis from synthesis gas. Chem. Eng. Sci. 54, 3587–3592. https://doi.org/10.1016/S0009-2509(98)00514-4

[9]   Bjórnbom, P.H., 1965. The independent reactions in calculations of complex chemical equilibria, Ind. Eng. Chem., Fund-am.

[10]   Yin, F., 2010. A simple method for finding independent reactions. Chem. Eng. Commun. 83, 117–127. https://doi.org/10.1080/00986448908940657

[11]   Yin, F., 1989. A simpler method for finding independent reactions. Chem. Eng. Commun. 83, 117–127. https://doi.org/10.1080/00986448908940657

[12]   G Di Marcoberardino, M Binotti, G Manzolini, J L Viviente, A Arratibel, L Roses, F Gallucci, 2017, Achievements of European projects on membrane reactor for hydrogen production, Journal of Cleaner Production, 161, 1442-1450

[13]   T Hou, S Zhang, Y Chen, D Wang, 2015, W Cai, Hydrogen production from ethanol reforming: Catalysts and reaction mechanism, Renewable and Sustainable Energy Reviews, 44, 132-148

[14]   G A Deluga, J R Salge, L D Schmide, X E Verykios, 2004, Renewable hydrogen from ethanol by autothermal reforming, Sciences, 303, 993-997

[15]   C Graschinsky, P Giunta, N Amadeo, M Laborde, 2012, Thermodynamic analysis of hydrogen production by autothermal reforming of ethanol, International Journal of Hydrogn Energy, 37 (13), 10118-10124

[16]   Sempuga, B. C. and Yao, Y., 2017, CO_2 hydrogenation from a process synthesis perspective: Setting up process targets', Journal of CO_2 Utilization, 20, 34–42

Chapter 3: Solid Waste to Hydrogen

3.1: CSP-Hybrid Staged-gasification of Solid Waste to Produce Hydrogen:

Hydrogen (H_2) production from solid waste through concentrated solar power (CSP) hybrid staged-gasification is an attractive technology because of environmental benefits and economic issues. In this study, the effects of gasification temperature and steam to biomass ratio on yield of syngas are investigated to predict the optimum operating conditions with maximum H_2 productivity. Aspen Plus® is used to develop a simple model for gasification followed by reforming of syngas and water gas shift (WGS) reaction. Heat load of a gasifier is balanced by injection of solar energy while heat load of a reformer is balanced by combustion of produced syngas. The main objective of this study is to compare the benefits of reforming syngas, the WGS reaction and the incorporation of CSP. The feed of 1000 kg/h feedstock is gasified at 700-900 °C @ 1 bar$_a$. Simulation results showed that with increase in temperature of the gasifier and steam flow rate to the gasifier significantly increased the carbon conversion, yield of hydrogen and yield of syngas. Simulation results revealed that H_2 production efficiency with CSP is about 12.5 kmol/MW$_{th}$ for PW as a feedstock and 13.2 kmol/MW$_{th}$ in case of MSW.

It is noted that adding CSP into the system can boost H_2 production up to 50% to 146 g/kg of wet pinewood sawdust (PW) as a feedstock while 61% to 224 g/kg of municipal solid waste (MSW). Simulation results from all the cases indicate that CSP-hybrid staged-gasification is a promising alternative process to produce secondary fuel in the form of H_2. Hydrogen enriched syngas production from solid waste and concentrated solar power is established in Aspen Plus® process simulator is shown in the Figure 3.1(i).

3.1.1: Background of Hydrogen Production from Solid Waste

Biomass derived H_2 can be used as a clean secondary energy fuel to reduce the greenhouse gases emissions with high energy conversion efficiency and with water as the only by-product [1]. Solid waste (crops residue, pinewood sawdust and municipal solid waste) has potential to produce H_2 via staged-gasification process [2,3], which is a thermochemical process to convert solid waste

into syngas with various gasifying agents, e.g. carbon dioxide (CO_2), oxygen (O_2), steam (H_2O) or air [4-6], followed by steam reforming and/or WGS reaction. There has been some experimental study to produce H_2 via gasification. The H_2 yield is in the range of 30-165 gH_2/kg of wet biomass.

The yield of syngas per unit biomass can be increased by using pure H_2O or pure O_2 as a gasifying agent [4,7]. Steam gasification has higher H_2 concentration, higher product gas efficiency and higher heating value per unit of biomass as compared to air or O_2 gasification [8]. However, steam gasification requires a significant amount of external heat to carry out a series of endothermic reactions as compared to air or O_2 gasification [9]. About 30% of the feedstock is combusted to provide the enthalpy of reaction for conventional gasification system [10,11]. CSP can play a key role to balance the enthalpy of reaction of gasification process and the entire biomass can be converted into H_2 and CO [12]. By combining CSP and biomass gasification, it shows great potential to convert solar energy into H_2.

Because gasification is a complex process [13-15] simulation models are essential to investigate the effects of operating conditions on the performance of gasification and to predict process behavior. It will save time and money to conduct a series of costly experiments and allow us to study different scenarios to optimize the process. Many researchers have developed the simplest possible models in Aspen Plus® [16-19]. These models have considered the complex chemical reactions, characteristics of the reactor and important physical characteristics of feedstock. The results generally included energy, exergy analyses of syngas production, combined biomass gasification with methane reformation, integrated biomass gasification plus catalytic reforming of syngas, determination of optimum temperature and steam to biomass ratio.

Because of extensive range of published literature, simulation-based study has been applied to design a hybrid biomass gasification for H_2 production. Such hybrid process provides an opportunity to convert solar energy to H_2 [20,21]. The proposed system has considered of two distinct section to balance the heat load: the injection of CSP-thermal energy to the gasifier; the addition of heat of combustion of a fraction of produced syngas to the reforming section. The heat from the WGS reaction has been recovered to reduce the energy requirement of the system. However, main technical challenges with gasification are endothermic gasification reactions, higher tar in syngas, lower H_2 contents in syngas.

The H_2 contents can be boosted by adding reforming or WGS reaction following by the gasification. The reforming reaction ($CH_4 + H_2O = CO + 3H_2$) is an equilibrium-limited reaction to convert CH_4 and CO_2 into CO and H_2 (Ren et al., 2019). The WGS reaction ($CO + H_2O = H_2 + CO_2$) is an equilibrium-limited and mildly exothermic reaction to convert CO through its chemical reaction with water into H_2 and CO_2. The WGS reaction is thermodynamically favored at a lower temperature, i.e.190-250 °C [22], whereas CO conversion is 99% at 200 °C [23].

The aim of this study is to investigate gasification at lower temperature, which will ease the injection of CSP-thermal energy as an external thermal energy input to the gasifier unit. The significance of present study is its focus on utilization of renewable energy resource, such as solar energy, to increase the H_2 production efficiency. In this study, the effect of temperature, steam to biomass (S/B) ratio and effects of CSP on H_2 production efficiency has been investigated in terms of yield of syngas, H_2/CO ratio, CO/CO_2 ratio, higher heating value of syngas, H_2 boost up by CSP and H_2 production efficiency in terms of kmol/MW$_{solar\ thermal\ energy}$. The best operating parameters for the proposed system have been determined and compared with the experimental results presented by other researchers to find out a sustainable pathway to produce H_2 from solar and solid waste resources via CSP-hybrid staged-gasification approach.

3.1.2: System Model with Process Flowsheet Description

The PW and MSW were selected as the feedstock to produce H_2. The Aspen Plus® software was used to develop a simple model and generate simulation results for the steam gasification. The results of proximate analysis, ultimate analysis and heating value of PW and MSW are presented in Table 3.1.2(i). The anticipated findings in this simulation study are in agreement with published experimental work done by other researchers [19,24,25].

A simple model was developed on the basis of Gibbs free energy minimization for gasification and reforming followed by equilibrium reactor for WGS reaction [18, 26, 27] as described in the Figure 3.1.2(i). The RYield reactor models were correspondingly used to obtain elemental yield of the solid waste to feed to the gasifier. This model is independent of gasifier design and represent maximum conversion efficiency [28].

Many researchers have applied some important operating parameters and basic

assumptions in order to develop a simple model, as shown in the Table 3.1.2(ii). Some assumptions may seem unrealistic. This is because of considering the theoretical conditions of the gasification process as an adiabatic process with zero heat loss at steady state. It is also assumed that all the components in the product gases behave as an ideal gas, and that residence time in the reactor is more than enough to reach equilibrium state.

In the RGibbs block, the gasification temperature was varied from 700 to 900 °C with an increment of 50 °C and pressure of 1 bar$_a$. In the reformer section, the reforming temperature was kept constant at 900 °C and 1 bar$_a$. While in REquil block, temperature was kept at 200 °C and 1 bar$_a$ for WGS reaction. 1000 kg/h feedstock was fed to the RYield reactor at 25 °C and 1 bar$_a$. The feedstock was decomposed in the RYield reactor into C, H, O, N, ash and water in a percentage composition corresponding to ultimate and proximate analysis (wet basis). The water was fed to the heat exchanger at 25 °C and 1 bar$_a$ to generate steam at 100 °C and 1 bar$_a$ sent to the RGibbs reactor as gasification agent. The steam flowrate fed to the gasifier was set to the minimum value, so that no solid carbon formed in the gasifier at different gasification temperatures.

The heat needed by the gasifier was supplied by CSP-solar-thermal energy. When no CSP was available, then a fraction of syngas was combusted to produce heat to meet the heat load of the gasifier. The produced syngas was cleaned in the cyclone separator to remove out the ash and cleaned syngas was further reformed to increase the H_2 content in the syngas. The reformed syngas was followed by WGS reaction to produce H_2. The CO in the produced syngas is about 1.0 kmol/h with maximum H_2. The detailed descriptions of the Aspen blocks used in the developed model are given in Table 3.1.2(iii).

3.1.3: Results and Discussion

The obtained yield of gH_2 per kg of wet biomass from gasification of PW and MSW was compared with literature as presented in Table 3.1.3(i). The optimum H_2 production at 800 °C is 98 gH_2 per kg of wet biomass, which is higher than what has been reported by other researchers. Similarly, the yield of H_2 from gasification of MSW at 800 °C is 140 gH_2 per kg of wet MSW, which is much better than as reported by experimental work.

The effect of temperature on HHV of syngas is shown in the Figure 3.1.3(i) (d). The gasifier performance can be evaluated by the HHV of syngas [24]:

$$HHV_{syngas} = 12.74*y_{H2} + 12.63*y_{CO} + 39.82*y_{CH4} \qquad (1)$$

Where, y_i indicates molar fraction of the main combustible components (H_2, CO and CH_4) on a dry basis. The model predicted that HHV of syngas always remains lower than measured value by experimentation. After steam gasification and reforming of syngas, the HHV has slightly increased from 10.80 to 12.50 MJ/Nm^3 at 700-900 °C in agreement with experimental data [47]. However, this trend is not reported by other authors [14]. The increase in HHV of syngas is because of a higher concentration of combustible components (H_2, CO and CH_4) with an increase in gasification temperature. The calorific value of H_2-enriched syngas is reduced with increasing temperature. In the literature, the higher heating value of produced syngas from solid waste gasification with different gasifying agents is presented in Table 3.1.3(ii).

3.1.3a: Effect of Temperature and Steam to Biomass Ratio

The gasification temperature is the key parameter to study solid waste gasification. The solid waste (PW and MSW) were gasified from 700 to 900 °C with the increment of 50 °C and pressure 1 bar$_a$. Figure 3.1.3a(i) (a-c) illustrates the effect of gasification temperature and S/B ratio on the yield of syngas and composition of syngas from gasification of PW with S/B ratio of 0.15 to 0.39 (w/w). The S/B ratio is calculated as steam flowrate (kg/h) fed to the gasifier divided by the biomass flowrate introduced into the gasifier in terms of kg/h. Figure 3.1.3a(i) (d) illustrates the effect of gasification temperature on the higher heating value (HHV) of syngas. Figure 3.1.3a(i) (e-f) describes the effect of adding CSP-thermal energy on H_2 productivity, H_2 boost up (in %) and H_2 production efficiency (kmol/MW$_{solar\ thermal\ heat}$) with respect to temperature in the gasifier.

The solid lines on the plot indicate the variation in syngas composition, H_2 productivity with temperature and S/B ratio for gasification without reforming and WGS reaction while the dotted lines indicate the gasification with reforming and dashed lines indicate the gasification with reforming and WGS reaction as predicted by the Aspen Plus® model. Herein, the H_2 productivity is calculated as amount of H_2 increased by adding CSP-thermal energy into the gasifier. H_2 boost up (in %) is calculated as the percent increase in H_2 with addition of solar-thermal energy to the

gasifier. While H_2 production efficiency is calculated as amount of H_2 produced with CSP divided by the heat load of the gasifier.

All the components (H_2, CO, CO_2, CH_4, H_2O) are classified as gas yield in the produced syngas. The trends for syngas composition by the model at higher temperature (800-900 °C) are similar to the experimental data while it is slightly different at lower temperature (700-750 °C). The possible reason for this could be the assumption of complete devolatilization of the solid waste or tar formation at low temperature.

Figure 3.1.3a(i) (a) shows that H_2 concentration slightly decreasing with temperature while CO concentration increasing with temperature. Similarly, the concentration of CO_2 decreasing at the higher temperature. In staged gasification, methane is reformed at high temperature to increase the concentration of H_2. After reforming of syngas, the concentration of CH_4 drops down to the minimum value. But the concentration of CO has increased with reforming of methane. The concentration of H_2 was maximized by the WGS reaction with addition of more water.

The molar ratio of H_2/CO and CO/CO_2 was analyzed with gasification temperature. Figure 3.1.3a(i) (b) shows the effect of gasification temperature on molar ratio of H_2/CO and CO/CO_2. After gasification alone, the CO/CO_2 ratio increases from 3.0 to 64.0 while the H_2/CO molar ratio varied from 1.50 to 1.0 could be useful for production of various chemicals [53-56]. Gasification with reforming and WGS reaction, the H_2/CO molar ratio can be increased up to 73.0 while the CO/CO_2 molar ratio can be decreased up to 0.03. The CO/CO_2 ratio increases with temperature because CO_2 content decreases with higher temperature. Adding reforming and WGS reaction can boost up the H_2 production.

3.1.3b: Effect of CSP on H_2 Productivity

By incorporating CSP-thermal energy to the gasifier, almost 30-35% of syngas can be saved [10,11]. It is clearly shown in the Figure 3.1.3b(i) (e-f) that when no CSP is available, then maximum amount of H_2 is about 49.0 kmol/h at 700-900 °C. When CSP is available, the produced amount of H_2 can reached to 73.0 kmol/h at same temperature range. It is clear that adding CSP thermal energy into the gasifier can increase the H_2 productivity up to 24.0 kmol/h. The proposed system shows that an opportunity to convert solar energy into H_2 fuel. It is noted that adding CSP into the system can boost H_2 production up to 50% at 700-900 °C. Results also showed that with

increasing temperature the H_2 productivity has slightly decreased from value of 13.30 to 11.70 kmol/h. The H_2 productivity with reforming and WGS reaction has slightly decreased from 24.90 to 23.0 at 700-900 °C. The maximum H_2 production efficiency with reforming and WGS reaction is 12.50 kmol/MW$_{th}$, which indicates that 750 °C is the best gasification temperature for this operation.

Similarly, Figure 3.1.3b(ii) (a-c) illustrates the effect of temperature and S/B ratio on the yield of syngas and composition of syngas from steam gasification of MSW with S/B ratio in the range of 0.62 to 0.90 (w/w). Figure 3.1.3b(ii) (d) illustrates the effect of temperature on higher heating value (HHV) of syngas. Figure 3.1.3b(ii) (e-f) describes the effect of adding CSP on H_2 productivity, H_2 boost up (in %) and H_2 production efficiency (kmol/MW$_{solar thermal energy}$) with respect to the temperature in the gasifier.

Figure 3.1.3b(ii) (a) shows that the H_2 concentration increases slightly with temperature, while the CO concentration increases sharply with an increase in the gasification temperature. Similarly, the concentration of CO_2 sharply decreasing at the higher temperature. Because the gasification is an endothermic process, the production of H_2 is influenced by reaction temperature. In staged gasification, the higher temperature will favor steam reforming of methane to increase the concentration of H_2. After reforming of syngas, the concentration of CH_4 drops down to the minimum value. Hence, the concentrations of CH_4 and H_2O decreases with reforming of syngas. The concentration of H_2 was maximized by WGS reaction with addition of more water to minimize the concentration of CO up to 1.00 kmol/h.

The molar ratio of H_2/CO and CO/CO_2 was analyzed with gasification temperature. Figure 3.1.3b(ii) (b) shows the effect of gasification temperature on molar ratio of H_2/CO and CO/CO_2. After gasification alone, the CO/CO_2 ratio increases from 3.5 to 79.6 while the H_2/CO molar ratio varied from 2.0 to 1.50 could be useful for production of various chemicals. Gasification with reforming and WGS reaction, the H_2/CO molar ratio can be increased up to 112.0 while the CO/CO_2 molar ratio can be decreased up to 0.02.

The effect of temperature on higher heating value (HHV) of syngas is shown in the Figure 3.1.3b(ii) (d). The model predicted HHV of the syngas always remains lower than measured value by experimentation. After steam gasification and reforming of syngas, the HHV has slightly

increased from 11.40 to 12.60 MJ/Nm^3 from 700-900 °C as predicted by experimental data. The increase in HHV of syngas is because of higher concentration of combustible components (H_2, CO and CH_4) with increasing gasification temperature.

Figure 3.1.3b(ii) (e-f) shows that when no CSP is available, the maximum amount of H_2 is about 70.0 kmol/h at 700-900 °C. When CSP is available, the produced amount of H_2 can reached to 112.0 kmol/h at same temperature range. It is convincing that adding CSP thermal energy into the gasifier can increase the H_2 productivity up to 42.0 kmol/h. It is noted that adding CSP into the system can boost H_2 production up to 61% from 700-900 °C. Results also showed that with increasing temperature the H_2 productivity has slightly decreased from value of 13.30 to 11.70 kmol/h. The H_2 productivity with reforming and WGSR has slightly decreased from 42.60 to 39.40 from 700-900 °C. The maximum H_2 production efficiency with reforming and WGS reaction is 13.20 kmol/MW$_{th}$, which indicates that 700 °C is the best gasification temperature for this operation.

The HHV of H_2 enriched syngas did not change significantly for both feedstock types at various temperatures. Many researchers have described that HHV of the produced syngas should be more than 4 MJ/Nm^3 so that it can be used in downstream applications such as combustion engines. Therefore, it can be concluded that both MSW and PW has an acceptable potential to produce clean fuel gas in order to be used in the existing combustion engines without any modification. As predicted that there is no significant increase in HHV of H_2 enriched syngas. Further detailed feasibility study including different blending ratio of PW and MSW should be considered in the future studies.

3.1.4: Conclusions

In conclusion, a new configuration of a CSP-hybrid solid waste gasification is proposed to produce clean and green H_2 from biomass and solar energy resources. This study showed that the H_2 production efficiency is about 13.0 kmol/MW$_{th}$. This number shows that a good potential to convert solar into H_2 fuel. It is noted that adding CSP into the system can boost H_2 production up to 50% for PW as a feedstock while 61% in case of MSW. From solid waste gasification of 100% MSW as compared to 100% PW, the concentration of H_2 increased from 73.0 to 112.0 kmol/h

while same trends for CO_2 and CH_4.

As the limitation of the available CSP technology, 700–800 °C might be the best temperature for the CSP-hybrid solid waste-gasification. It can be observed that the present model shows acceptable values of H_2 production as found in the experiments. It shows that both PW and MSW has an acceptable potential to produce H_2 in order to be used in combustion engines. As predicted that there is no significant increase in HHV of H_2 enriched syngas. Follow up studies can analyze other operating conditions, such as catalyst and residence time, to improve H_2 production efficiency. The results are promising, which makes the hybrid CSP steam gasification process a good option to convert renewables resources (biomass and solar) into H_2 fuel. This study provides a parametric analysis to transform biomass and solar into valuable and carbon-neutral alternative fuels. Steam gasification with WGS reaction is a promising technology to produce H_2 enriched syngas as an alternative fuel.

Tables

Table 3.1.2(i). Proximate analysis and ultimate analysis and higher heating value of pinewood sawdust and municipal solid waste (MSW) [24]

Analysis of feedstock		PW	MSW
Moisture content % by weight (wet basis)		11.70	07.50
Proximate analysis % by weight (dry basis)	Fixed carbon (FC)	12.80	24.83
	Volatile matter (VM)	75.10	51.28
	Ash	00.40	16.34
Ultimate analysis % by weight (dry basis)	Carbon (C)	50.70	60.17
	Hydrogen (H)	05.30	06.44
	Oxygen (O)*	42.20	15.22
	Nitrogen (N)	01.00	01.51
	Sulfur (S)	00.40	00.32
HHV (MJ/kg) dry basis		19.45	26.42
*Calculated by difference			

Table 3.1.2(ii). Some basic assumptions are presented in the literature to develop biomass gasification model in Aspen Plus$^{®}$

Operating parameters		Basic assumptions for thermodynamic equilibrium model	Reference
Ambient temperature (°C)	25	The gasifier is operated at steady state conditions, no change in parameters with time.	[14,24]
Ambient pressure (bar)	1	The gasification is an adiabatic process at atmospheric pressure and mixing of feed is perfect with gasification agent.	[29]
Gasification temperature range (°C)	600-900	The gasification is isothermal and isobaric process with no pressure and temperature gradient in the gasifier.	[30]
Gasification pressure (bar$_a$)	1	Pressure in the gasification system is considered to be constant at 1 bar$_a$. Zero heat loss.	[31]
Biomass feed rate (kg/h)	1000	The gasification reactions are very fast and achieve equilibrium state quickly and near to balance at higher temperature.	[32]
Exit temperature (°C)	25	Changes in exergies, kinetic and potential energies are very small as compared to temperature related properties, they can be neglected.	[33]
Steam temperature (°C)	130	All the components in the product gases behave as an ideal gas and residence time in the reactor is more enough to reach equilibrium state.	[34]
Steam to biomass ratio(S/B)		Flowrate was selected so no solid carbon is formed. Tar-free and solid carbon free syngas is produced from biomass.	[35]
		Ash and nitrogen are inert.	[36]
		All the components in the product gases leaves the gasifier at uniform temperature.	[37]
		The produced char is considered as pure carbon.	[38]

Table 3.1.2(iii). Description of Aspen Plus® blocks considered in the development of a simple model

Unit operation ID used in this study	Block ID in Aspen Plus®	Description	Process	Reference
RYield	RYield	Reaction stoichiometry and kinetics are unknown, but elements distribution yield is known then this type of reactor is used. The function is to decompose the biomass into its elements according to proximate analysis.	Decomposition	[27,39]
GASIFIER, REFORMER and DECOMB	RGibbs	Based on Gibbs free energy phase equilibrium model. It does not follow any specific chemical reaction because reaction stoichiometry is unknown. Gasification temperature and pressure is known. It considers feed composition and operating parameters. Phase equilibrium and chemical equilibrium based on Gibbs free energy.	Gasification, reforming of syngas and combustion of syngas	[19,40,41]
BASEP	Sep	It separates ash and solid carbon from the syngas. It considers ideal separation of gas and solid.	Separation	[42]
REQUILIB	REquil	Equilibrium reactor. It	Water gas shift	[43-45]

		considers the known reaction stoichiometry to reach rigorous equilibrium state. The equilibrium model helps to predict mass balance based on stoichiometric approach for the reactions, which are very fast and reversible in nature.	reaction	
WATRHEX1, WATRHEX2, SYNGCOLR and SYNGCOL1	Heater	It is used to exchange heat between cold and hot streams.	Heat recovery	[46]

Table 3.1.3(i). H_2 yield per kg of biomass on wet basis

Feedstock	gH_2/kg biomass	Reference
Pinewood sawdust	80	[14,25]
Municipal solid waste	32	[20,24]
Pinewood sawdust without CSP	98	This study
Municipal solid waste without CSP	140	This study
Pinewood sawdust with CSP	146	This study
Municipal solid waste with CSP	224	This study

Table 3.1.3(ii). Higher heating value of syngas produced from solid waste gasification with different gasifying agents

Feedstock	Gasifying agent	HHV (MJ/Nm^3)	Reference
Pinewood sawdust, Eucalyptus wood, Oak wood	Steam	10-16	[48]
Pinewood	Oxygen and steam	9-11	[49]
Pinewood	Steam	14	[50]

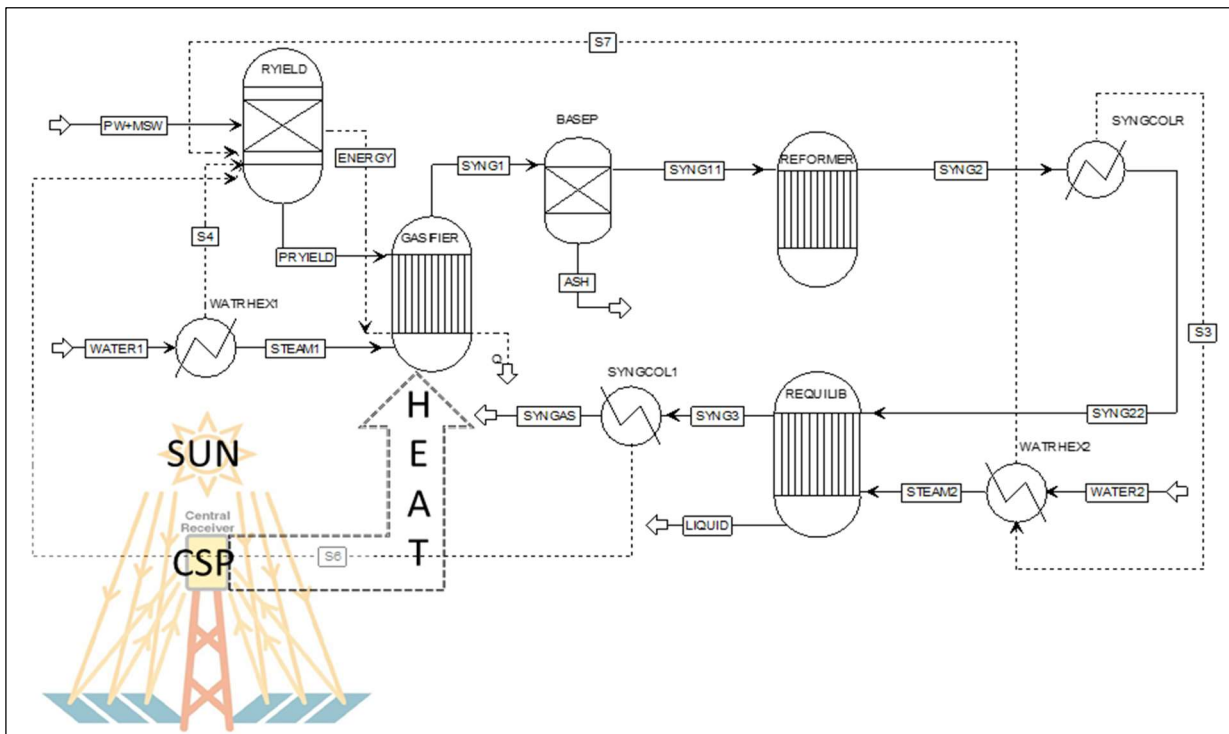| Woodchips	Steam	4-5	[51]
Cypress mulch	Air	4-5	[52]
Municipal solid waste	Air	9-13	[20]
Combined municipal solid waste and biomass	Steam	6-10	[24]
Pinewood sawdust	Steam	11-13	This study
Municipal solid waste	Steam	12-13	This study

Figures

Figure 3.1(i): Hydrogen enriched syngas production from solid waste and concentrated solar power is established in Aspen Plus®
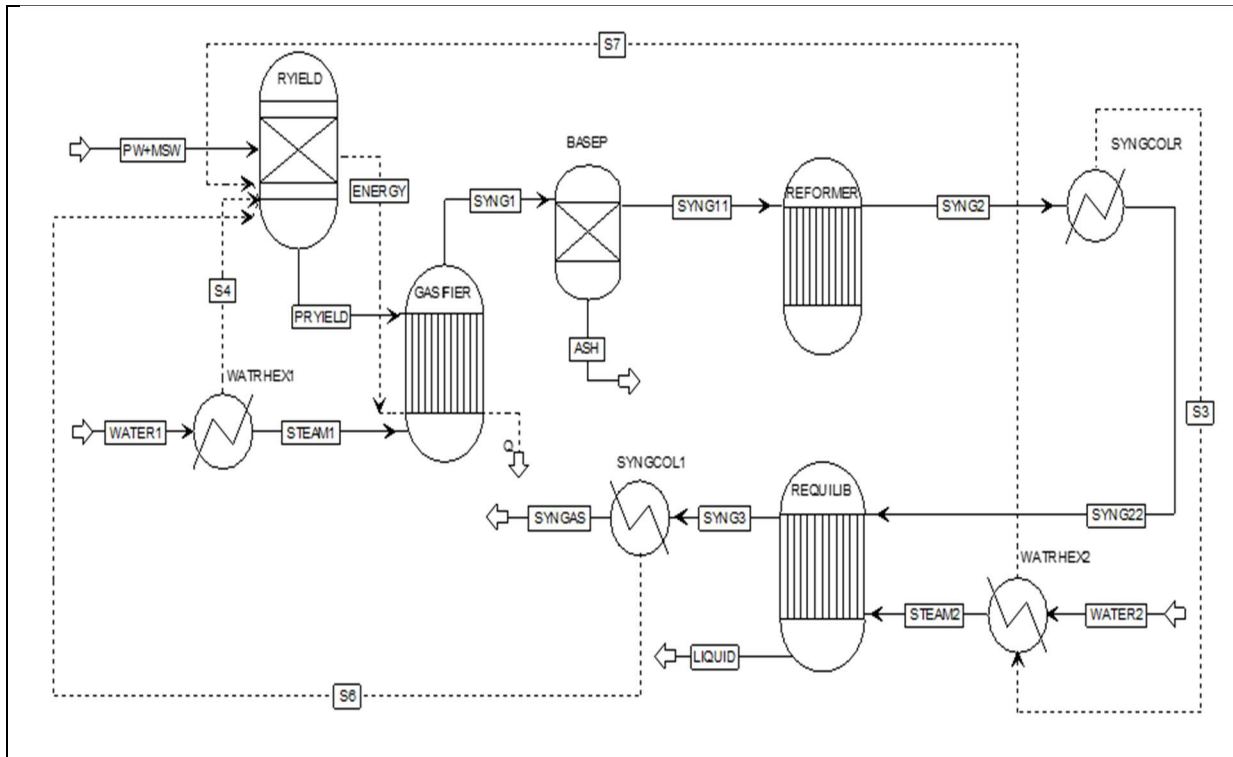
Figure 3.1.2(i): Process flowsheet for the staged-gasification of pinewood sawdust or municipal solid waste
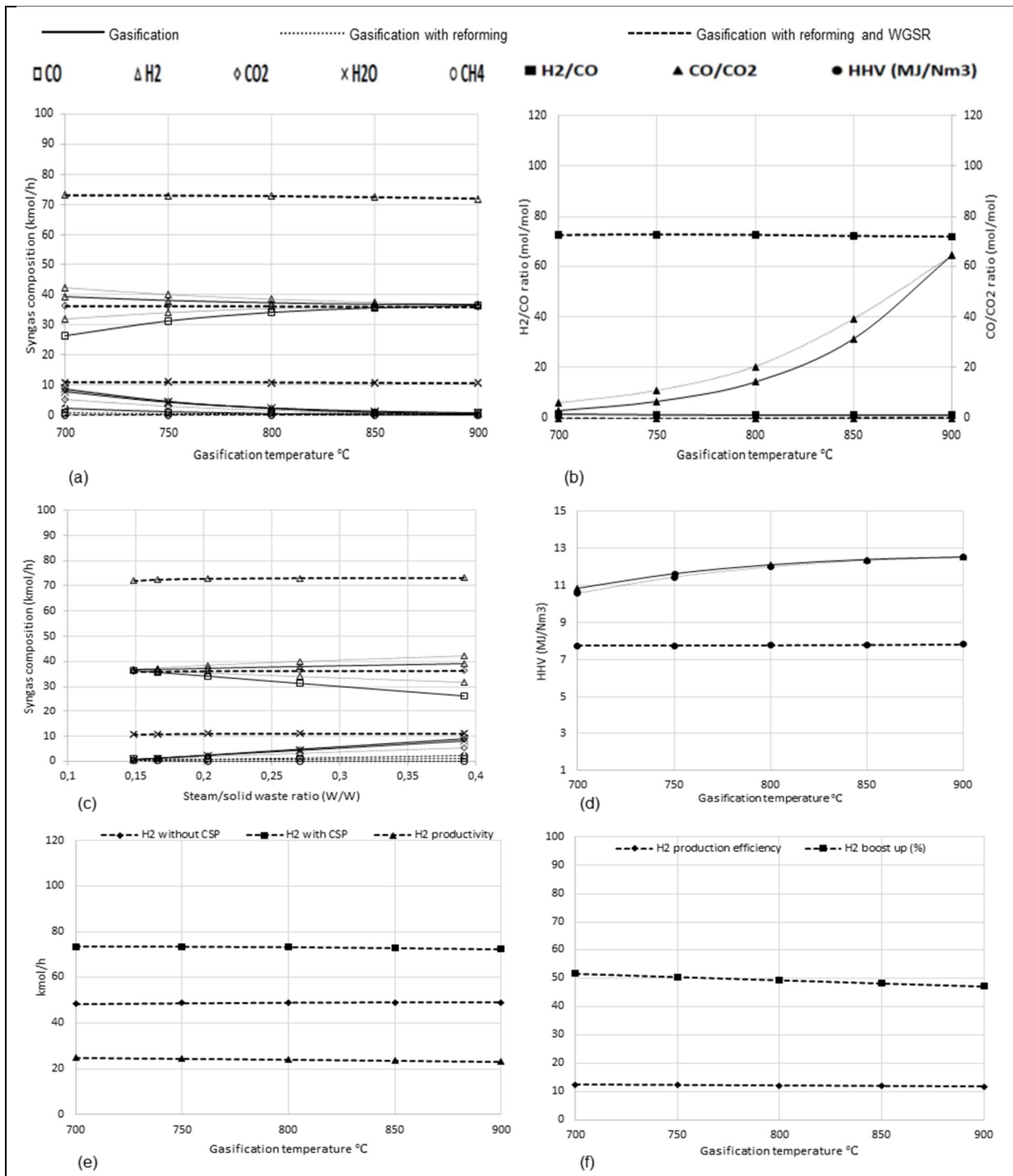
Figure 3.1.3b(i): Simulation results from steam gasification of PW, showing the effect of: (a) temperature on the yield of syngas and composition of syngas; (b) temperature on the H_2/CO molar ratio and CO/CO_2 molar ratio; (c) S/B ratio on the yield of syngas and composition of syngas; (d) temperature on the HHV of syngas; (e) temperature on the yield of H_2 without CSP, H_2 with CSP and H_2 productivity; (f) temperature on H_2 production efficiency and H_2 boost up.
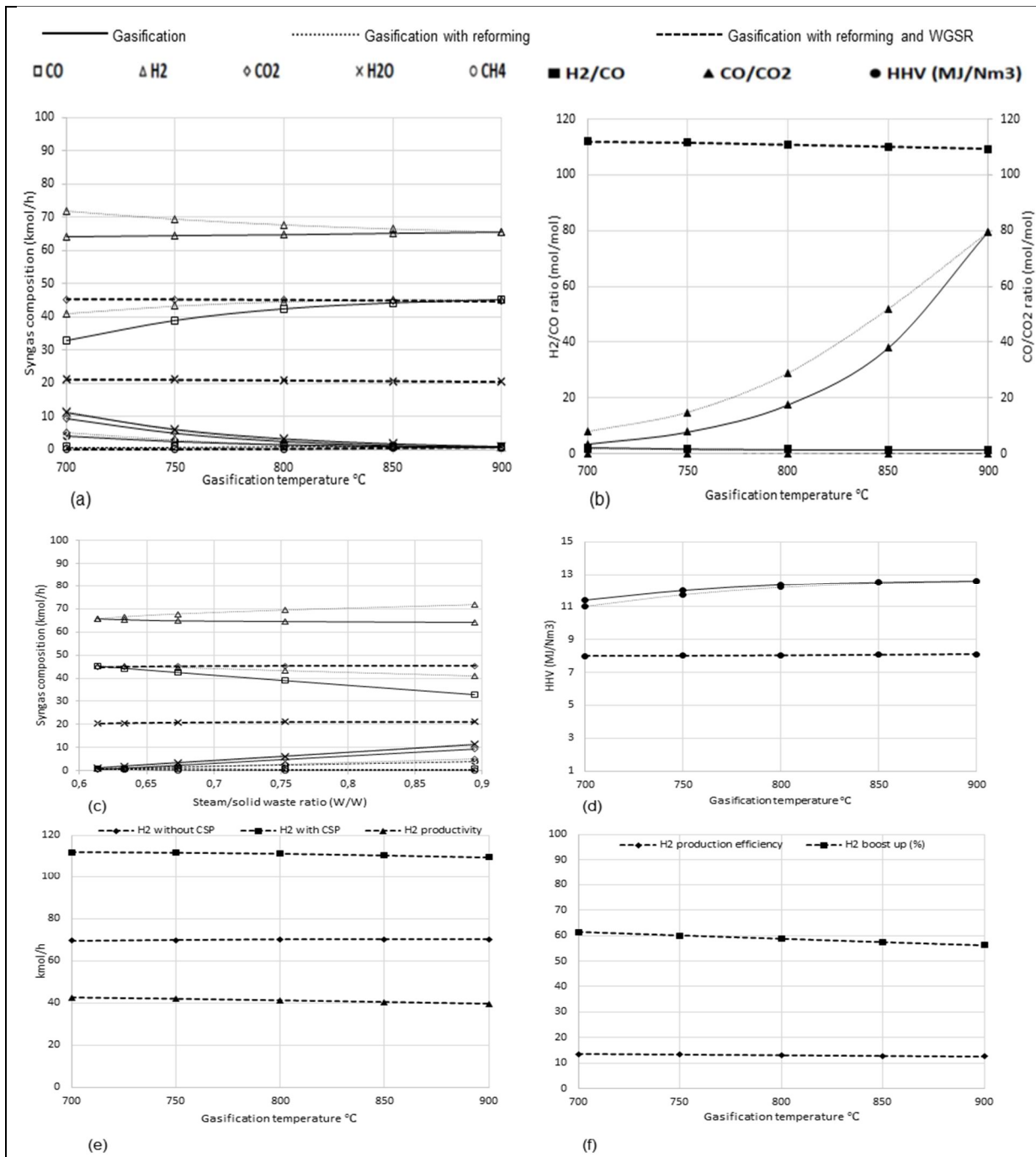
Fig. 3.1.3b(ii): Model results from steam gasification of municipal solid waste. (a) The effect of temperature on the yield of syngas and composition of syngas. (b) The effect of temperature on the H_2/CO molar ratio and CO/CO_2 molar ratio. (c) The effect of S/B ratio on the yield of syngas and composition of syngas. (d) The effect of temperature on the HHV of syngas. (e) The effect of temperature on the yield of H_2 without CSP, H_2 with CSP and H_2 productivity. (f) The effect of temperature on H_2 production efficiency and H_2 boost up.

References

[1]   Sharma, K., 2019. Carbohydrate-to-hydrogen production technologies: A mini-review. Renew. Sustain. Energy Rev. 105, 138–143. https://doi.org/10.1016/j.rser.2019.01.054

[2]   Gu, H., Tang, Y., Yao, J., Chen, F., 2019. Study on biomass gasification under various operating conditions. J. Energy Inst. 92, 1329–1336. https://doi.org/10.1016/j.joei.2018.10.002

[3]   Zeng, X., Dong, Y., Wang, F., Xu, P., Shao, R., Dong, P., Xu, G., Dong, L., 2016. Fluidized bed two-stage gasification process for clean fuel gas production from herb residue: Fundamentals and demonstration. Energy and Fuels 30, 7277–7283. https://doi.org/10.1021/acs.energyfuels.6b00765

[4]   Meng, F., Ma, Q., Wang, H., Liu, Y., Wang, D., 2019. Effect of gasifying agents on sawdust gasification in a novel pilot scale bubbling fluidized bed system. Fuel 249, 112–118. https://doi.org/10.1016/j.fuel.2019.03.107

[5]   Sadhwani, N., Adhikari, S., Eden, M.R., Li, P., 2018. Aspen Plus simulation to predict steady state performance of biomass-CO2 gasification in a fluidized bed gasifier. Biofuels, Bioprod. Biorefining 12, 379–389. https://doi.org/10.1002/bbb.1846

[6]   Shen, Y., Li, X., Yao, Z., Cui, X., Wang, C.H., 2019. CO2 gasification of woody biomass: Experimental study from a lab-scale reactor to a small-scale autothermal gasifier. Energy 170, 497–506. https://doi.org/10.1016/j.energy.2018.12.176

[7]   AlNouss, A., McKay, G., Al-Ansari, T., 2020a. A comparison of steam and oxygen fed biomass gasification through a techno-economic-environmental study. Energy Convers. Manag. 208, 112612. https://doi.org/10.1016/j.enconman.2020.112612

[8]   Singh Siwal, S., Zhang, Q., Sun, C., Thakur, S., Kumar Gupta, V., Kumar Thakur, V., 2020. Energy production from steam gasification processes and parameters that contemplate in biomass gasifier – A review. Bioresour. Technol. https://doi.org/10.1016/j.biortech.2019.122481

[9]   Hu, Y., Cheng, Q., Wang, Y., Guo, P., Wang, Z., Liu, H., Akbari, A., 2020. Investigation of biomass gasification potential in syngas production: Characteristics of dried biomass gasification using steam as the gasification agent. Energy and Fuels 34, 1033–1040. https://doi.org/10.1021/acs.energyfuels.9b02701

[10]   Ansari, S.H., Ahmed, A., Razzaq, A., Hildebrandt, D., Liu, X., Park, Y.K., 2020. Incorporation of solar-thermal energy into a gasification process to co-produce bio-fertilizer and power. Environ. Pollut. 266, 115103. https://doi.org/10.1016/j.envpol.2020.115103

[11]   Boujjat, H., Yuki Junior, G.M., Rodat, S., Abanades, S., 2020. Dynamic simulation and control of solar biomass gasification for hydrogen-rich syngas production during allothermal and hybrid solar/autothermal operation. Int. J. Hydrogen Energy 45, 25827–25837. https://doi.org/10.1016/j.ijhydene.2020.01.072

[12]   Milani, R., Szklo, A., Hoffmann, B.S., 2017. Hybridization of concentrated solar power with biomass

gasification in Brazil's semiarid region. Energy Convers. Manag. 143, 522–537. https://doi.org/10.1016/j.enconman.2017.04.015

[13] Al-Zareer, M., Dincer, I., Rosen, M.A., 2018. Influence of selected gasification parameters on syngas composition from biomass gasification. J. Energy Resour. Technol. Trans. ASME 140. https://doi.org/10.1115/1.4039601

[14] Shayan, E., Zare, V., Mirzaee, I., 2018. Hydrogen production from biomass gasification: A theoretical comparison of using different gasification agents. Energy Convers. Manag. 159, 30–41. https://doi.org/10.1016/J.ENCONMAN.2017.12.096

[15] Tian, T., Li, Q., He, R., Tan, Z., Zhang, Y., 2017. Effects of biochemical composition on hydrogen production by biomass gasification. Int. J. Hydrogen Energy 42, 19723–19732. https://doi.org/10.1016/j.ijhydene.2017.06.174

[16] Acar, M.C., Böke, Y.E., 2019. Simulation of biomass gasification in a BFBG using chemical equilibrium model and restricted chemical equilibrium method. Biomass and Bioenergy 125, 131–138. https://doi.org/10.1016/j.biombioe.2019.04.012

[17] Li, Q., Song, G., Xiao, J., Sun, T., Yang, K., 2019. Exergy analysis of biomass staged-gasification for hydrogen-rich syngas. Int. J. Hydrogen Energy 44, 2569–2579. https://doi.org/10.1016/J.IJHYDENE.2018.11.227

[18] Tavares, R., Monteiro, E., Tabet, F., Rouboa, A., 2020. Numerical investigation of optimum operating conditions for syngas and hydrogen production from biomass gasification using Aspen Plus. Renew. Energy 146, 1309–1314. https://doi.org/10.1016/j.renene.2019.07.051

[19] Terrell, E., Theegala, C.S., 2019. Thermodynamic simulation of syngas production through combined biomass gasification and methane reformation. Sustain. Energy Fuels 3, 1562–1572. https://doi.org/10.1039/c8se00638e

[20] Chen, G., Jamro, I.A., Samo, S.R., Wenga, T., Baloch, H.A., Yan, B., Ma, W., 2020. Hydrogen-rich syngas production from municipal solid waste gasification through the application of central composite design: An optimization study. Int. J. Hydrogen Energy 45, 33260–33273. https://doi.org/10.1016/j.ijhydene.2020.09.118

[21] Zhao, L., Qi, Y., Song, L., Ning, S., Ouyang, S., Xu, H., Ye, J., 2019. Solar-driven water–gas shift reaction over CuOx/Al2O3 with 1.1 % of light-to-energy storage. Angew. Chemie Int. Ed. 58, 7708–7712. https://doi.org/10.1002/anie.201902324

[22] Zhai, Y., Pierre, D., Si, R., Deng, W., Ferrin, P., Nilekar, A.U., Peng, G., Herron, J.A., Bell, D.C., Saltsburg, H., Mavrikakis, M., Flytzani-Stephanopoulos, M., 2010. Alkali-stabilized Pt-OHx species catalyze low-temperature water-gas shift reactions. Science (80). 329, 1633–1636. https://doi.org/10.1126/science.1192449

[23] Yao, S., Zhang, X., Zhou, W., Gao, R., Xu, W., Ye, Y., Lin, L., Wen, X., Liu, P., Chen, B., Crumlin, E., Guo, J., Zuo, Z., Li, W., Xie, J., Lu, L., Kiely, C.J., Gu, L., Shi, C., Rodriguez, J.A., Ma, D., 2017. Atomic-layered Au clusters on α-MoC as catalysts for the low-temperature water-gas shift reaction. Science (80). 357, 389–393. https://doi.org/10.1126/science.aah4321

[24] Cao, Y., Fu, L., Mofrad, A., 2019. Combined-gasification of biomass and municipal solid waste in a fluidized bed gasifier. J. Energy Inst. 92, 1683–1688. https://doi.org/10.1016/j.joei.2019.01.006

[25] Gao, N., Li, A., Quan, C., 2009. A novel reforming method for hydrogen production from biomass steam gasification. Bioresour. Technol. 100, 4271–4277. https://doi.org/10.1016/j.biortech.2009.03.045

[26] Cohce, M.K., Dincer, I., Rosen, M.A., 2010. Thermodynamic analysis of hydrogen production from biomass gasification. Int. J. Hydrogen Energy 35, 4970–4980. https://doi.org/10.1016/j.ijhydene.2009.08.066

[27] Han, J., Liang, Y., Hu, J., Qin, L., Street, J., Lu, Y., Yu, F., 2017. Modeling downdraft biomass gasification process by restricting chemical reaction equilibrium with Aspen Plus. Energy Convers. Manag. 153, 641–648. https://doi.org/10.1016/j.enconman.2017.10.030

[28] Ahmed, T.Y., Ahmad, M.M., Yusup, S., Inayat, A., Khan, Z., 2012. Mathematical and computational approaches for design of biomass gasification for hydrogen production: A review. Renew. Sustain. Energy Rev. https://doi.org/10.1016/j.rser.2012.01.035

[29] Aydin, E.S., Yucel, O., Sadikoglu, H., 2017. Development of a semi-empirical equilibrium model for downdraft gasification systems. Energy 130, 86–98. https://doi.org/10.1016/j.energy.2017.04.132

[30] Qi, T., Lei, T., Yan, B., Chen, G., Li, Z., Fatehi, H., Wang, Z., Bai, X.-S., 2019. Biomass steam gasification in bubbling fluidized bed for higher-H2 syngas: CFD simulation with coarse grain model. Int. J. Hydrogen Energy 44, 6448–6460. https://doi.org/10.1016/J.IJHYDENE.2019.01.146

[31] Lan, W., Chen, G., Zhu, X., Wang, X., Liu, C., Xu, B., 2018. Biomass gasification-gas turbine combustion for power generation system model based on Aspen Plus. Sci. Total Environ. 628–629, 1278–1286. https://doi.org/10.1016/J.SCITOTENV.2018.02.159

[32] Bader, A., Hartwich, M., Richter, A., Meyer, B., Salgansky, E.A., Zaichenko, A.Y., Podlesniy, D.N., Salganskaya, M.V., Tsvetkov, M.V., 2017. Numerical and experimental study of heavy oil gasification in an entrained-flow reactor and the impact of the burner concept. Fuel Process. Technol. 169, 491–496. https://doi.org/10.1016/j.fuproc.2017.09.003

[33] Ramzan, N., Athar, M., Begum, S., Ahmad, S.W., Naveed, S., 2015. Simulation of circulating fluidized bed gasification for characteristic study of Pakistani coal 17, 66–78. https://doi.org/10.1515/pjct-2015-0011

[34] Silva, I.P., Lima, R.M.A., Silva, G.F., Ruzene, D.S., Silva, D.P., 2019. Thermodynamic equilibrium model based on stoichiometric method for biomass gasification: A review of model modifications. Renew. Sustain.

Energy Rev. https://doi.org/10.1016/j.rser.2019.109305

[35]   Hejazi, B., Grace, J.R., 2020. Simulation of tar-free biomass syngas enhancement in a calcium looping operation using Aspen Plus built-in fluidized bed model. Int. J. Greenh. Gas Control 99, 103096. https://doi.org/10.1016/j.ijggc.2020.103096

[36]   Beheshti, S.M., Ghassemi, H., Shahsavan-Markadeh, R., 2015. Process simulation of biomass gasification in a bubbling fluidized bed reactor. Energy Convers. Manag. 94, 345–352. https://doi.org/10.1016/J.ENCONMAN.2015.01.060

[37]   Gagliano, A., Nocera, F., Patania, F., Bruno, M., Castaldo, D.G., 2016. A robust numerical model for characterizing the syngas composition in a downdraft gasification process. Comptes Rendus Chim. 19, 441–449. https://doi.org/10.1016/j.crci.2015.09.019

[38]   AlNouss, A., Parthasarathy, P., Shahbaz, M., Al-Ansari, T., Mackey, H., McKay, G., 2020b. Techno-economic and sensitivity analysis of coconut coir pith-biomass gasification using Aspen Plus. Appl. Energy 261, 114350. https://doi.org/10.1016/j.apenergy.2019.114350

[39]   Nikoo, M.B., Mahinpey, N., 2008. Simulation of biomass gasification in fluidized bed reactor using Aspen Plus. Biomass and Bioenergy 32, 1245–1254. https://doi.org/10.1016/J.BIOMBIOE.2008.02.020

[40]   Huang, F., Jin, S., 2019. Investigation of biomass (pine wood) gasification: Experiments and Aspen Plus simulation. Energy Sci. Eng. 1–10. https://doi.org/10.1002/ese3.338

[41]   Moshi, R.E., Jande, Y.A.C., Kivevele, T.T., Kim, W.S., 2020. Simulation and performance analysis of municipal solid waste gasification in a novel hybrid fixed bed gasifier using Aspen Plus. Energy Sources, Part A Recover. Util. Environ. Eff. 1–13. https://doi.org/10.1080/15567036.2020.1806404

[42]   Safarianbana, S., Unnthorsson, R., Richter, C., 2019. Development of a new stoichiometric equilibrium-based model for wood chips and mixed paper wastes gasification by Aspen Plus, in: ASME International Mechanical Engineering Congress and Exposition, Proceedings (IMECE). American Society of Mechanical Engineers (ASME). https://doi.org/10.1115/IMECE2019-10586

[43]   Abdelouahed, L., Authier, O., Mauviel, G., Corriou, J.P., Verdier, G., Dufour, A., 2012. Detailed Modeling of Biomass Gasification in Dual Fluidized Bed Reactors under Aspen Plus. Energy & Fuels 26, 3840–3855. https://doi.org/10.1021/ef300411k

[44]   Ishaq, H., Dincer, I., 2020. A new energy system based on biomass gasification for hydrogen and power production. Energy Reports 6, 771–781. https://doi.org/10.1016/j.egyr.2020.02.019

[45]   Pala, L.P.R., Wang, Q., Kolb, G., Hessel, V., 2017. Steam gasification of biomass with subsequent syngas adjustment using shift reaction for syngas production: An Aspen Plus model. Renew. Energy 101, 484–492. https://doi.org/10.1016/J.RENENE.2016.08.069

[46]   Zheng, H., Kaliyan, N., Morey, R.V., 2013. Aspen Plus simulation of biomass integrated gasification combined cycle systems at corn ethanol plants. Biomass and Bioenergy 56, 197–210. https://doi.org/10.1016/J.BIOMBIOE.2013.04.032

[47]   Hernández, J.J., Aranda, G., Barba, J., Mendoza, J.M., 2012. Effect of steam content in the air-steam flow on biomass entrained flow gasification. Fuel Process. Technol. 99, 43–55. https://doi.org/10.1016/j.fuproc.2012.01.030

[48]   Franco, C., Pinto, F., Gulyurtlu, I., Cabrita, I., 2003. The study of reactions influencing the biomass steam gasification process. Fuel 82, 835–842. https://doi.org/10.1016/S0016-2361(02)00313-7

[49]   Lv, P., Yuan, Z., Ma, L., Wu, C., Chen, Y., Zhu, J., 2007. Hydrogen-rich gas production from biomass air and oxygen/steam gasification in a downdraft gasifier. Renew. Energy 32, 2173–2185. https://doi.org/10.1016/j.renene.2006.11.010

[50]   Xiao, X., Meng, X., Le, D.D., Takarada, T., 2011. Two-stage steam gasification of waste biomass in fluidized bed at low temperature: Parametric investigations and performance optimization. Bioresour. Technol. 102, 1975–1981. https://doi.org/10.1016/j.biortech.2010.09.016

[51]   Wang, Y., Yoshikawa, K., Namioka, T., Hashimoto, Y., 2007. Performance optimization of two-staged gasification system for woody biomass. Fuel Process. Technol. 88, 243–250. https://doi.org/10.1016/j.fuproc.2006.10.002

[52]   Akudo, C.O., 2014. Quantification of Tars, Particulates, and Higher Heating Values in Gases Produced from a Biomass Gasifier | Akudo | BioResources. Bioresour. Technol. 9, 5627.5635

[53]   Zeng, J., Xiao, R., Zeng, D., Zhao, Y., Zhang, H., Shen, D., 2016. High H2/CO ratio syngas production from chemical looping gasification of sawdust in a dual fluidized bed gasifier. Energy and Fuels 30, 1764–1770. https://doi.org/10.1021/acs.energyfuels.5b02204

[54]   Ren, J., Liu, Y.L., Zhao, X.Y., Cao, J.P., 2019. Biomass thermochemical conversion: A review on tar elimination from biomass catalytic gasification. J. Energy Inst. https://doi.org/10.1016/j.joei.2019.10.003

[55]   Sarafraz, M.M., Safaei, M.R., Jafarian, M., Goodarzi, M., Arjomandi, M., 2019. High quality syngas production with supercritical biomass gasification integrated with a water-gas shift reactor. Energies 12, 2591–2610. https://doi.org/10.3390/en12132591

[56]   Turn, S. 1998. An experimental investigation of hydrogen production from biomass gasification. Int. J. Hydrogen. Energy August 1998, Volume 23, Pages 641-648.

Chapter 4: Power Generation by Applying Different Agents for Biomass Gasification

4.1: Power Generation by Applying Different Agents for Biomass Gasification

The research investigates the possibility of producing a methane (CH_4) rich stream from syngas via a methanation reactor for power generation in a normal gas turbine. Effects of four gasification agents; water ($H_2O_{(g)}$), carbon dioxide (CO_2), air and oxygen (O_2) were considered to produce syngas from biomass ($CH_{1.496}O_{0.82}$) gasification. Simulation of gasification and the methanation process were developed using Aspen Plus® software for a target of 40% CH_4 mole concentration, which is the minimum level required for a gas turbine. The heat for gasification was supplied through heat integration from the energy generated during methanation resulting in no or less external energy supplied for gasification. The results showed that CH_4 concentration increased with a decrease in the quantity of gasification agent used at the cost of an increase in heat demand to the gasifier. Increasing temperature resulted in increase in CH_4 concentration but lower net power generation after methanation for all gasification agents. Using air as a gasification agent resulted in a CH_4 concentration of 42%, at 1000 °C. This is above the target 40% required for combustion in a normal gas turbine despite the high nitrogen (N_2) composition present in the feed.

Cases in which steam and no gasification agent was used recorded the highest CH_4 concentration (47%) at 900 °C. The use of steam as gasification agent resulted in the highest molar amount of CH_4 produced but a large amount of energy was required to heat the liquid water to making steam. For gasification at 800-900 °C without methanation, the maximum power generated is about 1-1.2 kWe/kg of wheat straw; with methanation, it is about 1.2-1.3 kWe/kg. Although energy efficiency is same but heat of enthalpy from exothermic methanation can be integrated with the gasification system. The overall simulations show that biomass can be used to produce the minimum CH_4 concentration required to generate power in a normal gas turbine. Concentrated solar power (CSP) applied to the gasification process will help to boost the CH_4 produced after methanation by about 20% for all systems.

4.1.1: Introduction

Natural gas can be obtained with varying composition of CH_4 and sometimes constituting inert gases such as N_2 and CO_2. Therefore, the focus has turned to manufacturing gas turbines that are flexible enough to deal with different gas composition without affecting the combustion process and with minimal or no hardware change to the turbines. Gas turbines with fuel flexibility are essentially driven by the discovery of new gas options from biomass with large variations in gas composition (including diluents and other hydrocarbons) [1]. Hence, the need to combust such fuels with variable composition without additional treatment to limit fuel cost [2]. Improvements have been made to combustion turbines to ensure maximum flexibility while maintaining extremely low emissions.

The high price of natural gas has also focused attention on the desirability of replacing it with combustible gas derived from biomass in gas turbine systems. Typical system analysis indicates that Integrated Gasification Combined Cycle (IGCC) plants have some potential to fulfil the requirement for a zero–emissions power [2]. Although modern, state-of-the art and costly gas turbines are commercially available to combust natural gas with higher H_2 content, additional development work is necessary to design more efficient turbines ready for using natural gas with higher CO_2 content. Generally, CO_2 emissions appear to be reduced by adding H_2 to natural gas. However, it is expensive to get the H_2 hence, there is an increase in research on converting waste biomass materials to CH_4 gas. Biomass is a renewable source and is considered one of the most important resources also to replace fossil fuels without increasing greenhouse effects [3]. Gasification is considered an attractive way to convert biomass into synthesis gas.

A syngas turbine is generally expensive for power generation when compared to normal gas turbines. Normal gas turbines utilise natural gas as a primary fuel and emits substantially less CO_2 per kilowatt-hour (kWh) generated than any other fossil technology in commercial use. Therefore, a normal gas turbine is preferred for biomass to power technology processes. The content of CH_4 plays a vital role because CH_4 enriched syngas has higher heating value and produce high combustion velocity in the combustion engine [4,5]. A CH_4 rich gas stream can be achieved by adding a methanation unit straight after gasification. However, the composition of produced syngas is dependent upon gasifier's technology and biomass source used. The

composition of syngas will affect the combustion performance and energy efficiency. Research shows that a minimum of 25% CH_4 content is required in order to use a normal gas turbine, but in reality, a minimum of 40% CH_4 content gives efficient power generation, hence that is the target in this research application. Most medium lower heating values (LHV) gaseous fuel contain less than 60% CH_4 with a LHV of between 11.2-30.0 MJ/Nm^3 [6]. Most biomass contains 60% volatile compounds compared to coal (which contains about 40%), and this makes biomass more reactive than coal [7]. CH_4 is chosen in preference to H_2 as a product for the present simulations because CH_4 is easier to handle and store, and it requires less complicated modifications of engine design.

Biomass gasification is an endothermic process. Conventionally, energy needed for gasification is provided by partial combustion of the biomass in the gasification unit, or external combustion of a fraction of syngas produced by gasification. This heat can also be provided by concentrated solar power (CSP). CS-assisted biomass gasification with IGCC process is considered as one of the emerging sustainable processes [8,9]. However, at the current state of technology, the viability of the CSP-hybrid biomass gasification process is yet to be established. Using CSP for biomass gasification serves the purposes of an external, renewable and unlimited energy source, and it can improve the utilization efficiency of the biomass.

In order to avoid complexities in development of a simple model for CSP-assisted biomass gasification, Aspen Plus® process simulator is extensively used in the literature [10,11]. This process simulator is based on sequential modelling with some input variables and equation-oriented simulation program. It is based on mass, energy, momentum balances and phase equilibrium data to simulate biomass gasification process [11-16]. Some researchers have modelled CSP-assisted biomass gasification to produce H_2 or CH_4 rich syngas and electric power [17-19]. Ansari et. al [20] have investigated Aspen Plus® simulation to boost power production in a gas turbine combustor by using CSP to the biomass gasification process. They concluded that there is a significant increase in overall energy efficiency up to 58% by using CSP. However, this research intends to take advantage of heat integration and use energy produced during methanation for gasification. This can reduce the external energy supplied to the gasifier or reduce the use of CSP when CH_4 is combusted to make power as compared to syngas.

It is concluded that simulation works on CSP-assisted biomass gasification and IGCC combined cycle to produce power from biomass derived methane rich syngas. The recent trend is to predict the performance of gasification system with the inclusion of sub-model for CSP energy to increase energy efficiency of the overall process. However, the objective of this simulation is to develop a simple model using Aspen Plus$^{®}$ to conclude the effects of four gasification agents; water ($H_2O_{(g)}$), carbon dioxide (CO_2), air and oxygen (O_2) on methane productivity from biomass gasification with CSP and without CSP. According to one eminent researcher [Krumpelt et al., 2002], production of CH_4 requires CO and H_2 in the presence of a catalyst (usually at an H_2/CO ratio of 3), and a water gas shift (WGS) reaction is necessary to achieve this. Reduced nickel can be used to catalyse the formation of CH_4 in gasification of biomass [21].

The aim of this research is to convert biomass into syngas, and thereafter convert the syngas into a target of 40% CH_4 in a methanation reactor for power generation via a normal gas turbine. The notion is to try and use a cheaper gas combustion engine system to generate energy for small scale purposes as well as reduce energy input to the overall system through heat integration. The research investigated possible oxidising agents (air, CO_2, O_2 and $H_2O_{(g)}$) for gasification of wheat straw. The overall energy efficiency for the whole process was investigated based on the various gasification agent feeds.

4.1.2: Process Modelling and Simulation

An integrated system model in Aspen Plus$^{®}$ was developed for biomass gasification with $H_2O_{(g)}$, air, O_2 and CO_2 being used as the gasifying agent and a special case in which no gasifying agent is applied. This was followed by methanation reaction to produce CH_4 enriched syngas. The developed model was studied to predict CH_4 production when combustion of part of the syngas produced is introduced to balance the heat load of the gasifier and when CSP was applied. The Aspen Plus$^{®}$ model with a process flowsheet is shown in Figure 4.1.2(i) and Figure 4.1.2(ii). This was used to simulate the potential of biomass gasification and subsequent syngas adjustment using methanation equilibrium reactor.

The process flowsheet was developed with following steps: specification of components (mixed, conventional and non-conventional), units set, selection of proper property method and selection of unit operation, material and energy streams. Each feed stream is specified with

temperature, pressure, composition and flowrate. The unit operation is specified with thermodynamic conditions. The model was based on RGibbs reactor with Gibbs free energy minimization approach. Biomass feed rate was 1000 kg/h and the possible injection of CSP was simulated as equivalence to the heat load of a gasifier. Temperature flow rate of H_2O as steam, air, O_2, CO_2 as a gasifying agent and no gasifying agent was simulated to optimize the overall process at 1 bar$_a$.

Flowrate of the gasifying agent was selected on the basis that no solid carbon (C) is formed in the product stream. Some assumptions are, steady state and isothermal process, temperature and pressure are uniform in the RGibbs, no heat and pressure loss and no tar formation. The ash was separated from the produced gas in the cyclone separator while the subsequent syngas adjustment was done in the REquil reactor (methanation reactor). The equilibrium model helps to predict mass balance based on stoichiometric approach for the reactions, which are very fast and reversible in nature. The restricted equilibrium is defined with specific chemical reaction and zero temperature approach. The REquil reactor calculates chemical equilibrium constant at specified temperature thereby giving the equilibrium gas composition. Equilibrium models were applied because the reactions are assumed to be fast enough not to consider kinetics.

The equilibrium reactor has considered both WGS reaction and methanation reaction. The WGS reaction ($CO + H_2O \leftrightarrow H_2 + CO_2$) is an equilibrium-limited and mildly exothermic reaction to convert CO through its chemical reaction with H_2O into H_2 and CO_2. At 200 °C, the CO conversion with H_2O is about 99% [22, 23]. The methanation reaction ($CO + 3H_2 \rightarrow CH_4 + H_2O$ and $CO_2 + 4H_2 \rightarrow CH_4 + 2H_2O$) is equilibrium limited and extremely exothermic to convert CO and CO_2 with H_2 into CH_4 and H_2O. The low temperature methanation is carried out at temperature less than 300 °C [24] to get maximum conversion of CO and CO_2. Here, in order to consider 100% conversion of CO and CO_2 with 100% yield of CH_4, 200 °C is the best temperature [25]. The methanation reactor was operated at temperature of 200 °C and 1 bar$_a$ for CO and CO_2 conversion to boost the CH_4 formation. A fraction of syngas was combusted in the RGibbs reactor at 130 °C and 1 bar to balance the heat load of a gasifier when no solar thermal energy is available.

Five cases were considered to simulate the gasification process using air, $H_2O_{(g)}$, O_2 and CO_2 for Case 1, Case 2, Case 3 and Case 4, respectively. With Case 5, no gasification agent was

used only applying to typical pyrolysis. The aim was to investigate and evaluate how the gasification agents affect syngas production in the specified process and in turn CH_4 composition for power generation. It was also to try and optimise energy in the form of combustion of the CH_4 gas over typical syngas (CO and H_2) for power generation on a normal gas turbine.

The overall CH_4 composition and energy demands would depend on the various amounts of gasification agents fed to the gasifier. In the simulations and calculations, biomass feed was set at 1 ton/h of wheat straw, which is equivalent to 37.55 kmol/h. If a higher quantity of feed is required for larger scale plants, the results in the simulation can be scaled up linearly. The gasification simulations assumed thermodynamic equilibrium is reached. The operating conditions and the thermodynamic models used in each unit in the process are summarised in Table 4.1.2(i).

The process input parameters for a biomass was based on ultimate and proximate analysis of wheat straw. The proximate analysis as fixed carbon (FC), volatile matter (VM), ash (ASH) and ultimate analysis as carbon (C), hydrogen (H), oxygen (O), nitrogen (N) and lower heating value (LHV) of the investigated biomass is given in the Table 4.1.2(ii). These values were used in the developed model, where the chemical formula of the dry biomass is $CH_{1.496}O_{0.82}$. The contents of chlorine and sulphur were ignored, because they exist in small amounts, which has little effect on the simulation results.

The treated wheat straw fed into a gasifier for gasification at high temperatures (700-1000 °C). Air, O_2, CO_2 and steam are supplied at the lowest flowrate at which the formation of C is zero. We assume that the product gas does not constitute undesired gases (e.g. chlorine, hydrogen sulphide and sulphur); therefore, the product gas is passed through cyclone separator to remove out the ash. A WGS unit may be of particular importance as it converts some H_2O into H_2 usually via a catalyst in order to meet the requirement of the H_2/CO ratio for the methanation unit as shown in Eq. (1). However, this was not considered in this would fix the CO to H_2 ratio before methanation. Fixing the CO to H_2 ratio would result in the overall output to be the same for all cases considered as the feed to the methanation reactor would be the same.

$$CO + H_2O \xrightarrow{\text{catalyst}} CO_2 + H_2 \tag{1}$$

The methanation of syngas is an exothermic reaction that converts CO) and/or CO_2 to CH_4 using H_2, Eq. (2) and Eq. (3) respectively. In the methanation reactor, high conversion is achieved to maximise CH_4 content in the gas stream for the power generator.

$$CO + 3H_2 = CH_4 + H_2O \Delta H = -206 \, kJ/mol \tag{2}$$

$$CO_2 + 4H_2 = CH_4 + 2H_2O \Delta H = -165 \, kJ/mol \tag{3}$$
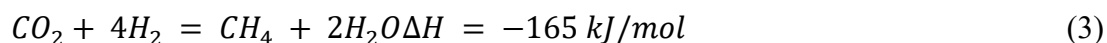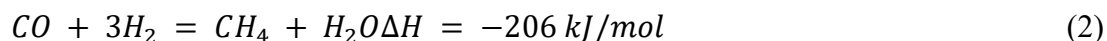
Provided that the product gas composition from the methanation units has a CH_4 concentration above 40%, then the gas can be combusted on a simple gas engine for power generation.

4.1.3: Results and Discussion

Case 1 - Air Feed (N₂: 78%, O₂: 21%, H₂O: 1%)

The cheap option of a gasification agent for small-scale biomass/waste to energy projects is air if other agents are not readily available. The simulation target was to achieve maximum CH_4 content from the methanation process at different gasification temperatures. Gas compositions before and after methanation are given in Figure 4.1.3(i) for the four temperatures studied with air as feed. The results show that CH_4 concentration increases after the methanation reaction with increasing temperature. It is shown that with air as gasification agent, CH_4 content can be increased from 21.64% to 42.38% when temperature is increased from 700 to 1000 °C respectively. The CH_4 content at 1000 °C meets the specified target composition for power generation via a normal gas turbine. Reducing the air feed to the gasifier as temperature is increased reduces the N_2 composition in the product gas from 37% to 5% for the respective temperature range limits studied. The presents of N_2 in product gas at lower temperatures result in a diluted end gas, requiring larger and expensive downstream equipment to use the gas, as well as reducing the heating value of the gas. Therefore, air can be recommended as the gasification agent at 1000 °C when a high CH_4 content for power generation is the target for the biomass-to-energy process because only a small molar composition of N_2 gas is present in the product stream. Figure 4.1.3(ii) also shows that the CO_2 content after methanation is high meaning that the reaction taking place may be producing both CH_4 and CO_2 from the C in CO. Thus, the typical reaction that may be happening in the

methanation section is shown by Eq. (4). CH_4 concentration after the methanation unit is above 40% for use in a normal gas turbine at temperatures above 900 °C.

$$2CO + 2H_2 = CH_4 + CO_2 \qquad\qquad (4)$$

Process heat loads, power generation and net power output from the whole process are shown in Table 4.1.3(ii). The first point to note from calculations was the heat energy released in the methanation unit can be used to supply some of energy for the demand of the gasifier through heat integration. It shows that as more air is fed to the gasifier less power input is required for gasification. However, high air feed requires more external power input to drive the fans for gasification and the syngas produced is diluted with N_2. The energy produced after combusting CO, H_2 and CH_4 after methanation and power produced from the heat recovery steam generation (HRSG) unit is also shown in Table 4.1.3(i). The net heat duty decreases as temperature to the gasifier is increased.

The use of CSP to supply energy to the gasification reactor can be beneficial in increasing the CH_4 concentration because part of the syngas will no longer be used to provide energy for the unit. Figure 4.1.3(iii) shows how the system can be improved if CSP can be applied. The results have shown that the molar percentage boost up is only 1% at 700 °C and can increase up to 20% at 1000 °C with CSP supplying the energy to the gasification reactor. CH_4 productivity is defined as the increase in the amount of CH_4 produced as a result of introducing CSP- thermal energy in the gasification system (also given as percentage CH_4 boost up, Eq. (5)). CH_4 production efficiency is calculated as the ratio of CH_4 productivity with the heat load of the gasifier, Eq. (6).

$$CH_4 \text{ boost up } (\%) = \frac{CH_4 \text{ with CSP} - CH_4 \text{ without CSP}}{CH_4 \text{ without CSP}} \; x \; 100 \qquad\qquad (5)$$

$$CH_4 \text{ production efficiency} = \frac{CH_4 \text{ Productivity}}{Gasifier \text{ heat load}} \; x \; 100 \qquad\qquad (6)$$

Case 2 – Steam as Gasification Agent

An alternative option for gasification agent is H_2O as it can provide both H and O atoms to the system. When H_2O is fed, the energy balance might be an issue due to the extra high energy required to heat up and vaporise $H_2O_{(l)}$ to steam. Therefore, waste heat from the power generation and methanation units must be recovered to turn water into steam. The temperature for steam fed

into gasification is assumed at 100 °C because the process is designed for low pressure. The minimum water feed flowrate was also set to a value that resulted in no C formation from the gasifier. Carbon production clogs the process, hence the idea was to analyse systems where the formation of C can be avoided, whilst using the minimum gasification agent.

There is a high concentration of H_2 and H_2O in the stream from the gasifier. When less H_2O was fed, less energy was required in the gasification unit, but the H_2/CO ratio decreased. Figure 4.1.3(v) shows the gas composition after the gasification and methanation reactions. H_2O concentration was produced in smaller amounts in the product stream for both sections above 900 °C. The analysis showed that for all cases, CH_4 increases after methanation. However, there was also an increase in the production of CO_2 concentration after methanation reactor as gasification temperature was increased to 800 °C and 900 °C but decreased slightly again at 1000 °C. The production of H_2 is high after gasification for all cases and this can be attributed to the WGS reaction.

Table 4.1.3(ii) shows energy of combustion, power generation and net power output from the whole process when steam was used as the gasification agent. The simulation shows that CH_4 content can be increased to 47% at 900 °C before the gas is sent for power generation, which is much higher than the value when air is used for gasification for the same temperature. However, from the overall energy balance, the net power generation is still very small, as seen in Table 4.1.3(ii).

The reason is the high energy supplied to the gasifier to heat the water to gasification temperature. The high concentration of CO_2 after the methanation stage also reduces the heating value of the gas. Because of the high energy demands, it is suggested that steam is not used as a gasification agent in biomass-to-energy process, unless the energy can be supplied by integrating the system with CSP. The results shown in Figure 4.1.3(v) indicate that the molar percentage boost up can be 19% at 700 °C and can increase up to 23% at 1000 °C with CSP supplying the energy to the gasification reactor. The power produced by combusting products after methanation is high and constant for all temperatures. However, the net heat duty is low and decreases with increase in temperature at 1000 °C.

Case 3 – O_2 as Gasification Agent

O_2 is usually the last option when considering a gasification agent because availability of pure O_2 may be limiting and expensive. However, it is worthwhile to investigate this option for comprehensiveness of the study. Gas compositions for the cases with O_2 feed after gasification and methanation are given in Figure 4.1.3(vi) and the results show that a huge amount of CO_2 is also produced in the methanation reactor. The highest CH_4 concentration after the methanation reactor is 44%, which is above the target concentration for use in a normal gas turbine. The H_2O compositions after the methanation reactions is low even at lower temperatures. Figure 4.1.3(vi) shows that the H_2 to CO ratio was less than 1 after gasification in all cases investigated as compared to the systems when air and H_2O were supplied as gasification agents. The H_2:CO ratio can be increased by adding water or adding the WGS unit, but this was not the scope of this study. If the H_2:CO ratio was to be adjusted and fixed by adding H_2O, this would have to be done for all systems and will result in the overall composition after methanation to be the same. The results showed that a lower concentration of CO_2 is observed after methanation as gasification temperature is increased.

Table 4.1.3(iii) gives the energy demands of the whole process when O_2 is used for gasification. Heat input to the gasifier increased as temperature increased. As gasification temperature is increased the CH_4 produced increases. The net power generation increases with increase in CH_4 concentration. However, the net power generation from CH_4 does not increase much after 900 °C. The total power produced from combusting CH_4 is the same as when air or H_2O are used as oxidising agents. This is shown even when N_2 has been excluded in the feed to the gasifier by using pure O_2. Therefore, cost-benefit analysis of producing CH_4 from the process using O_2 as a gasification agent does not bring much advantage to the overall process. The reason for the low power generation in the gas after the methanation reactor is the high concentration of CO_2 present in the gas. The gasification analysis at 700 °C is heat balanced and there is no need to combust part of the produced syngas to make up energy for gasification. This means there is no need to supply any extra energy in form of CSP.

Case 4 – CO_2 Agent as a Feed

The biomass was gasified with controlled amount of CO_2 so that no solid C is formed. The gasifying agent (CO_2) was fed at ambient temperature and pressure. The researchers believed that feeding CO_2 would reduce the net CO_2 produce by the whole system. Figure 4.1.3(vii) shows the

product compositions after the gasification and methanation sections. We note that the concentration of CO after methanation is high at all temperatures studied. CH_4 concentration increases with temperature to give a maximum concentration of 43% after the methanation unit at 1000 °C. Although still high, we also see that CO_2 concentration decreases with increase in temperature after methanation.

From Table 4.1.3(iv), the heat released by the methanation section is also high and is rather constant at different temperatures. The heat load of the gasification system is higher than air, H_2O and O_2 as a gasification agent. It was assumed that the benefit of using CO_2 as a gasification agent will help in reduction of overall CO_2 emissions. However, the net CO_2 emitted when producing power after methanation is similar to all other gasification agents studied. Table 4.1.3(iv) shows that the total power generation is constant at all temperatures. This is because the molar amount of CH_4 produced after methanation remains the same despite the huge concentration difference for the range of temperatures studied. Both H_2 and H_2O compositions after methanation are low, meaning the system may be hydrogen limited. The overall CH_4 boost up when CO_2 is used as a gasification agent is shown in Figure 4.1.3(viii). It averages about 22% for all temperatures with CSP applied. The concentration of CH_4 is shown in Figure 4.1.3(viii). It is higher at high temperatures, therefore, the concentration boost for the production of methane gas would be more beneficial at 1000 °C.

Case 5 – No Gasification Agent as a Feed

In the Aspen Plus® simulated case in which no gasification agent was fed into the gasifier, the biomass was decomposed in the gasifier at high temperatures to form synthesis gas. Gas compositions from the gasifier, after methanation, are shown in Figure 4.1.3(ix). The case in which no gasification agent was used for biomass gasification was a special case, and it was inevitable that C would not be formed. The produced C ends as soot in the ash instead of converting to CO, CH_4 or CO_2 and this is due to less O_2 being available in the respective biomass feed substrate or just kinetics.

The main reason for the research was to increase the CH_4 composition in the product gas and reduce the energy consumption in the gasifier. However, although the highest CH_4 content is 47% (above the specified 40% target), the amount of energy required by the gasifier increases with

gasification temperature. Table 4.1.3(v) shows the heat required for gasification, power generation and net power output from the whole process when no gasification agent was used. Heat required for gasification increases significantly with temperature as expected. The amount of solid C formed is higher (9.6 kmol/h) at 700 °C, but it decreases to 1 kmol/h at 1000 °C. Net CO_2 emission is after methanation is 22.32 kmol/h, which is 30% less than the CO_2 produced when using other gasification agents at 700 °C. As temperature increased above 700 °C the CO_2 emitted by the overall process increase and becomes 30.92 at 1000 °C.

The CH_4 produced remains constant at temperatures above 800 °C when no CSP is applied. However, the percentage CH_4 increase when all the syngas produced is sent to the methanation reactor increases from 6% at 700 °C to 20% at temperatures above 900 °C as shown in the Figure 4.1.3(x). This tells us that operating biomass gasification at temperatures above 800 °C or more will have no significant benefits in the amount and composition of CH_4 produced when gasifying with no gasification agent.

Solutions for reducing CO_2 emissions can be achieved by comprehensive process synthesis methods, which help to design systems in which CO_2 can be a feed, trying to increase energy efficiency or switching to biomass fuels. Syngas produced through gasification can be converted to power by direct combustion in a special syngas turbine. The purpose of adding the methanation after gasification was studied for possible benefits in two-fold. First, to try and use a normal gas turbine for power generation which is cheaper as compared to combusting syngas with high H_2 content via a syngas turbine.

The second intention was to apply process synthesis and investigate the advantage of using heat integration to reduce overall energy supply to the system by external means. Heat released by the methanation would be used for the gasification unit. Table 4.1.3(vi) shows the comparison for all cases studied showing that there is no case which can give all benefits in terms of energy, gas composition and zero carbon formation. However, results have shown that each case can provide specific benefits depending on the absolute gas product purpose and availability of heat energy (which can be supplied by CSP) and end-use requirements.

All gasification processes studied produce an H_2/CO ratio that is close to 1 except when CO_2 is used as a gasification agent (ratio increase from 0.56 to 0.86 with respective temperature

limits). Two cases; when steam was used as gasification agent and when no gasification agent was used produce the highest CH_4 concentration of 47% after methanation.

Generally, all the results have shown that it is inevitable not to produce an equivalent or higher amount of CO_2 to CH_4 in the methanation section even when CO_2 is fed to the gasification section. The use of steam and CO_2 resulted in the highest power generation despite requiring high heat energy supply in the gasification unit. When 4.20 kmol/h steam was used as gasification agent, the system produced the highest molar amount of CH_4 (15.32 kmol/h) from 37.55 mol/h of wheat husks ($CH_{1.496}O_{0.82}$). Using CSP to supply external energy to the gasification system resulted in the increase in CH_4 combusted for power generation. A fraction of syngas can be saved ranging between 17-19% if CSP is applied.

4.1.4:   Conclusions

The gasification process was simulated with air, O_2, CO_2 and steam as gasification agents to produce syngas. The syngas was passed through the methanation reactor to maximise CH_4 content in the stream before it is sent for power generation in a normal gas turbine. The results show that the highest the CH_4 concentration (47%) and total power is generated when steam is used as a gasification agent. High energy is required to heat the water to reaction temperature, but the energy can be supplied using a combination of heat integration and CSP supply. This makes the case when steam is used as the best case amongst all studied systems.

As for the case with no gasification agent, the molar amount of CH_4 produced was lower due to the formation of C in the gasification stage. When O_2 is used, the CH_4 fraction in the stream sent to the power generation is still much low despite the absence of N_2 from the feed. All processes studied produce a high CO_2 content after methanation and further detailed analysis to boost H_2 and CH_4 by adding water to the methanator should be considered in future studies. The ability to use heat generated in the methanation process for gasification (heat integration) offers an advantage in this system when trying to generate CH_4 for power production via a normal gas turbine. An application of CSP to the system increases the amount of CH_4 produced by about 20% for all cases thus increasing the efficiency of the processes.

Tables

Table 4.1.2(i): Operating conditions and the thermodynamic models used in the process

Items	Temperature	Pressure	Thermodynamic model
	°C	bar	
Steam	25	1	Ideal
Air/CO_2/O_2	25	1	Ideal
Gasifier	700-1000	1	R Yield /R Gibbs
Combustion	1200	15	R Stoic
Methanation reactor	200	1	R Equilibrium

Table 4.1.2(ii). The ultimate and proximate analysis and lower heating value (LHV) of biomass [26] (* Oxygen by difference)

Biomass Material	Moisture content wt. (%) (wet basis)	Proximate analysis wt. (%) (dry basis)			Ultimate analysis wt. (%) (dry basis)				LHV MJ/kg (dry basis)
		FC	VM	ASH	C	H	O*	N	17.988
Wheat straw	8.87	10.98	82.12	6.90	42.95	5.35	46.99	0.00	

Table 4.1.3(i): Energy of combustion, power generation and net heat duty from the whole process for different air feed as gasifying agent

Temperature (°C)	700	800	900	1000
Air input at 25 °C and 1 bar (kmol/h)	27.50	9.30	3.80	2.37
Fraction of syngas combusted to supply gasification energy in RGibbs reactor	0.01	0.12	0.16	0.17
CO for combustion (kmol/h)	0.00	0.03	2.43	3.06
H_2 for combustion (kmol/h)	0.08	0.00	0.00	0.00
CH_4 for combustion (kmol/h)	12.42	14.35	14.32	14.32
Power produced by combustion (kW$_e$)	-731.48	-848.15	-894.31	-906.33

Power produced by HRSG sys (kWₑ)	-323.76	-370.43	-391.16	-396.56
Total power generation (kWₑ)	-1055.24	-1218.59	-1285.48	-1302.91
Heat duty needed for gasifier (kW$_{th}$)	-120.00	460.00	640.00	696.00
Heat released by Methanation (kW$_{th}$)	-824.00	-997.00	-999.00	-1002.00
Net heat duty (kW$_{th}$)	-944.00	-537.00	-359.00	-306.00

Table 4.1.3(ii): Energy of combustion, power generation and net duty for the process with steam as gasifying agent

Temperature (°C)	700	800	900	1000
H_2O input at 25 °C and 1 bar (kmol/h)	**13.35**	**4.20**	**1.63**	**1.02**
Fraction of syngas combusted to supply gasification energy in RGibbs reactor	0.16	0.18	0.18	0.192
CO for combustion (kmol/h)	0.00	0.00	0.84	2.06
H_2 for combustion (kmol/h)	0.13	0.05	0.00	0.00
CH_4 for combustion (kmol/h)	15.30	15.32	15.12	14.82
Power produced by combustion (kWₑ)	-906.47	-906.93	-911.15	-916.80
Power produced by HRSG sys (kWₑ)	-394.92	-394.97	-396.80	-400.07
Total power generation (kWₑ)	-1301.39	-1301.91	-1307.97	-1316.88
Heat duty needed for gasifier (kW$_{th}$)	620.00	750.00	770.00	780.00
Heat released by Methanation (kW$_{th}$)	-903.00	-1035.00	-1054.00	-1037.00
Net heat duty (kW$_{th}$)	-283.00	-285.00	-284.00	-257.00

Table 4.1.3(iii): Energy of combustion, power generation and net heat duty for the process when O_2 is used as the gasifying agent

Temperature (°C)	700	800	900	1000
O_2 input at 25 °C and 1 bar (kmol/h)	**6.99**	**2.15**	**0.90**	**0.50**
Fraction of syngas combusted to supply gasification energy in RGibbs reactor	0.00	0.11	0.152	0.167
CO for combustion (kmol/h)	0.00	0.01	2.30	3.06
H_2 for combustion (kmol/h)	0.07	0.01	0.00	0.00

CH$_4$ for combustion (kmol/h)	11.82	14.25	14.31	14.31
Power produced by combustion (kW$_e$)	-696.85	-842.74	-890.91	-905.74
Power produced by HRSG sys (kW$_e$)	-307.95	-367.81	-389.50	-396.21
Total power generation (kW$_e$)	-1004.80	-1210.54	-1280.41	-1301.96
Heat duty needed for gasifier (kW$_{th}$)	-358.00	420.00	630.00	695.00
Heat released by Methanation (kW$_{th}$)	-769.00	-988.00	-999.00	-1001.00
Net heat duty (kW$_{th}$)	-1127.00	-568.00	-369.00	-306.00

Table 4.1.3(iv): Energy of combustion, power generation and net heat duty for the process when CO_2 is used as the gasifying agent

Temperature (°C)	700	800	900	1000
H$_2$O input at 25 °C and 1 bar (kmol/h)	**24.30**	**5.00**	**1.72**	**1.10**
Fraction of syngas combusted to supply gasification energy in RGibbs reactor	0.186	0.178	0.18	0.185
CO for combustion (kmol/h)	4.10	4.10	4.10	4.10
H$_2$ for combustion (kmol/h)	0.00	0.00	0.00	0.00
CH$_4$ for combustion (kmol/h)	14.31	14.31	14.31	14.31
Power produced by combustion (kW$_e$)	-915.18	-924.20	-925.55	-925.80
Power produced by HRSG system (kW$_e$)	-415.01	-407.47	-406.20	-405.95
Total power generation (kW$_e$)	-1330.2	-1331.69	-1331.76	-1331.76
Heat duty needed for gasifier (kW$_{th}$)	797.00	770.00	770.00	780.00
Heat released by Methanation (kW$_{th}$)	-1030.00	-998.00	-999.00	-1003.00
Net heat duty (kW$_{th}$)	-233.00	-228.00	-229.00	-223.00

Table 4.1.3(v): Energy of combustion, power generation and net heat duty from the process when no gasification agent is used

Temperature (°C)	700	800	900	1000
Fraction of a syngas combusted to supply gasification energy in RGibbs reactor	0.061	0.143	0.167	0.172
CO for combustion (kmol/h)	0.00	0.00	0.93	2.08

H$_2$ for combustion (kmol/h)	0.09	0.04	0.00	0.00
CH$_4$ for combustion (kmol/h)	10.51	13.43	14.31	14.31
Power produced by combustion (kW$_e$)	-622.36	-794.78	-864.62	-886.95
Power produced by HRSG system (kW$_e$)	-271.37	-346.18	-376.66	-387.12
Total power generation (kW$_e$)	-893.74	-1140.97	-1241.29	-1274.08
Heat duty needed for gasifier (kW$_{th}$)	200.00	568.00	690.00	727.00
Heat released by Methanation (kW$_{th}$)	-620.00	-909.00	-997.00	-1001.00
Net heat duty (kW$_{th}$)	-420.00	-341.00	-307.00	-274.00

Table 4.1.3(vi): Comparison of the five cases when different gasification agents were used for methane production

Gasification agent	Merit	Demerits
Air	Readily available. CH$_4$ composition increase from 21% to 42% (700 to 1000 ℃), respectively.	More energy is required to feed air to the system because of the huge N$_2$ composition. Synthesis gas produced is diluted with N$_2$.
H$_2$O	Highest CH$_4$ composition (47.3%) after methanation at 900 ℃. Highest total power generated (-1316.88 kW$_e$) at 1000 ℃.	Requires high energy to produce steam for gasification.
O$_2$	Less energy is required to blow oxygen into the gasification reactor as compared to other gasification agents. Highest net heat duty (-1127.00 kW$_{th}$).	Expensive to get and not readily available. Overall energy produced after methanation is similar to the case when air is used.
CO$_2$	Using a greenhouse gas as fee. Highest power produced by combusting products of methanation (-925.80 kW$_e$) at	No benefit on net CO$_2$ produced when compared against other gasification agents.

|	1000 °C.	No energy gain with increasing temperature. Requires high energy for gasification.
No gasification agent	No energy required to blow gasification agent into the gasification reactor. High CH_4 composition (47.1 %) after methanation at 900 °C. Net CO_2 emission is after methanation is 30% less than using other agent at 700 °C.	Carbon is formed. Net CO_2 produced increase with temperature.

Figures
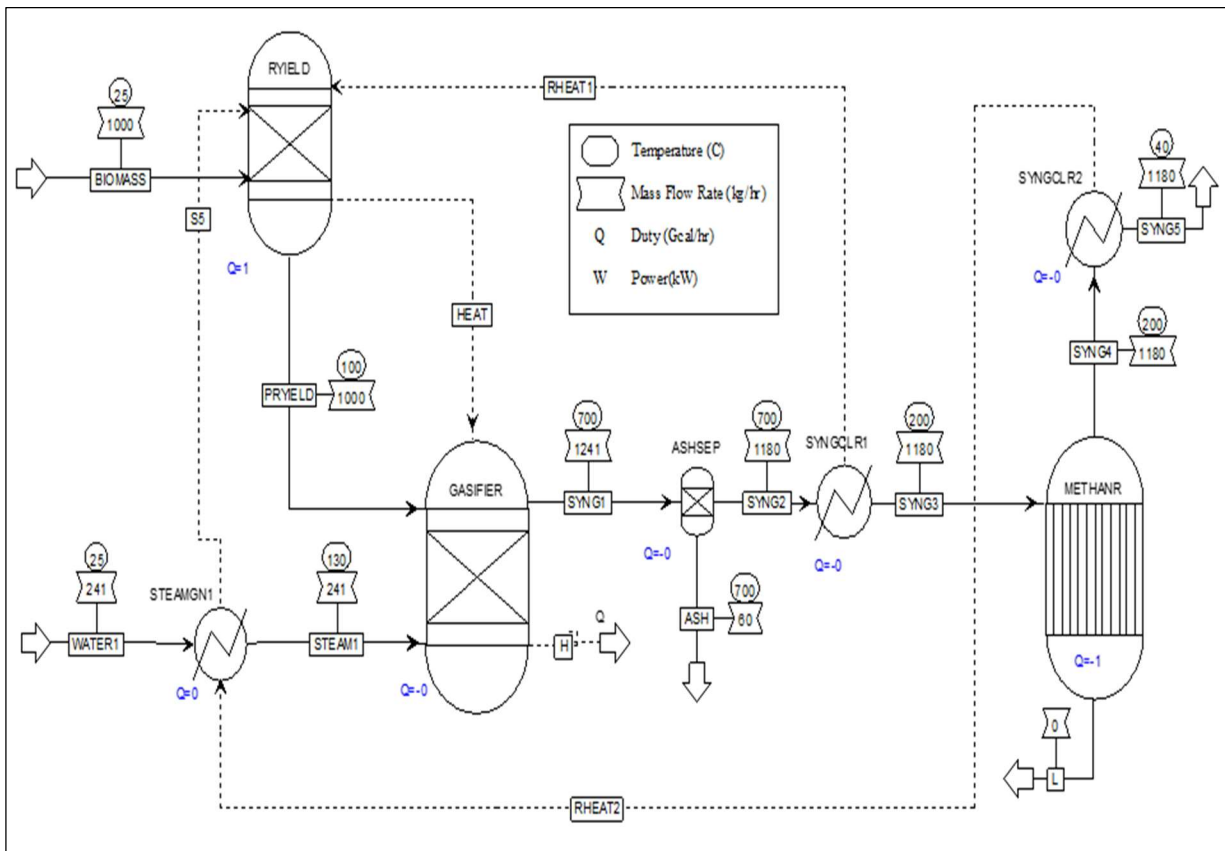
Figure 4.1.2(i). Process flowsheet of biomass gasification with subsequent methanation process
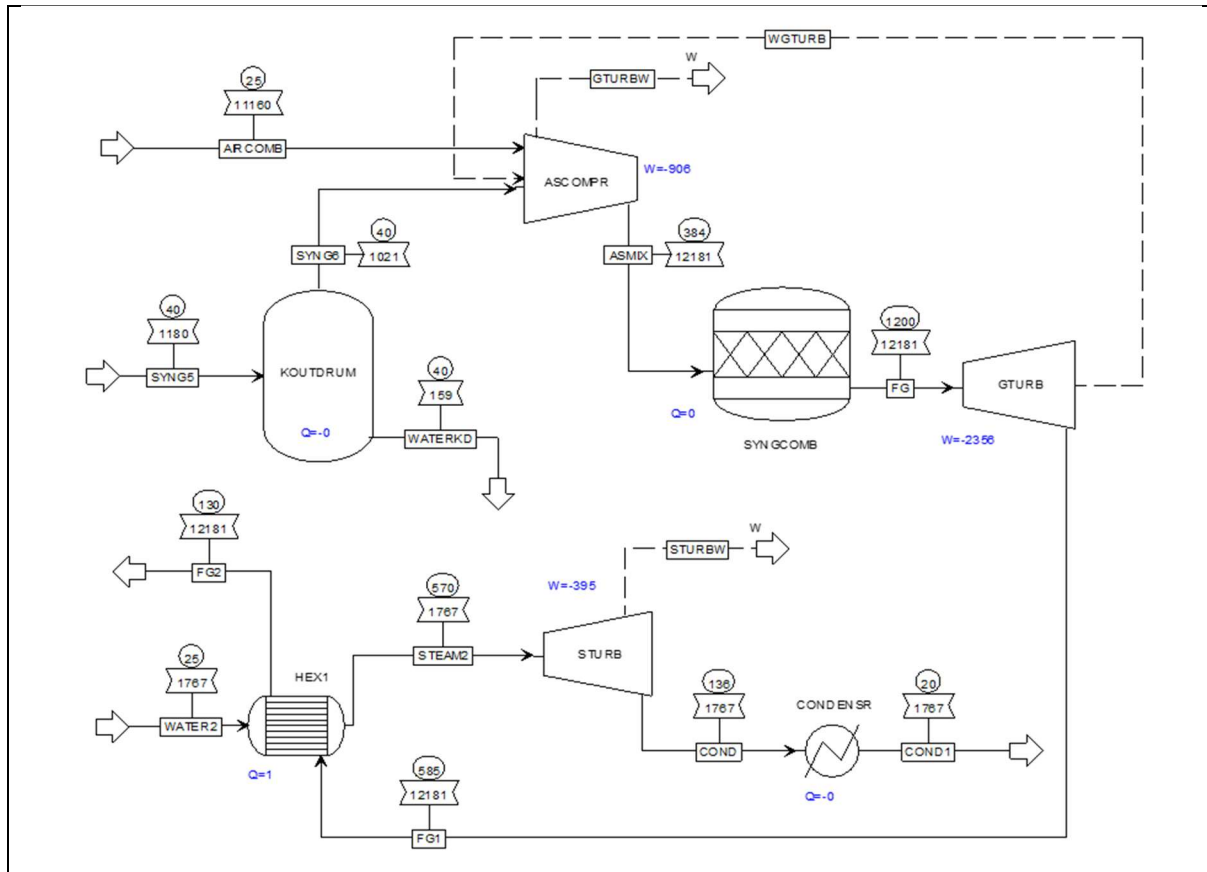
Figure 4.1.2(ii). Process flowsheet of power generation from syngas after methanation
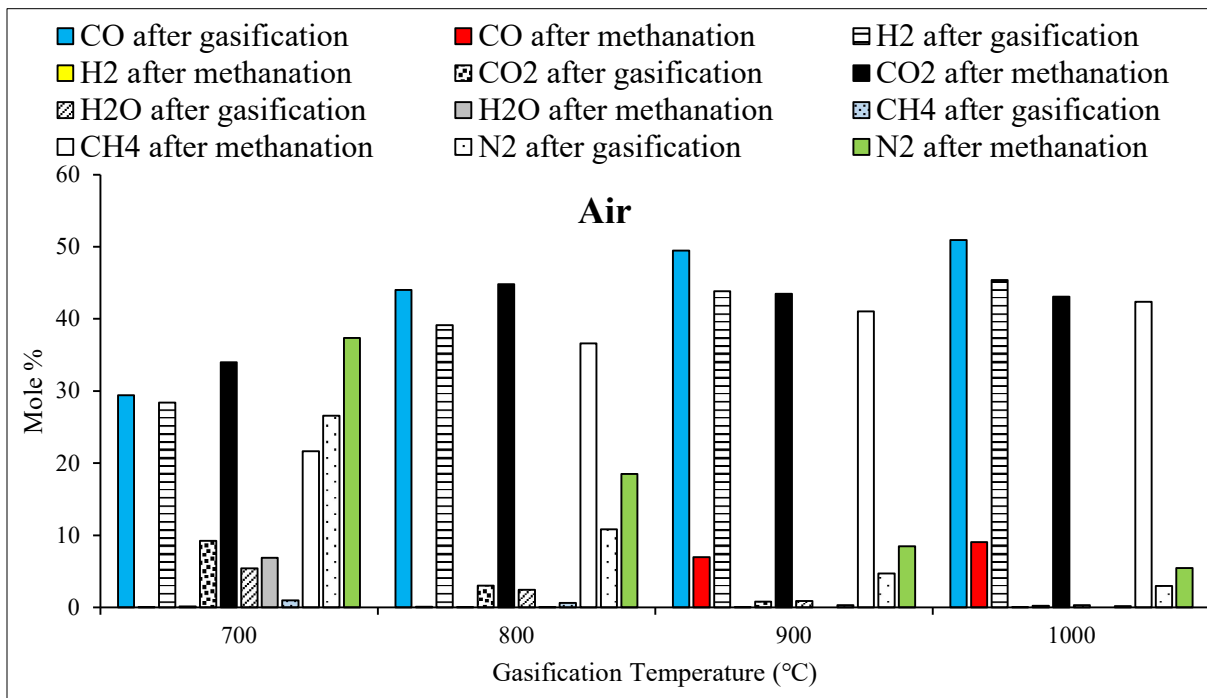
Figure 4.1.3(i): Gas composition from gasifier and methanation unit at different temperatures when air is used as gasification agent.
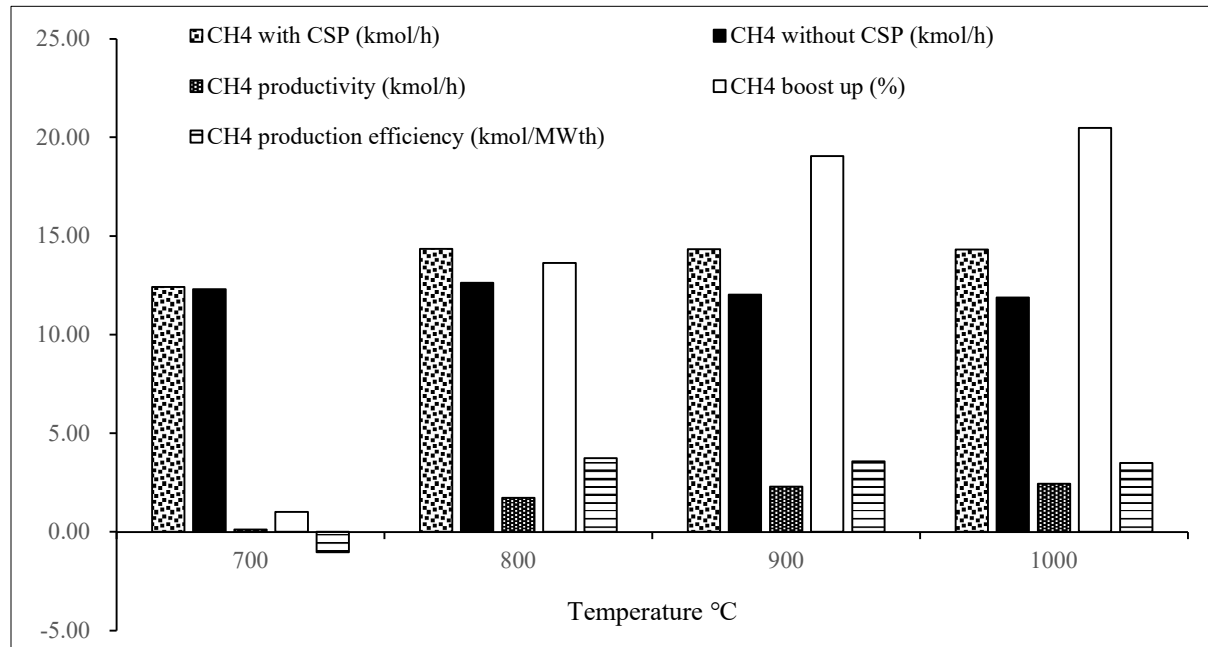

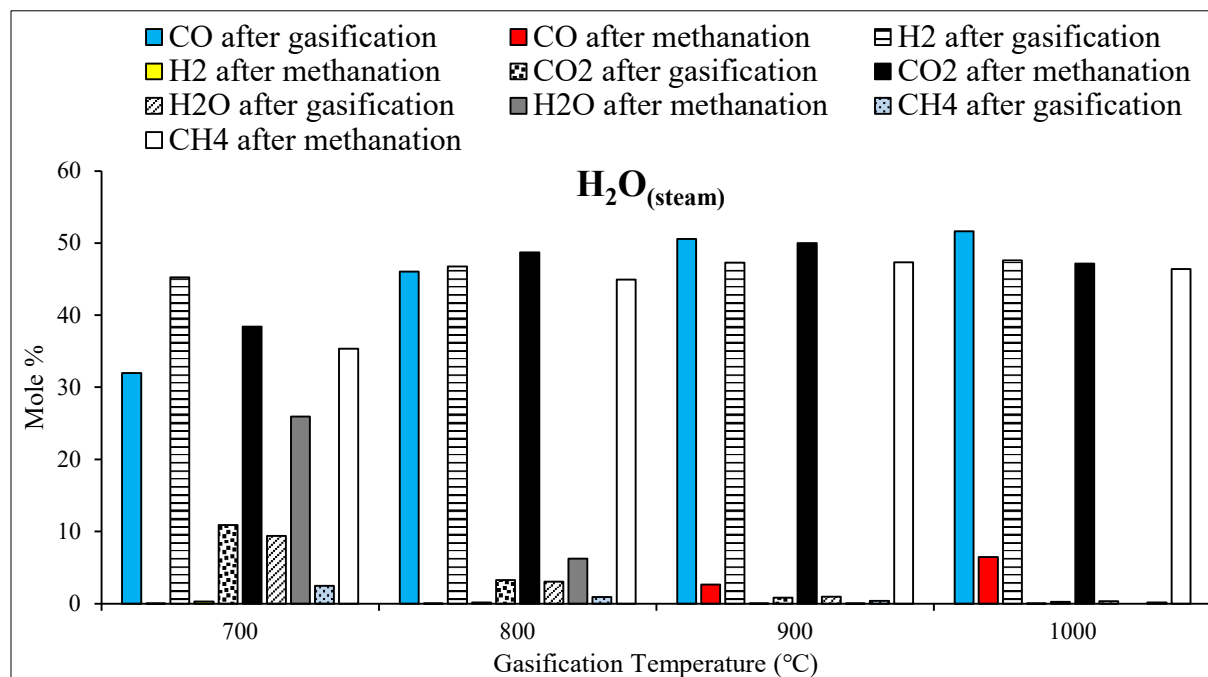Figure 4.1.3(ii): Percentage CH_4 boost with CSP when air is used as a gasification agent.

Figure 4.1.3(iii): Gas composition from gasifier and methanation unit at different temperatures when steam is used as gasification agent.
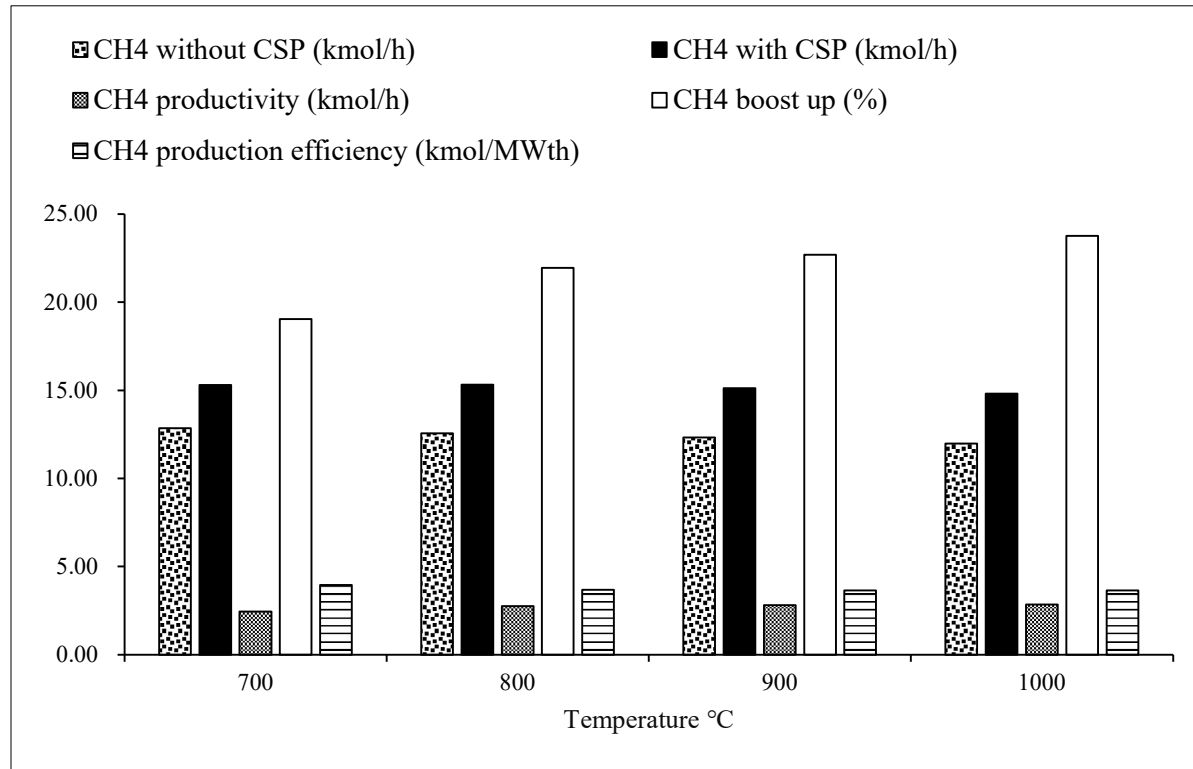
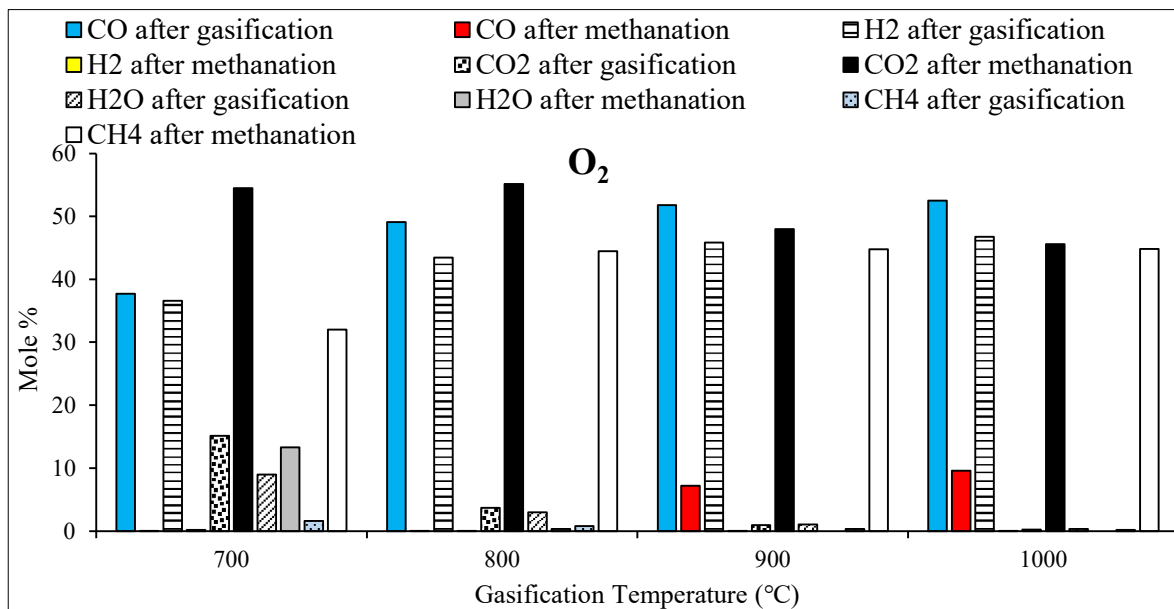Figure 4.1.3(iv): Percentage CH$_4$ boost with CSP when steam is used as a gasification agent.

Figure 4.1.3(v): Gas composition from gasifier and methanation unit at different temperatures when O$_2$ is used as gasification agent.

Figure 4.1.3(vi): Percentage CH_4 boost with CSP when pure O_2 is used as a gasification agent.

Figure 4.1.3(vii): Gas composition from gasifier and methanation unit at different temperatures when CO_2 is used as gasification agent.
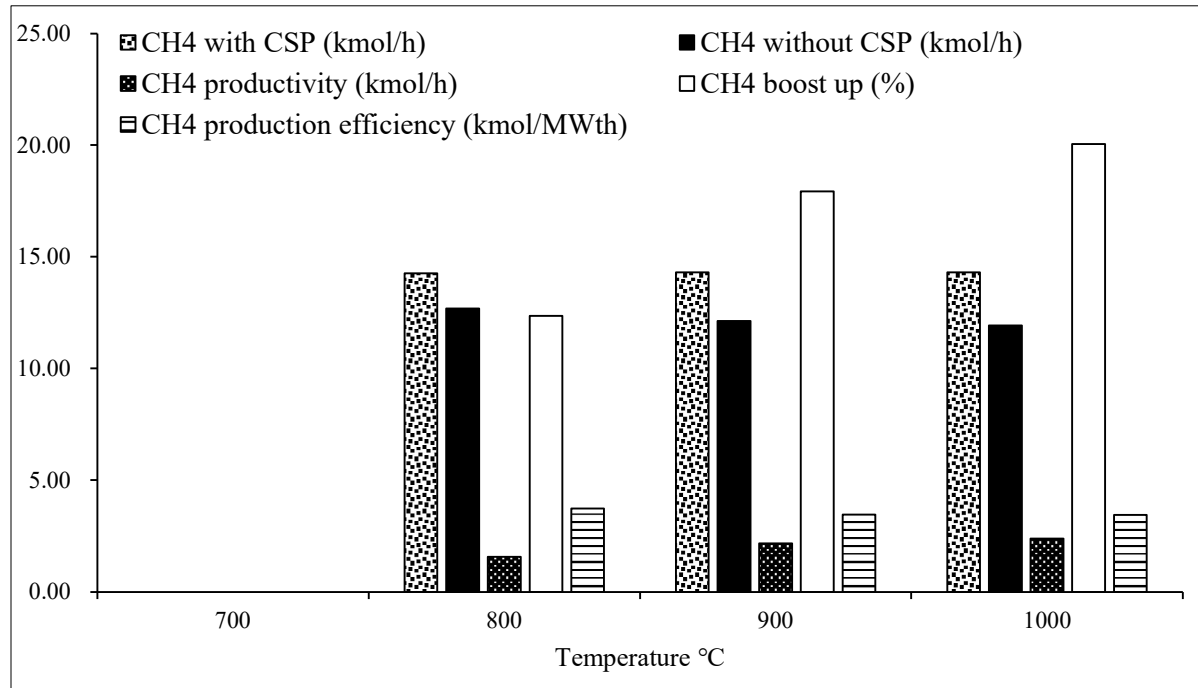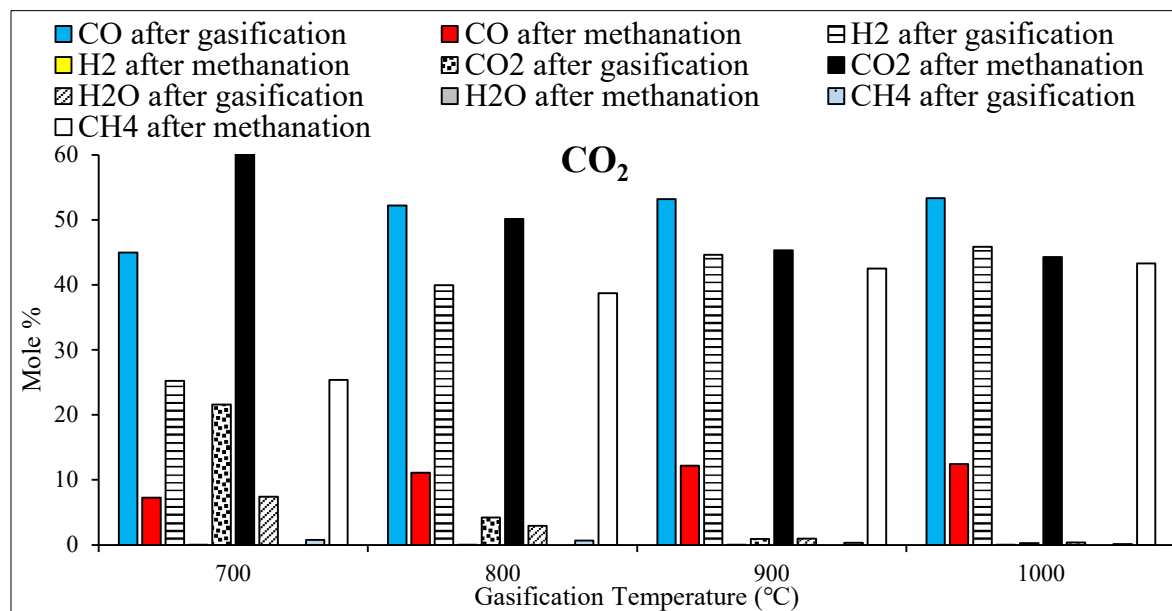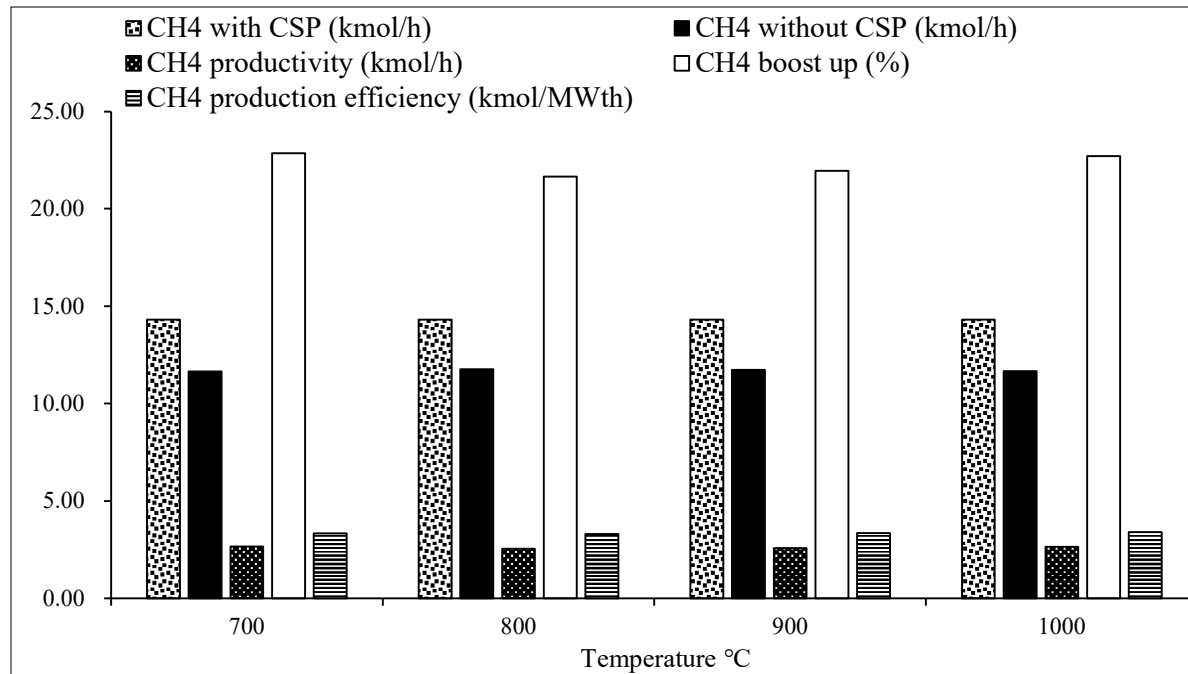
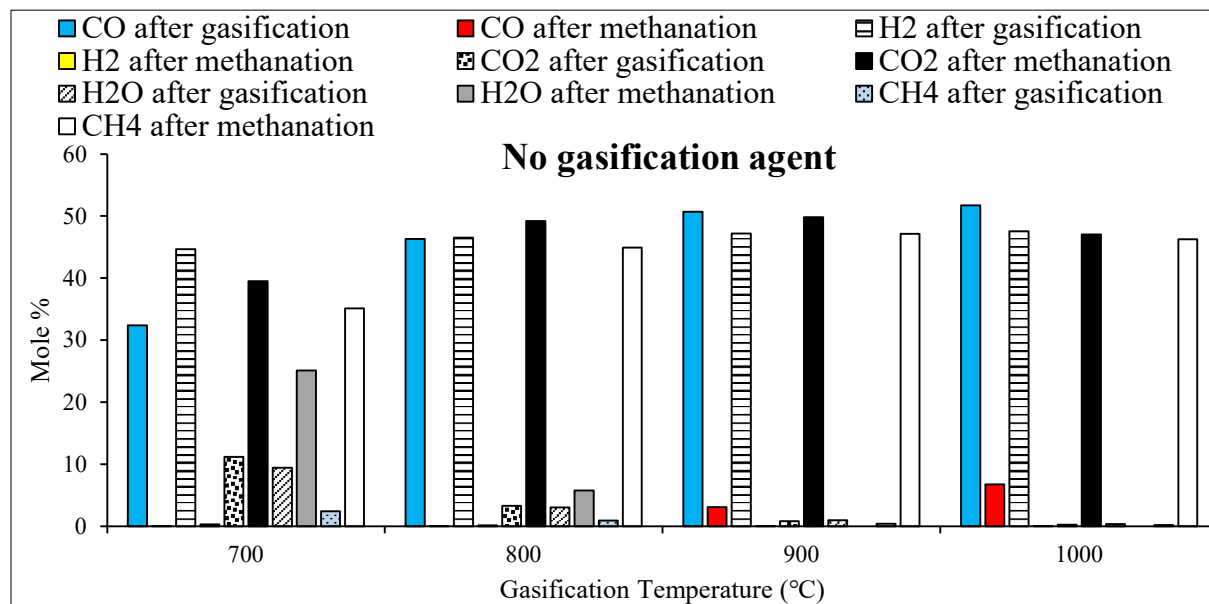Figure 4.1.3(viii): Percentage CH_4 boost with CSP when CO_2 is used as the gasification agent.

Figure 4.1.3(ix): Gas composition from gasifier and methanation unit at different temperatures when no gasification agent is used.
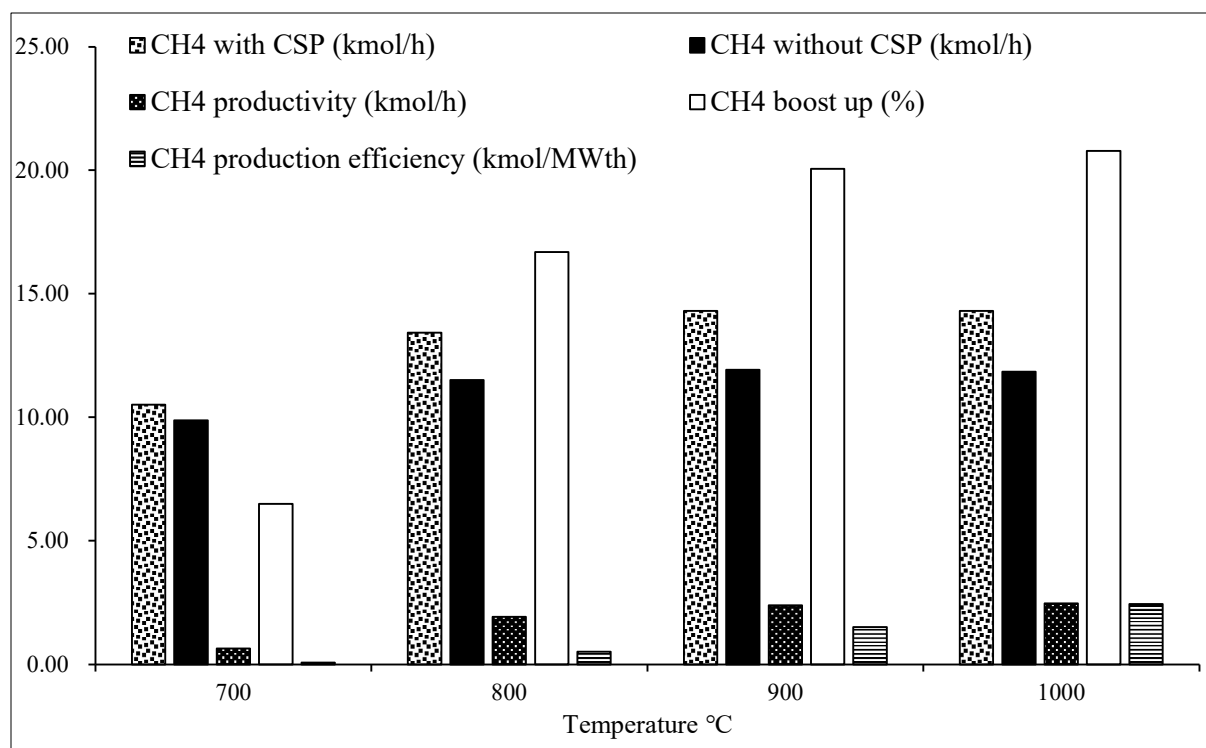
Figure 4.1.3(x): Percentage CH$_4$ boost with CSP when pure no gasification agent is used as a gasification agent.

References

[1] Prasad, L., Pala, R., Wang, Q., Kolb, G., Hessel, V., 2017. Steam gasification of biomass with subsequent syngas adjustment using shift reaction for syngas production: An Aspen Plus model. https://doi.org/10.1016/j.renene.2016.08.069

[2] Flohr, P., Stuttaford, P., 2013. Combustors in gas turbine systems, in: Modern Gas Turbine Systems: High Efficiency, Low Emission, Fuel Flexible Power Generation. Elsevier Ltd., pp. 151–187. https://doi.org/10.1533/9780857096067.2.151

[3] Boerrigter H., R.R., 2006. Review of applications of gases from biomass gasification, in: Handbook Biomass Gasification, Edited by H.A.M. Knoef. Biomass Technology Group (BTG). p. ECN-RX-06-066

[4] Ajvad, M., Shih, H.Y., 2020. Modeling syngas combustion performance of a can combustor with rotating casing for an innovative micro gas turbine. Int. J. Hydrogen Energy 45, 31188–31201 https://doi.org/10.1016/j.ijhydene.2020.08.113

[5] Park, J., Lee, M.C., 2016. Combustion instability characteristics of H2/CO/CH4 syngases and synthetic natural gases in a partially-premixed gas turbine combustor: Part i - Frequency and mode analysis. Int. J. Hydrogen Energy 41, 7484–7493. https://doi.org/10.1016/j.ijhydene.2016.02.047

[6]   Jones, R., Goldmeer, J., Monetti, B., 2011. Addressing gas turbine fuel flexibility. GE Energy. GER4601 (05/11) revB

[7]   Krumpelt, M., Krause, T.R., Carter, J.D., Kopasz, J.P., Ahmed, S., 2002. Fuel processing for fuel cell systems in transportation and portable power applications. Catalysis Today. Elsevier, pp. 3–16. https://doi.org/10.1016/S0920-5861(02)00230-4

[8]   Milani, R., Szklo, A., Hoffmann, B.S., 2017. Hybridization of concentrated solar power with biomass gasification in Brazil's semiarid region. Energy Convers. Manag. 143, 522–537. https://doi.org/10.1016/j.enconman.2017.04.015

[9]   Soria, R., Portugal-Pereira, J., Szklo, A., Milani, R., Schaeffer, R., 2015. Hybrid concentrated solar power (CSP)–biomass plants in a semiarid region: A strategy for CSP deployment in Brazil. Energy Policy 86, 57–72. https://doi.org/10.1016/J.ENPOL.2015.06.028

[10]   AlNouss, A., McKay, G., Al-Ansari, T., 2020. Production of syngas via gasification using optimum blends of biomass. J. Clean. Prod. 242, 118499. https://doi.org/10.1016/j.jclepro.2019.118499

[11]   Herdem, M.S., Mazzeo, D., Matera, N., Wen, J.Z., Nathwani, J., Hong, Z., 2020. Simulation and modeling of a combined biomass gasification-solar photovoltaic hydrogen production system for methanol synthesis via carbon dioxide hydrogenation. Energy Convers. Manag. 219, 113045. https://doi.org/10.1016/j.enconman.2020.113045

[12]   Gu, H., Tang, Y., Yao, J., Chen, F., 2019. Study on biomass gasification under various operating conditions. J. Energy Inst. 92, 1329–1336. https://doi.org/10.1016/j.joei.2018.10.002

[13]   Han, J., Liang, Y., Hu, J., Qin, L., Street, J., Lu, Y., Yu, F., 2017. Modeling downdraft biomass gasification process by restricting chemical reaction equilibrium with Aspen Plus. Energy Convers. Manag. 153, 641–648. https://doi.org/10.1016/j.enconman.2017.10.030

[14]   Kaushal, P., Tyagi, R., 2017. Advanced simulation of biomass gasification in a fluidized bed reactor using Aspen Plus. Renew. Energy 101, 629–636. https://doi.org/10.1016/j.renene.2016.09.011

[15]   Nikoo, M.B., Mahinpey, N., 2008. Simulation of biomass gasification in fluidized bed reactor using Aspen Plus. Biomass and Bioenergy 32, 1245–1254. https://doi.org/10.1016/J.BIOMBIOE.2008.02.020

[16]   Sadhwani, N., Adhikari, S., Eden, M.R., Li, P., 2018. Aspen Plus simulation to predict steady state performance of biomass-CO2 gasification in a fluidized bed gasifier. Biofuels, Bioprod. Biorefining 12, 379–389. https://doi.org/10.1002/bbb.1846

[17]   Bet Sarkis, R., Zare, V., 2018. Proposal and analysis of two novel integrated configurations for hybrid solar-biomass power generation systems: Thermodynamic and economic evaluation. Energy Convers. Manag. 160, 411–425. https://doi.org/10.1016/J.ENCONMAN.2018.01.061

[18]   Cohce, M.K., Dincer, I., Rosen, M.A., 2011. Energy and exergy analyses of a biomass-based hydrogen production system. Bioresour. Technol. 102, 8466–8474. https://doi.org/10.1016/j.biortech.2011.06.020

[19]   Pan, Z., Chan, W.P., Veksha, A., Giannis, A., Dou, X., Wang, H., Lisak, G., Lim, T.T., 2019. Thermodynamic analyses of synthetic natural gas production via municipal solid waste gasification, high-temperature water electrolysis and methanation. Energy Convers. Manag. 202, 112160. https://doi.org/10.1016/j.enconman.2019.112160

[20]   Ansari, S.H., Ahmed, A., Razzaq, A., Hildebrandt, D., Liu, X., Park, Y.K., 2020. Incorporation of solar-thermal energy into a gasification process to co-produce bio-fertilizer and power. Environ. Pollut. 266, 115103. https://doi.org/10.1016/j.envpol.2020.115103

[21]   Minowa, T., Ogi, T., Dote, Y., Yokoyama, S. ya, 1994. Methane production from cellulose by catalytic gasification. Renew. Energy 5, 813–815. https://doi.org/10.1016/0960-1481(94)90094-9

[22]   Yao, S., Zhang, X., Zhou, W., Gao, R., Xu, W., Ye, Y., Lin, L., Wen, X., Liu, P., Chen, B., Crumlin, E., Guo, J., Zuo, Z., Li, W., Xie, J., Lu, L., Kiely, C.J., Gu, L., Shi, C., Rodriguez, J.A., Ma, D., 2017. Atomic-layered Au clusters on α-MoC as catalysts for the low-temperature water-gas shift reaction. Science (80). 357, 389–393. https://doi.org/10.1126/science.aah4321

[23]   Zhai, Y., Pierre, D., Si, R., Deng, W., Ferrin, P., Nilekar, A.U., Peng, G., Herron, J.A., Bell, D.C., Saltsburg, H., Mavrikakis, M., Flytzani-Stephanopoulos, M., 2010. Alkali-stabilized Pt-OHx species catalyze low-temperature water-gas shift reactions. Science (80). 329, 1633–1636. https://doi.org/10.1126/science.1192449

[24]   Lee, W.J., Li, C., Prajitno, H., Yoo, J., Patel, J., Yang, Y., Lim, S., 2020. Recent trend in thermal catalytic low temperature CO2 methanation: A critical review. Catal. Today. https://doi.org/10.1016/j.cattod.2020.02.017

[25]   Gao, J., Wang, Y., Ping, Y., Hu, D., Xu, G., Gu, F., Su, F., 2012. A thermodynamic analysis of methanation reactions of carbon oxides for the production of synthetic natural gas. RSC Adv. 2, 2358–2368. https://doi.org/10.1039/c2ra00632d

[26]   Channiwala, S.A., Parikh, P.P., 2002. A unified correlation for estimating HHV of solid, liquid and gaseous fuels. Fuel 81, 1051–1063. https://doi.org/10.1016/S0016-2361(01)00131-4

Chapter 5: Concentrated Solar Energy to Hydrogen

5.1: Concentrated Solar Energy to Produce Hydrogen

Biomass gasification is an endothermic process which can be used to produce hydrogen (H_2). This study presents a simulation model using Aspen Plus® to design biomass gasification process with water gas shift reaction (WGSR) to obtain maximum H_2. This was done by optimizing the process conditions via modeling to understand the fundamental of the gasification process. Gibbs free minimization and thermodynamics equilibrium approach was used to find out best operating conditions for H_2 production. After conditioning of syngas, WGSR at 200 °C was introduced to produce H_2 as an alternative fuel. Both steam and CO_2 as gasification agents were investigated. The effect of temperature and flowrate of steam and CO_2 were optimized in such a way so that no solid carbon produced in the syngas. Higher temperature is favourable while temperature higher than 800 °C has an adverse effect on H_2 yield. The aim of present study is to determine H_2 production per kg of biomass feed and H_2 productivity per MW_{th} solar-thermal energy input to the gasification system. To validate the results from a model were compared with experimental data to adjust the validity of steam and CO_2 gasification model.

5.1.1: Introduction

Clean H_2 production from biomass and solar energy is considered as a sustainable energy alternative. H_2 has potential to contribute toward green environment, economically feasible and energetically efficient solution in the future. Therefore, it will be inevitable to shift from traditional energy system to innovative alternatives [1]–[4]. Biomass gasification is one of the thermochemical conversions of low-density energy resources into high-energy density fuels and chemicals. Steam, air and CO_2 are used as oxidizing agent during biomass gasification [5].

Conventionally, energy needed for gasification is provided by biomass partial combustion in the gasification unit, or external combustion of a fraction of syngas produced by gasification. This heat can also be provided by concentrated solar power (CSP). CSP-assisted biomass gasification is an emerging sustainable process. CSP-hybrid biomass gasification is a competitive technology to diversify away from utilization of traditional fossil fuels [6]–[8]. However, at the

current state of technology, the viability of the CSP-hybrid biomass gasification process is yet to be established. Vidal et. al has modelled the integration of CSP with biomass gasification to produce H_2 and electric power [9]. Using CSP for biomass gasification serves the purposes of an external, renewable and unlimited energy source [10], and it can improve the utilization efficiency of the biomass.

There have been simulation studies on steam or CO_2-gasification using Aspen Plus®. Some researchers predicted that steam gasification with shift reaction is a promising technology for H_2 production or to adjust the H_2/CO molar ratio [11]–[14]. The produced syngas from steam gasification is primarily composed of H_2, CO, CO_2, water (H_2O) and methane (CH_4) with H_2/CO ratio is in the range of 1 and 2. WGSR was introduced after biomass gasification to increase H_2 fraction in the syngas. In Aspen Plus® simulation, solar-hybrid biomass gasification with WGSR based on restricted equilibrium was added to produce H_2 [15], [16]. The yield and quality of syngas produced from gasification depends upon the type of biomass, type of a gasifier, gasifying agent, operating conditions and complex chemical reactions [17]. The purpose of present study is to develop a model of gasification with WGSR to predict syngas composition. The parametric analysis like gasification temperature, CO_2 as a gasifying agent, and shift reaction temperature on CO conversion to increase the H_2 content in the final product has been studied. The predicted simulation results are validated with already published experimental results.

5.1.2: Process Modelling and Simulation Details

An integrated system model in Aspen Plus® was developed for H_2 production using a biomass gasifier with steam and CO_2 as a gasifying agent followed by water gas shift reaction. The developed model was studied to predict H_2 production per kg of biomass input and H_2 productivity per MW_{th} solar-thermal energy input to the gasification system and H_2 production with or without CSP. The solar energy contribution of the CSP system was modeled in terms of solar-thermal heat injection into the gasifier unit. When there was no CSP, combustion of syngas was introduced to balance the heat load of the gasifier. The share of solar thermal energy into the gasification system results in more syngas per unit of biomass.

The Aspen Plus® model with a process flowsheet shown in Figure 5.1.2(i) was used to simulate the potential of a hybrid CSP-biomass gasification and subsequent syngas adjustment

using shift reactor. The process flowsheet was developed with following steps: specification of components (mixed, conventional and non-conventional), units set, selection of proper property method and selection of unit operation, material and energy streams. Each feed stream is specified with temperature, pressure, composition and flowrate. The unit operation is specified with thermodynamic conditions. The model was based on RGibbs reactor with Gibbs free energy minimization approach. Steam or CO_2 is used as gasification agent. Biomass feed rate was 1000 kg/h and solar-thermal input was simulated as equivalence to the heat load of a gasifier. Temperature (600-1000 °C), flow rate of steam or CO_2 was simulated to optimize the overall process at 1 bar_a. Flowrate of steam and CO_2 was selected on the basis that no solid carbon is formed in the syngas.

Some assumptions are, steady state and isothermal process, temperature and pressure are uniform in the RGibbs, no heat and pressure loss and no tar formation. The ash was separated from the produced gas in the cyclone separator while the subsequent syngas adjustment was done in the REquil reactor (shift reactor) with adding steam basis on restricted chemical equilibrium approach. The restricted equilibrium is defined with specific chemical reaction and zero temperature approach. The REquil reactor calculates chemical equilibrium constant at specified temperature thereby giving the equilibrium gas composition. Firstly, minimum amount of steam supply to WGSR to get a target amount of CO (0.6 kmol/h or 0.7%) in the product gas of shift reactor. The shift reactor was operated at temperature of 200 °C and 1 bar_a with controlled amount of steam for CO conversion to boost the hydrogen productivity. A fraction of syngas was combusted in the RGibbs at 200 °C and 1 bar_a to balance the heat load of a gasifier when no CSP-thermal energy is available.

The process input parameters for a biomass was based on ultimate and proximate analysis of wheat straw. The proximate analysis as fixed carbon (FC), volatile matter (VM), ash (ASH) and ultimate analysis as carbon (C), hydrogen (H), oxygen (O), nitrogen (N) and lower heating value (LHV) of the investigated biomass is given in the Table 5.1.2(i). These values were used in the developed model. The chlorine and sulfur content was ignored, because of the small quantities, which have little effect on the simulation results. The syngas cleanup was simplified as a separation unit.

5.1.3: Results and Discussions

The effect of temperature on performance of steam gasification of biomass at temperature (600-1000 °C) and pressure 1 bar$_a$ is shown in Figure 5.1.3(i). By adding CSP-thermal energy to the gasifier, almost 20% of syngas can be saved. Figure 5.1.3(ii) (a and b) is for steam gasification, describing about H_2 production without CSP, H_2 production with CSP, H_2 productivity, H_2 boost up (in %) and H_2 production efficiency in terms of CSP-solar-thermal energy injection with respect to temperature.

Figure 5.1.3(ii) (a) shows that when no CSP-thermal energy is available, the maximum amount of H_2 is about 48 kmol/h at 800 °C. When CSP-thermal energy is available, the produced amount of H_2 reached to 58 kmol/h at same temperature. It means that using CSP can increase the H_2 productivity by 10 kmol/h. The proposed system shows that an opportunity to convert solar energy into H_2 fuel. Figure 5.1.3(ii) (b) shows that adding CSP into the system can boost hydrogen production by 10% at 600 °C and over 15% for temperature range from 700-900 °C. Results also showed that the hydrogen production efficiency increased from 9.36 kmol/MW$_{th}$ to 14.4 kmol/MW$_{th}$ as gasification temperature increased from 600 to 800 °C, but dropped slightly to 14.3 kmol/MW$_{th}$ when the temperature increased further. This indicates that 800 °C is the best temperature for this operation.

The effect of temperature on performance of CO_2-gasification of biomass at temperature (600-1000 °C) and pressure 1 bara is shown in Figure 5.1.3(ii). The heat duty of a gasifier with CO_2 as a gasifying agent is slightly higher than steam as a gasifying agent. Figure 5.1.3(ii) (a and b) is for CO_2-gasification, describing about H_2 production without CSP, H_2 production with CSP, H_2 productivity, H_2 boost up (in %) and H_2 production efficiency in terms of CSP-solar-thermal energy injection with respect to temperature. Figure 5.1.3(ii) (a) shows that when no CSP-thermal energy is available the maximum amount of H_2 is about 49 kmol/h at 800 °C. When CSP-thermal energy is available, the produced amount of H_2 reached to 59 kmol/h at same temperature. It means that using CSP will increase the H_2 productivity of 10 kmol/h. The proposed system shows that an opportunity to convert solar energy into H_2 fuel. Figure 5.1.3(ii) (b) shows that for CO_2-gasification case, adding CSP into the gasification can boost hydrogen production by 25% between 600-1000 °C, while the hydrogen production efficiency peaked

also at 700 °C to 14.42 kmol/MW$_{th}$. For a fixed amount of biomass, the hydrogen produced from a CO_2 gasification process is slightly more (0.02 kmol/MW$_{th}$) than the steam gasification process. While for the hydrogen production efficiency, the steam gasification process has a very little advantage. In CO_2-gasification case, 700 °C is the best gasification temperature providing the best efficiency.

Adding solar into steam and CO_2-gasification offers a substantial benefit to boost H_2 production from biomass gasification. At 800 °C, the heat load is 0.66 MW$_{th}$ for steam-gasification case while it is 0.687 MW$_{th}$ for CO_2-gasification of biomass. The heat load for CO_2-gasification is slightly higher (0.027 MW$_{th)}$ than steam gasification but it has several advantages; alternative option to utilize CO_2 and less corrosive gasification system. In CO_2-gasification, the heat load of a gasifier unit is varied with temperature in the range of 0.7-0.8 MW$_{th}$. As the limitation of the available heat storage temperature, 700–800 °C might be the best temperature for the concentrated solar-assisted steam or CO_2-gasification system. The available experimental work on H_2 production per kg of wheat straw biomass is 30 g/kg biomass [19], 46 g/kg biomass [20] and the maximum is 128 g/kg of dry ash-free biomass [21].

In order to validate the model for both cases, a comparison has been made between H_2 production obtained through gasification from developed model with already mentioned experimental data. For comparison, the predicted simulation results were obtained by running the model at 800 °C. Without CSP, for steam-gasification case, it is 96 g/kg of wet biomass while for CO_2-gasification, it is 98 g/kg of wet biomass. With CSP, for steam gasification case, it is 117 g/kg of wet biomass and for CO_2-gasification, it is 119 g/kg of wet biomass. It can be observed that the present model shows acceptable values of H_2 production as found in the experiments. The model predicted higher values because model does not consider the formation of tar and higher hydrocarbons in the syngas. Both models predicted H_2 efficiency of 14-15 kmol per MW$_{th}$. This study provides a parametric analysis to transform biomass, solar and CO_2 into valuable and carbon-neutral alternative fuels. Steam or CO_2 gasification with shift reaction is a promising technology to produce H_2 as an alternative fuel or to adjust the H_2/CO molar ratio as required.

5.1.4: Conclusion

In conclusion, we have found that in both steam and CO_2 gasification processes, the best gasification temperature is 700-800 °C with hydrogen production efficiency at 14.5 kmol/MW$_{th}$. Higher H_2 recovery with application of CSP technology showing that solar energy can play a vital role in thermochemical conversion biomass gasification process. There is no significant difference between steam gasification and CO_2-gasification regarding efficiency. The results are promising, which makes the hybrid CSP steam or CO_2-gasification process a good option to convert renewables resources (biomass and solar) into H_2 fuel.

Note: This paper is published in proceedings of the 26th International Conference on Concentrating Solar Power and Chemical Energy Systems SolarPACES-2020.

Tables

Table 5.1.2(i): The ultimate and proximate analysis and lower heating value (LHV) of biomass[18] (* oxygen by difference)

Sr. No.	Material	Moisture content (%) by weight (wet basis)	Proximate analysis (%) by weight (dry basis)			Ultimate analysis (%) by weight (dry basis)				LHV MJ/kg (dry basis)
			FC	VM	ASH	C	H	O*	N	
1	Wheat straw	8.87	10.98	82.12	6.90	42.95	5.35	46.99	0.00	17.988

Figures
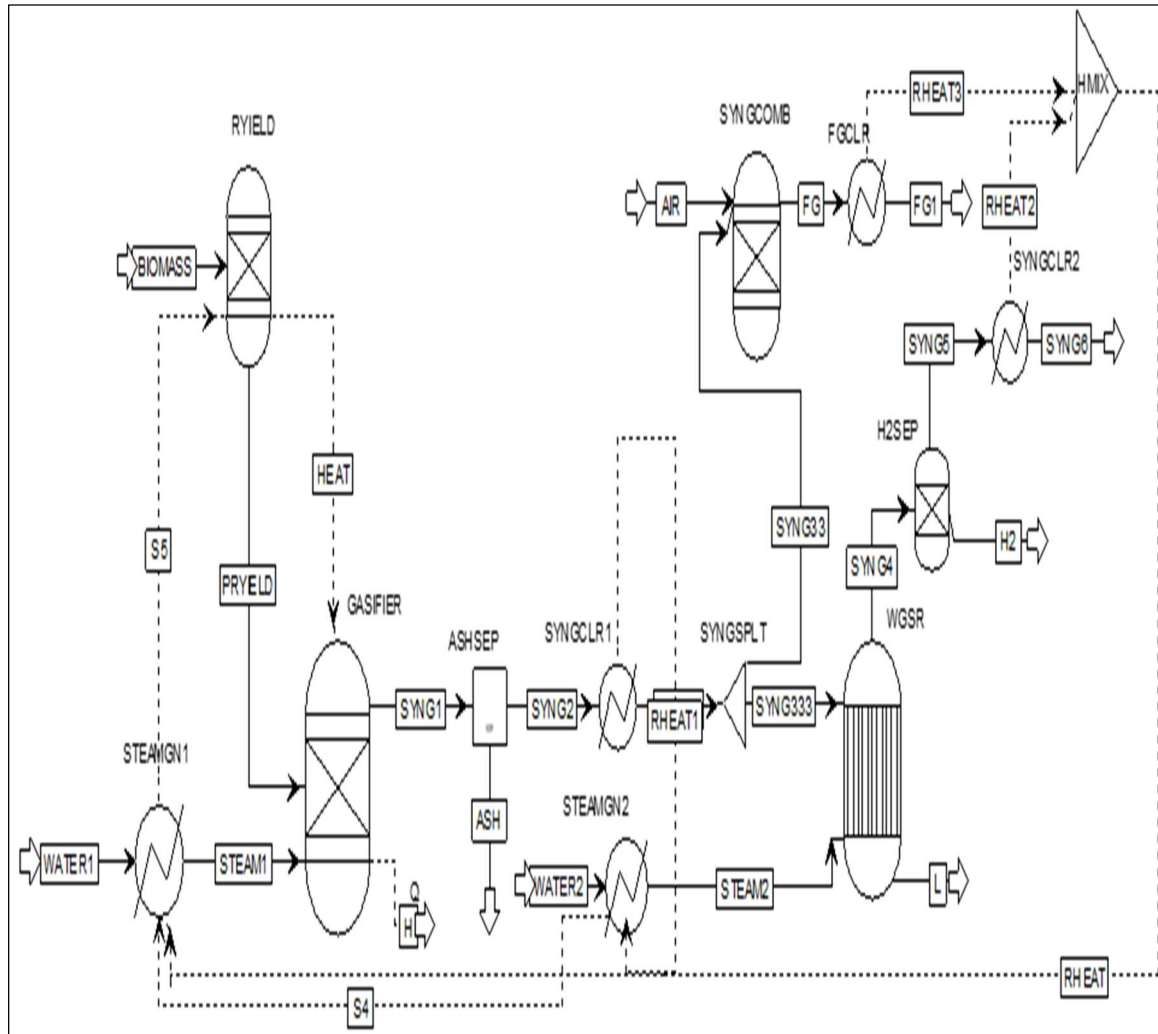

Figure 5.1.2(i): Process flowsheet of biomass gasification with subsequent syngas adjustment with water gas shift reaction.

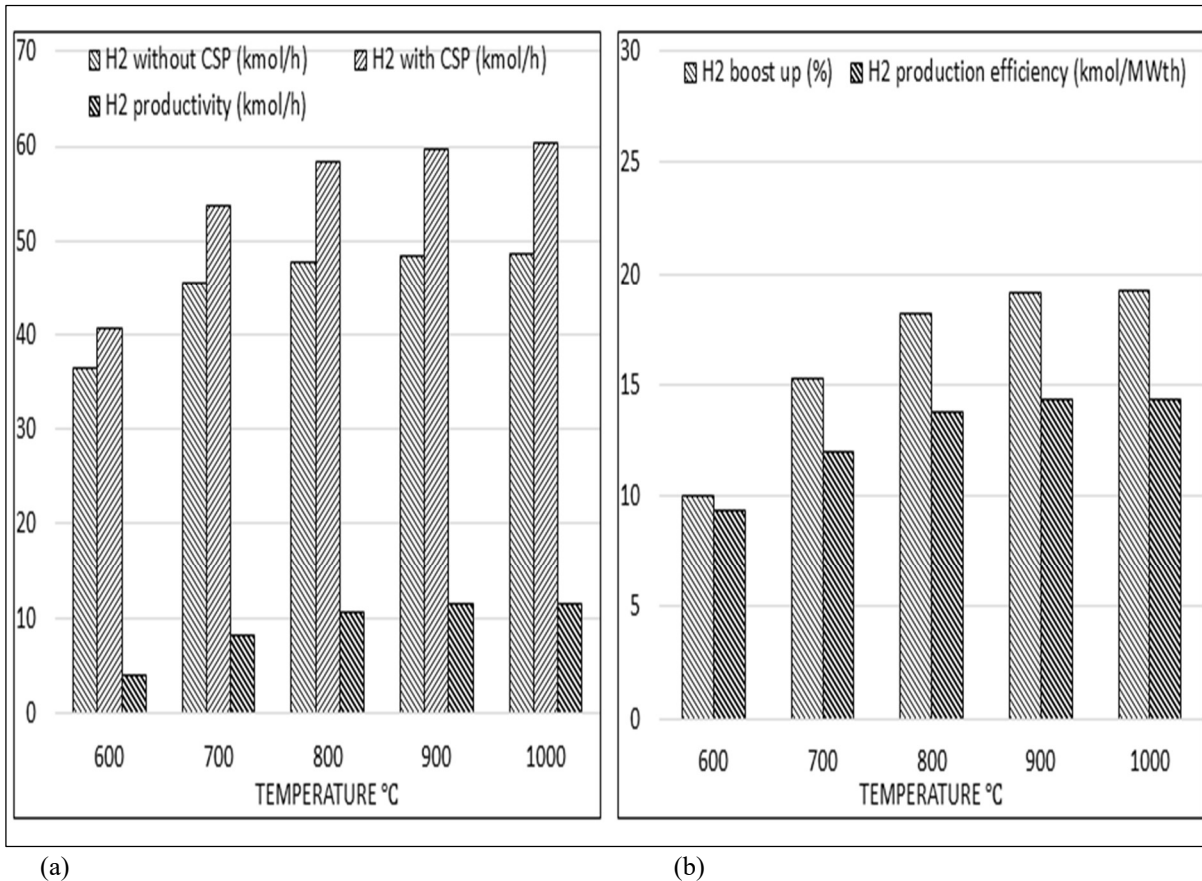(a)   (b)

Figure 5.1.3(i) (a) Effect of temperature on H_2 without CSP, H_2 with CSP and H_2 productivity. (b) Effect of temperature on H_2 boost up and H_2 production efficiency by steam-gasification of biomass.

* H_2 without CSP is the amount of H_2 produced after WGSR, as a fraction of syngas is combusted to balance the heat load of a gasifier at specified temperature while remaining syngas is shifted through WGSR

** H_2 with CSP is the amount of H_2 produced after WGSR, CSP-thermal energy is used to balance the heat load of a gasifier at specified temperature while the whole syngas from gasifier is passed through WGSR

*** H_2 productivity in the increase of amount of H_2 boosted by injection of CSP-thermal energy into gasification system

**** H_2 boost up is calculated as the percent increase in H_2 production by the injection of CSP-thermal energy to gasifier

***** H_2 production efficiency is calculated as H_2 productivity divided by the heat load of a gasifier, i.e. the CSP thermal energy injected to the gasification process
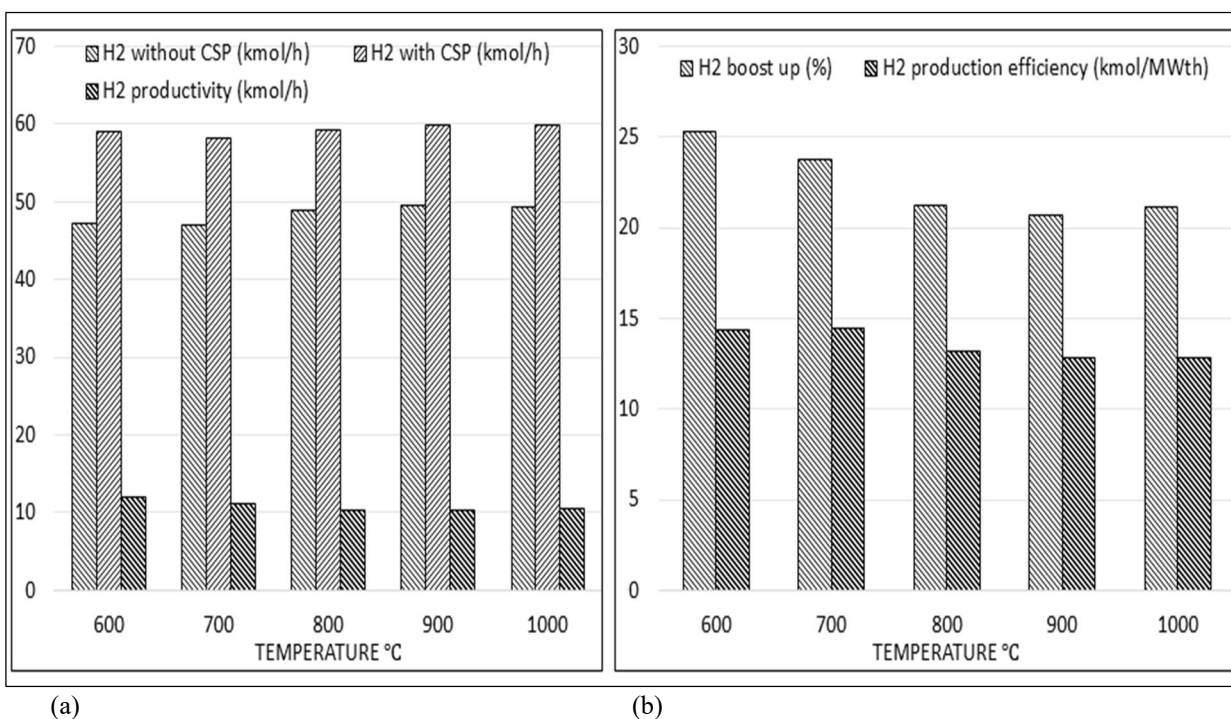
(a) (b)

Figure 5.1.3(ii) (a) Effect of temperature on H_2 without CSP, H_2 with CSP and H_2 productivity. (b) Effect of temperature on H_2 boost up and H_2 production efficiency by CO_2-gasification of biomass.

References

[1] E. Shafiei, B. Davidsdottir, J. Leaver, H. Stefansson, and E. I. Asgeirsson, "Energy, economic, and mitigation cost implications of transition toward a carbon-neutral transport sector: A simulation-based comparison between hydrogen and electricity," *J. Clean. Prod.*, vol. 141, pp. 237–247, Jan. 2017

[2] I. Dincer and C. Acar, "Review and evaluation of hydrogen production methods for better sustainability," *Int. J. Hydrogen Energy*, vol. 40, pp. 11094–11111, 2015

[3] P. Nikolaidis and A. Poullikkas, "A comparative overview of hydrogen production processes," *Renew. Sustain. Energy Rev.*, vol. 67, pp. 597–611, 2017

[4] L. Cao *et al.*, "Biorenewable hydrogen production through biomass gasification: A review and future prospects," *Environ. Res.*, vol. 186, p. 109547, Jul. 2020

[5] Shahid H. Ansari and X. Liu, "Aspen Plus hybrid CSP biomass CO2-gasification process for power production: Aspen Plus simulation," in SolarPACES-2019

[6]   E. G. Hertwich and X. Zhang, "Concentrating-solar biomass gasification process for a 3rd generation biofuel," *Environ. Sci. Technol.*, 2009

[7]   Z. Bai, Q. Liu, J. Lei, H. Hong, and H. Jin, "New solar-biomass power generation system integrated a two-stage gasifier," *Appl. Energy*, vol. 194, pp. 310–319, May 2017

[8]   R. Milani, A. Szklo, and B. S. Hoffmann, "Hybridization of concentrated solar power with biomass gasification in Brazil's semiarid region," *Energy Convers. Manag.*, vol. 143, pp. 522–537, 2017

[9]   M. Vidal and M. Martín, "Optimal coupling of a biomass based polygeneration system with a concentrated solar power facility for the constant production of electricity over a year," *Comput. Chem. Eng.*, vol. 72, pp. 273–283, Jan. 2015

[10]   S. Pramanik and R. V. Ravikrishna, "A review of concentrated solar power hybrid technologies," *Appl. Therm. Eng.*, vol. 127, pp. 602–637, Dec. 2017

[11]   S. Banacloche, I. Herrera, and Y. Lechón, "Towards energy transition in Tunisia: Sustainability assessment of a hybrid concentrated solar power and biomass plant," *Sci. Total Environ.*, vol. 744, p. 140729, Nov. 2020

[12]   L. P. R. Pala, Q. Wang, G. Kolb, and V. Hessel, "Steam gasification of biomass with subsequent syngas adjustment using shift reaction for syngas production: An Aspen Plus model," *Renew. Energy*, vol. 101, pp. 484–492, Feb. 2017

[13]   J. Han *et al.*, "Modeling downdraft biomass gasification process by restricting chemical reaction equilibrium with Aspen Plus," *Energy Convers. Manag.*, vol. 153, pp. 641–648, Dec. 2017

[14]   K. Im-orb, L. Simasatitkul, and A. Arpornwichanop, "Techno-economic analysis of the biomass gasification and Fischer-Tropsch integrated process with off-gas recirculation," *Energy*, vol. 94, pp. 483–496, Jan. 2016

[15]   M. S. Herdem, D. Mazzeo, N. Matera, J. Z. Wen, J. Nathwani, and Z. Hong, "Simulation and modeling of a combined biomass gasification-solar photovoltaic hydrogen production system for methanol synthesis via carbon dioxide hydrogenation," *Energy Convers. Manag.*, vol. 219, p. 113045, Sep. 2020

[16]   H. Ishaq and I. Dincer, "A new energy system based on biomass gasification for hydrogen and power production," *Energy Reports*, vol. 6, pp. 771–781, Nov. 2020

[17]   A. M. Sharma, A. Kumar, S. Madihally, J. R. Whiteley, and R. L. Huhnke, "Prediction of biomass-generated syngas using extents of major reactions in a continuous stirred-tank reactor," *Energy*, vol. 72, pp. 222–232, Aug. 2014

[18]   S. A. Channiwala and P. P. Parikh, "A unified correlation for estimating HHV of solid, liquid and gaseous fuels," *Fuel*, vol. 81, pp. 1051–1063, 2002

[19]   M. Kraussler, M. Binder, P. Schindler, and H. Hofbauer, "Hydrogen production within a polygeneration

concept based on dual fluidized bed biomass steam gasification," *Biomass and Bioenergy*, vol. 111, pp. 320–329, Apr. 2018

[20]   S. Fail *et al.*, "Wood gas processing to generate pure hydrogen suitable for PEM fuel cells," *ACS Sustain. Chem. Eng.*, vol. 2, no. 12, pp. 2690–2698, Dec. 2014

[21]   S.Turn, C.Kinoshita, Z.Zhang, D.Ishimura, and J.Zhou, "An experimental investigation of hydrogen production from biomass gasification," *Int. J. Hydrog. Energy August 1998,* vol. Volume 23, no. Issue 8, p. Pages 641-648, 1998

Chapter 6: Hybrid CSP Biomass CO$_2$-gasification Process

6.1: Hybrid CSP Biomass CO$_2$-gasification Process for Power Production

Generally, biomass gasification takes place in the presence of a gasifying agent such as steam, air, oxygen or carbon dioxide (CO$_2$), or any combination of these gasifying agents. There have been recent interests of utilizing CO$_2$ as a gasification agent, with the advantage of less tar production and better char quality. In this study, CO$_2$ is used as a gasifying agent in the hybrid CSP-biomass integrated gasification combined cycle (IGCC) process for power generation and the simulation results were compared with CSP – biomass steam IGCC system. The aim is to assess the potential use of CO$_2$ as a gasifying agent and to learn more about its effects on the gasification process. In this study, Aspen Plus was used to develop a simple model for CSP-assisted biomass gasification to produce synthetic gas (syngas). This was followed by an integrated gasification combined cycle (IGCC) system for power production.

The effect of operating temperature of the gasification system was studied to determine the optimum temperature. It was found that gasification temperature of about 800 ºC is good enough to achieve maximum energy efficiency. The peak net efficiency of hybrid CO$_2$-gasification IGCC system is 46% which is slightly higher than steam IGCC process which is 45%; it is higher than other hybrid options found in the literature. A solar thermal to power efficiency of 55% is achieved in hybrid CO$_2$ gasification which is less than hybrid steam gasification which is 58%. Hybrid CSP CO$_2$-biomass IGCC is a promising process for dispatchable power supply.

Use CO$_2$ as gasification agent will help to mitigate the greenhouse gases (GHG) emissions mainly carbon dioxide (CO$_2$) which is a major cause of global warming and serious health issues [1], [2]. There have been several experimental and simulation studies using CO$_2$ or CO$_2$/steam to enhance the gasification of carbonaceous feedstock [3], [4]. Marco J. Castaldi et al. have presented a novel catalytic combustion (steam CO$_2$-coal gasification) concept to gasify coal into syngas followed by hydrogen separation and power generation. The process was

carried out with recycling up to 25% of CO_2 to the gasifier which results with extra hydrogen and higher power production [5]. Renganathan et al. have studied thermodynamics analysis of utilization of CO_2 for biomass gasification based on Gibbs minimization approach using Aspen Plus® [4]. They have reported that the use of CO_2 has influenced on more CO but less H_2 in syngas and 850 °C is optimal temperature with a wide-ranging ratio of H_2/CO.

In a hybrid CSP biomass steam IGCC system proposed by us [6], solar-thermal energy through concentrated solar energy (CSP) is incorporated into a biomass gasifier unit to increase the yield of syngas to boost power produced from a gas turbine. It would be interesting to compare the performance of hybrid CSP biomass CO_2-gasification and hybrid CSP biomass steam-gasification in terms of energy efficiency. In the present study, a thermodynamics analysis of biomass gasification using CO_2 is carried out on the basis of Gibbs free energy minimization approach using Aspen Plus® process simulator. The performance is analyzed in terms of energy efficiency with solar and without solar. A comparative study has been performed to evaluate the advantages and disadvantages of steam and CO_2 as a gasifying agent. Further, hybrid CSP biomass CO_2-gasification to power is studied. Finally, optimum operating conditions for CSP biomass CO_2-gasification are investigated.

6.1.1: Process Modelling and Simulation Details

Thermodynamic modelling of biomass CO_2-gasification process can be done using Gibbs free minimization approach. An integrated system model was developed for power generation using a biomass gasifier with CO_2 as a gasifying agent followed by syngas combustion turbine. CO_2-gasification of biomass is an endothermic and highly energy-intensive process. The heat needed for gasification is normally provided by combustion of biomass, inside the gasification or externally through syngas combustion or CSP. The gasification unit utilize external heating to provide the energy needed. The heat recovery steam generation system for power generation by steam turbine was also introduced. The developed model was studied to predict gasifier performance, energy efficiency of IGCC system, with or without CSP. The process was modeled for a plant with a capacity of 1000 kg/h of wet biomass feedstock. The solar energy contribution of the CSP system was modeled in terms of solar-thermal heat injection into the gasifier unit. When there was no CSP, combustion of syngas was introduced to balance the heat

load of the gasifier. The share of solar thermal energy into the gasification system results in more syngas per unit of biomass.

The Aspen plus$^®$ model with a process flowsheet shown in Figure 6.1.1(i) was used to simulate the potential of a hybrid CSP CO_2-biomass IGCC of wheat straw. The process uses concentrated solar power as heat for the gasification process when sun is available, while heat from the combustion of produce gas is used during no-sun hours to ensure a continuous process. The char and ash separated from the produce gas in the cyclone separator while the syngas is combusted in the gas turbine to produce mechanical power that drives electrical generator. The heat from exhaust gases of the gas turbine and that from hot syngas is recovered in heat recovery steam generators (HRSG) to produce steam that drives steam generators for electrical power production.

This model was run based on the following general assumptions; steady state operation, moisture content of the biomass was adequate for CO_2 gasification of the biomass, heat loss from the piping network was negligible, ambient conditions are constant, peak electric power generation and adiabatic conditions and no pressure drop in combustors and heat exchangers.

Thermodynamics equilibrium-based RGibbs model was used to simulate the biomass gasification process. Wheat straw was selected as the biomass feedstock[7]. The biomass was gasified at a temperature of 600-1000 °C @ 1 bar$_a$ with a controlled amount of CO_2, so that no solid carbon formed. The gasifying agent (CO_2) was fed at ambient temperature and pressure. The proximate analysis as fixed carbon (FC), volatile matter (VM), ash (ASH) and ultimate analysis as carbon (C), hydrogen (H), oxygen (O), nitrogen (N) and lower heating value (LHV) of the investigated biomass is given in the Table 6.1.1(i). The contents of chlorine and sulfur were ignored, because of the small amounts, which have little effect on the simulation results. The syngas cleanup was simplified as a separation unit. The produced syngas is cooled down to remove water and other impurities before compressed and sent to syngas turbine for power generation. The heat from the hot syngas from the gasification unit and exhaust gas of the syngas turbine is recovered in heat recovery steam generation (HRSG) system to produce more power.

The IGGC model was based on a combined cycle using a syngas combustion turbine (Brayton cycle) and steam turbine (Rankine cycle). The combustion turbine was operated at 1200 °C and 15 bar_a with exit at 585 °C @ 1 bar_a. The super-heated steam was generated using a heat recovery steam generation (HRSG) system to recover heat from hot syngas in the gasifier and hot flue gases in the combustion turbine. The steam turbine was operated at 125 bar_a and 570 °C with exit at 20 °C @ 0.02 bar_a. Energy efficiency and solar efficiency is calculated for biomass CO_2-gasification and IGCC system. The cogeneration gas-steam combined cycle is an environmentally friendly technology that produces high energy efficiency for power generation system.

6.1.2: Results and Discussion

The effect of temperature on performance of a gasifier for CO_2-gasification of biomass is shown in Figure 6.1.2(a and b). The Figure 6.1.2(a and b) shows the effect of energy efficiency (E.E.) for IGCC without CSP, IGCC with CSP, net energy efficiency, cold gas efficiency and solar efficiency with respect to temperature. The simulation results show that energy efficiency for IGCC system without CSP is varying from 38% to 46% for CO_2-gasification while it is varying from 38% to 43% for steam gasification.

The energy efficiency for IGGC system integrated with CSP is in the range of 60-68% for CO_2-gasification while it is 52-59% for steam gasification. The results showed that the energy efficacy can be boost up to 32% by application of CSP into CO_2-gasification while 30% for steam gasification. The net energy efficiency is varying from 36-48% for CO_2-gasification while it is 42-46% for steam gasification and solar energy efficiency is in the range of 34-55% for CO_2-gasification while it is 57-58% for steam gasification.

Adding solar into gasification offers a substantial benefit because it reduces electricity prices, reduces the need to build additional power plants to meet power demand and promotes energy security. Adding solar thermal energy through CSP for CO_2-gasification is less than steam gasification but it has several advantages; less CO_2 emissions, alternative option to utilize CO_2, more reactive char, more flexibility in H_2/CO ratio and less corrosive gasification system. In CO_2-gasification, the heat load of a gasifier unit is varied with temperature. As the limitation of the available heat storage temperature, 750 – 800 °C might be the best temperature for the

concentrated solar-assisted biomass CO_2-gasification system. The available CSP power generation methods and energy efficiency are presented in Table 6.1.2(i). The solar energy efficiency observed by proposed CSP-CO_2-gasification with IGCC system is 55%, which is still in comparable range for CSP-steam gasification power generation method. The main outcome of this simulation work is that to utilize CO_2 as a gasifying agent in a hybrid CSP-biomass gasification is still better than available CSP power generation methods with higher energy efficiency.

6.1.3: Conclusions

CO_2-gasification of biomass shows the potential benefit on slightly higher energy efficiency with less GHG emissions to the environment as compared to hybrid CSP biomass steam-gasification. The increase in energy efficiency is a good indicator to meet power demand. However, the study reveals that solar thermal to power efficiency for CO_2-gasification system is slightly less than steam-IGCC system. The results are promising, which makes the hybrid CSP-CO_2-gasification process a good option to convert renewables resources (biomass and solar) into electricity.

Note: This paper is already published in proceedings of the 25th International conference on concentrating solar power and chemical energy systems SolarPACES-2019.

6.2: Supercritical Carbon Dioxide Cycle for Power Generation

Hybrid CSP biomass gasification process with supercritical carbon dioxide (sCO_2) cycle for power generation was numerically investigated by aid of Aspen Plus® simulation model from which data was generated and further processed to determine the system efficiencies. The system comprised of sCO_2 Brayton cycle integrated to solar aided biomass gasification that utilized the sCO_2 –rich gases from a pressurized combustor to run closed loop recompressed sCO_2 Brayton cycle for mechanical power generation. Specifically, the influences of sCO_2 turbine inlet and outlet pressures and the amount of sCO_2 recycled back to the combustor in relation to net thermal efficiency of the system were examined.

Further, comparisons to performances of the systems with indirect heating of the sCO_2 and that without solar power input were done. The results show that net thermal efficiency of about 60% is attainable, which is better than most biomass based IGCC. Recycling sCO_2 back to the combustor dilutes the syngas in the combustor and thus oxy-combustion at lower temperatures are attainable. This points to a potential highly efficient Allam cycles operating at a practical condition for the current IGCC equipment technology. Further, higher inlet turbine pressure safeguards stable efficient operation of the Allam cycle for a wider range of exit pressures. Additionally, solar-assisted Allam cycle affords higher net thermal efficiencies because of the extra power which is attained by avoiding combustion of syngas to provide heat for gasification. Further, it is shown that the performance of the system is superior to that of indirectly heated sCO_2 and that without solar aid. The injected solar power boosts the power output as high as 52% and its conversion efficiency is about this value. Thus, the solar aided Allam cycle looks promising.

6.2.1: Introduction

There has been recent interest of applying supercritical carbon dioxide (sCO_2) Brayton cycle in CSP applications for power generation. The closed loop recompression sCO_2 offers the potential of equivalent or higher cycle efficiency versus supercritical or superheated steam cycle at temperature relevant for CSP applications, with a potential simple and compactable design resulting in lower installation, maintenance, and operation cost of the system. To avoid heat storage, other fuels can be used to provide heat to the system during off-sun hours, e.g. biomass. Nevertheless, direct combustion of biomass cannot be used because its combustion temperature is lower than what is required in sCO_2 cycles. On the contrary, combustion temperature of syngas is high enough for operation of sCO_2 [17].

Besides, biomass is considered carbon neutral and thus emitting carbon dioxide from a combustion of syngas yielded from biomass is less harmful to the environment than natural gas and coal based integrated gas combined cycles (IGCC). The experimental studies of such IGCCs are limited in literature. However, the scholarship on numerical modelling of biomass gasification is advancing. The work of Lan, Chen [18], Tavares, Monteiro [19] Ansari and Liu [20] and others have provided a solid foundation for simulation of biomass gasification using Aspen

Plus. McClung, Brun & Chordin [21], Milani, Luu, McNaughton & Abbas [22] reported on simulations of the sCO_2 Brayton cycle. Hence, tapping from these studies and integrating the biomass and sCO_2 simulation models gives a platform of exploring an integrated system that employs solar thermal energy for biomass gasification whose syngas is combusted in pressurized combustor in the presence of pure oxygen to produce exhaust gases reach in sCO_2 and water that are expanded in sCO_2 turbine to produce work.

There are many areas that can be investigated to show technical and economic feasibility of a closed loop recompression sCO_2 cycle integrated to solar biomass gasification. To get first insight of such a system, this work investigates the influence of sCO_2 turbine pressure ratio, inlet pressure, and the amount of sCO_2 recycled back to the combustor. Further, comparisons to performances systems with indirect heating of the sCO_2 and that without solar power input are done.

6.2.2: Methodology

The proposed hybrid CSP Biomass Gasification Process with sCO_2 Cycle for power generation was numerically investigated in Aspen Plus® simulation platform. Simulations runs yielded data that was further processed to determine the effect of recycled sCO_2 on combustion temperature, turbine power output, and sCO_2 concentration in in the turbine. Additionally, the generated data enabled an examination basis on sCO_2 turbine inlet and exit pressures in relation to their influence on the net thermal efficiency. The description of the Aspen Plus® model and the simulation data processing procedures are detailed under model description and post data processing sections that follow.

6.2.3: Aspen Plus Model Description

Figure 6.2.3 depicts schematic diagram of the Allam cycle considered in this study. It is a typical Allam cycle that converts solid biomass wastes to syngas via allothermal gasification that utilizes CO_2 as gasification agent. The hybrid system (not dipicted in the figure) consisting of concentrated solar power (CSP) and combusted of syngas meets heat load (+Q1) of the gasification process. However, a performance comparison is conducted for: Allam cycle with

solar assist (AC_SA); Allam Cycle without solar assist (AC_WSA); IGCC with an indirect supercritical carbon dioxide Brayton cycle (ISC_IGCC).

The gasification utilizes biomass from agricultural wastes with sCO_2 as gasifying agent. The gasification process was assumed to be in thermodynamic and chemical equilibrium, as such the process was modeled using Gibbs free energy minimization method. RYield and RGibbs reactor models in Aspen Plus were correspondingly used to obtain elemental yields of the biomass and gasify the biomass to yield syngas at chemical equilibrium composition. The sCO_2 feed rate was controlled to yield syngas with zero solid carbon and ash was assumed to be the only solid present in the syngas which was subsequently separated from the gaseous phase in the separator model. This gasification process proceeded at 700 °C. During simulations, PENG-ROB method predicted thermodynamic properties.

To improve system performance, the heat from the hot syngas was recovered in heat recovery steam generator (HRSG) whose steam powered a low temperature steam turbine to produce mechanical power. Pumping power for feed water to HRSG was manipulated in way that the water flow could be just enough to achieve steam quality of 1 at 125 bars and 328 °C. STEAM-TA method estimated thermodynamic properties of water in the Rankine steam cycle model. The syngas was cooled to 60 °C in heat recovery steam generator (HRS) before knocking out water using flash model. The gas free of raw water was then cleaned of N_2 and water vapor before being pressurized to sCO_2 and then combusted in presence of pure oxygen, which was also pressurized to match sCO_2 pressure. The combustion was assumed to undergo stoichiometric reaction and hence RSTOIC reactor model was used for the combustion process. The combustion reactions produced H_2O (g), and sCO_2 from a complete oxy-combustion of the clean syngas.

The high temperature sCO_2:H_2O mixture was expanded in a turbine to produce mechanical power. It was envisaged that the stream from the combustor would be rich in sCO_2 because of the refeeding of sCO_2 into the combustor and hence the Brayton cycle was regarded as sCO_2 based. To improve thermodynamic performance of the Brayton cycle, exhaust gases were utilized to preheat CO_2 streams that were recycled to combustor as well as the gasifier.

Further, the air separation unit was modelled by compressing air (at ambient condition) to 7 bar pressure before separated to pure oxygen and nitrogen in the separator model. The separated oxygen was further compressed to match the operating pressure of sCO_2.

6.2.4: Post Data Processing

The exploration of the system's responses to different operating conditions was achieved through sensitivity analyses which varied sCO_2 turbine outlet and inlet pressures as well sCO_2 to biomass ratio (mass flow ratio of sCO_2 recycled to combustor and biomass feed). For each variation step, the design specification blocks were used to manipulate the flows of air, sCO_2 to the gasifier, and feed water to HRSG to correspondingly achieve zero oxygen in the combust gases; zero solid carbon in syngas and steam quality of 1. The transfer blocks were used to equalize the operation pressure in all units that required pressure input.

At each step of the sensitivity analyses, net-work of sCO_2 and steam turbines (WT as well as net-work required for compressors (WC) and pump (WP) were read and recorded. These values in conjunction to literature values of low heating value of biomass ($LHV_{Biomass}$) and the Q_{solar} (CSP power injected into the gasifier to meet its heat load) were used to calculate the net thermal efficiency of the entire system by using equation (1). However, the heat losses in the pipe networks and other system accessories were regarded negligible when compared to power required in the turbines, compressors and pump.

$$Net \ thermal \ efficiency = \frac{\sum WT - \sum Wc - W}{LHV Biomass + Q} \qquad (1)$$

In case of the solar aided gasification, the syngas that could otherwise be combusted to provide heat of gasification is utilized in the power production. Hence, the difference in the net mechanical power (NMPs) of the system with solar assistance and that without (NMPns) is regarded as additional power arising from solar injection into the system. Therefore, the

conversion efficiency of the injected solar power to mechanical power was calculated using equation (2).

$$solar \text{ to mechanic}al \text{ } power \text{ } efficiency = \frac{NMPs - NMPns}{Solar \text{ } power \text{ } injected \text{ } to \text{ } gasifier} \qquad (2)$$

6.2.5: Results and Discussion

The effect of recycled sCO_2 on combustor temperature; sCO_2 turbine power output; and concentration of sCO_2 in the sCO_2 turbine are shown in Figure 6.2.4(i). The amount of recycled sCO_2 is presented as the ratio of mas flows of recycled sCO_2 and biomass feed (sCO_2/biomass ratio). Considering that biomass feed was fixed at 1000kg/hr, then sCO_2/biomass ratio > 1 implies sCO_2 recycle in the excess of 1000 kg/hr. The blue curve seen in Figure 6.2.4 shows that when sCO_2 is not recycled to the combustor, the combustion process at temperatures too high for practical applications considering limitations of materials that can withstand high temperatures. However, a steep gradient at the beginning of the curve entails that slight recycling of sCO_2 into the combustor, sharply decreases the combustion temperature due to extinguishing effects of sCO_2 during combustion process. However, when temperatures <1000 °C is attained, there is a slow decrease of combustion temperature. Despite slow combustor temperature reduction, further increase of sCO_2 amount increases both the sCO_2 turbine power output and sCO_2 concentration.

Attainment of ~97% sCO_2 concentration in the turbine at practical temperatures within 750-850 °C ensures operation of the turbine in the very near conditions of pure sCO_2 turbines employed in indirect sCO_2 Brayton cycles. Besides, the sharp increase of turbine power to as high as 80-90% more power than when there is no recycle safeguards the potential of producing adequate power that can overcome the power it takes to compress the recycled sCO_2 back to combustor and thus ensuring positive net power.

Figure 6.2.4(i) depicts the influence of inlet and exit sCO_2 turbine pressures on net thermal efficiency of the system. The results are for a system that was operated at 800 °C combustor temperature and thus yielding at least 80% more turbine power and higher (~97%) sCO_2 concentration as can be read from Figure 6.2.4(i). As can be seen from dotted curves in the figure, inlet pressure <200 bar does not favor efficient operation of the system higher exit pressures. The energy efficiencies sharply drops for exit pressures more than 10 bars. This can be attributed to the fact that a wider pressure drop is required in for the turbine to produce substantial amount of power. Nonetheless, these low- pressure operated turbines exhibited highest net thermal efficiency as high as 60%. However, the sudden drop in the efficiencies when the exit pressure is increased beyond 10 bar is due to much work, which is expended in compressing carbon dioxide (CO_2) from its subcritical conditions to supercritical conditions It is also shown that if the inlet pressure is more than 300 bar, the system can operate at stable efficiencies for a wider range of exit pressures. (See the solid lines in Figure 6.2.4(i)) The gradual decline in efficiency for high inlet and exit pressures can be attributed to less power which is needed to compress CO_2 to supercritical conditions as well as the wider pressure drop across the turbine.

The peaks shown in Figure 6.2.4(ii) suggest that for an efficient operation of Allam cycle, there is limiting exit pressure despite the general knowledge that lowering exit pressure of turbine increases the power output. Although the system was not optimized and that it used a simple model, it is encouraging to not that peak net thermal efficiencies of the investigated system ranges from 40 to 60%. This gives hope that with an improved model and proper optimization, an Allam cycle with a net thermal efficiency of about 60% is attainable and can be better than those of the current IGCCs [23].

Figure 6.2.4(iii) shows a comparison of the following in relation to their net thermal and solar-to-mechanical power efficiency: Allam cycle with solar assist (AC_SA); IGCC with an indirect supercritical carbon dioxide Brayton cycle (ISC_IGCC); and Allam Cycle without solar assist (AC_WSA). For purposes of comparison, the AC_SA that yielded 61% net thermal efficiency shown in Figure 6.2.4(iii) was used against ISC-IGCC and AC_WSA operated at similar conditions. AC_SA offered highest net thermal efficiency out of all systems compared.

This shows the superiority of utilizing solar heat in meeting gasification heat load as shown. With the trend in high powered CSP, research aimed at developing solar aided Allam cycles will be worth pursuing.

Further, evaluation of equation (2) at all sCO_2/Biomass ratio indicate that when solar power is utilized in biomass gasification, its conversion efficiency i.e. solar-to-mechanical-efficiency can be as high as 52% and the system's power performance can improve by the same percentage. However, a lower conversion efficiency is expected when direct normal irradiance (DNI) is considered instead of amount of solar power received at the gasifier.

Further, Figure 6.2.4(iii) illustrates the superiority of directly heating sCO_2 in the combustor as opposed to indirectly heat sCO_2 via a heat exchanger. The net thermal energy efficiency of the indirect heating stagers at 41%, representing a 31% lower performance than the direct heating counterpart. From heat transfer perspective it is known that indirect heating incurs more heat losses compared to direct heat and hence the inferiority of indirectly heating sCO2 in the Brayton cycle. Notwithstanding the results of this study, more analysis of the proposed system is required to better understand its superiority in relation to other sCO_2 based IGCCs.

6.2.6: Conclusions

From the results of this study, solar aided Allam cycle looks promising and this study specially concludes the following;

1. Recycling sCO_2 back to the combustor dilutes the syngas in the combustor and thus oxy-combustion at lower temperatures are attainable. This points to a potential highly efficient Allam cycles operating at a practical condition for the current IGCC equipment technology.

2. Higher inlet turbine pressure safeguards stable efficient operation of the Allam cycle for a wider range of exit pressures.

3. Solar-assisted Allam cycle affords higher net thermal efficiencies because of the extra power which is attained by avoiding combustion of syngas to provide heat for gasification.

Note: This paper has already been published in proceedings of the 25th International Conference on Concentrating Solar Power and Chemical Energy Systems, SolarPACES-2019.

Tables

Table 6.1.1: The ultimate and proximate analysis and lower heating value (LHV) of biomass[7]
(* oxygen by difference)

Sr. No.	Material	Moisture content (%) by weight (wet basis)	Proximate analysis (%) by weight (dry basis)			Ultimate analysis (%) by weight (dry basis)				LHV MJ/kg (dry basis)
			FC	VM	ASH	C	H	O^*	N	
1	**Wheat straw**	8.87	10.98	82.12	6.90	42.95	5.35	46.99	0.00	17.988

Table 6.1.2(i): CSP power generation method, solar collector temperature and energy efficiency

CSP power generation method	Solar collector temperature (°C)	Solar energy efficiency (%)	Reference
Organic Rankine cycle	300	~20%	[8], [9]
Sub-critical steam Rankine cycle	400-450	35-40%	[10], [11]
Supercritical CO_2	500-800	25-50%	[12], [13]

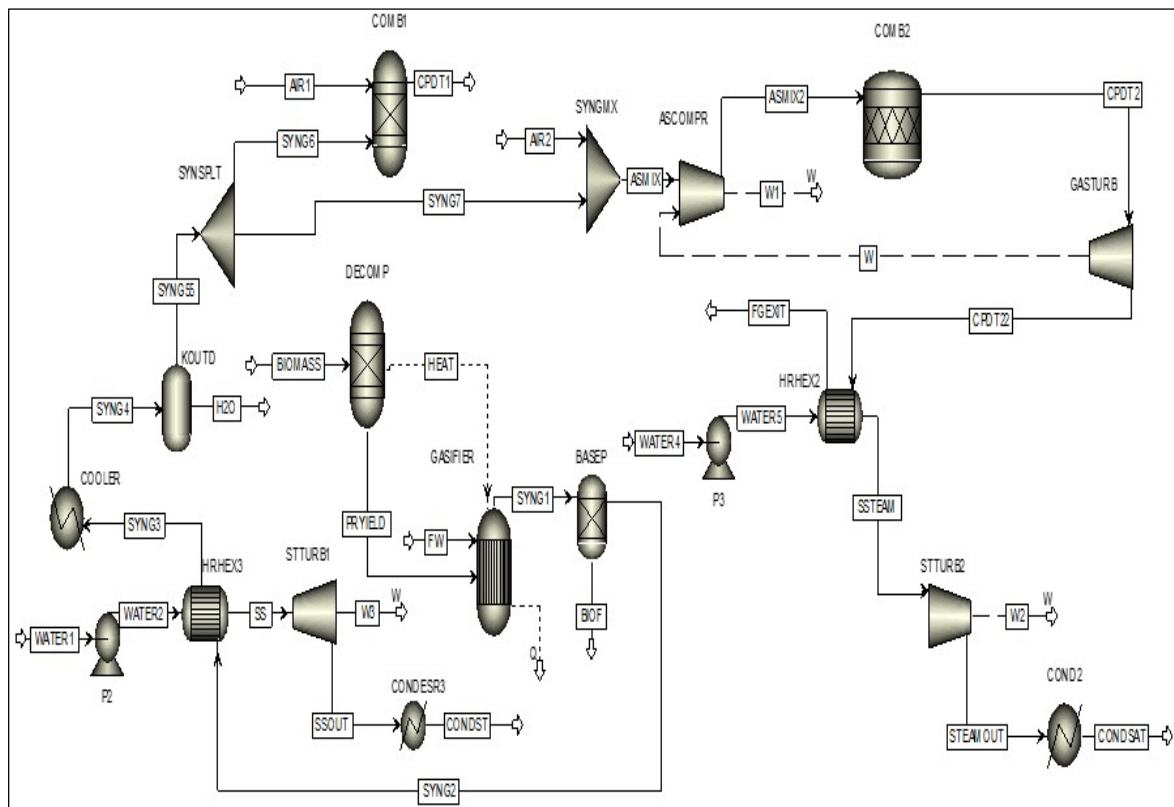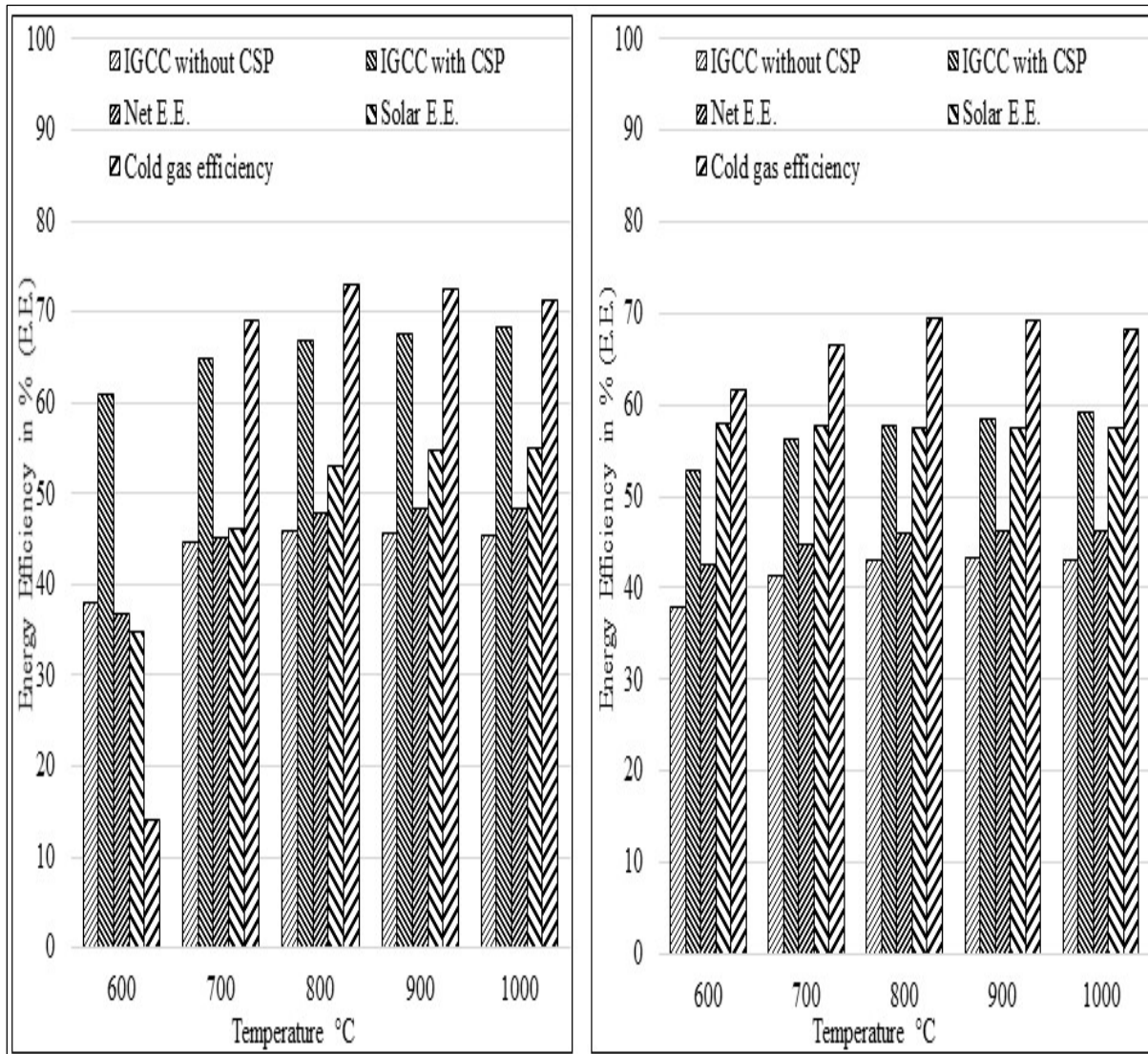| Stirling engine | 800-1000 | ~50% | [14], [15] |
Air Brayton cycle	1000-1100	50-55%	[16]
Steam gasification	800-1200	~58%	[6]
CO_2-gasification	800-1000	~55%	This study

Figures

Figure 6.1.1: Process flowsheet of biomass integrated gasification combined cycle (IGCC).

(a) CO_2-gasification of biomass

(b) Steam-gasification of biomass

Figure 6.1.2: (a) CO_2-gasification of biomass. (b) Steam-gasification of biomass.

The steam condition for power generation is 570 °C and 125 bar$_a$.

* E.E. for IGCC without CSP is calculated as electricity output versus biomass thermal energy input.

* E.E. for IGCC with CSP is calculated as the peak electricity output versus biomass thermal energy input.

* Net E.E. is calculated as the peak electricity output versus biomass plus peak solar thermal energy input.

* Solar E.E. is calculated as addition peak electricity output with solar versus peak solar thermal input into gasifier.

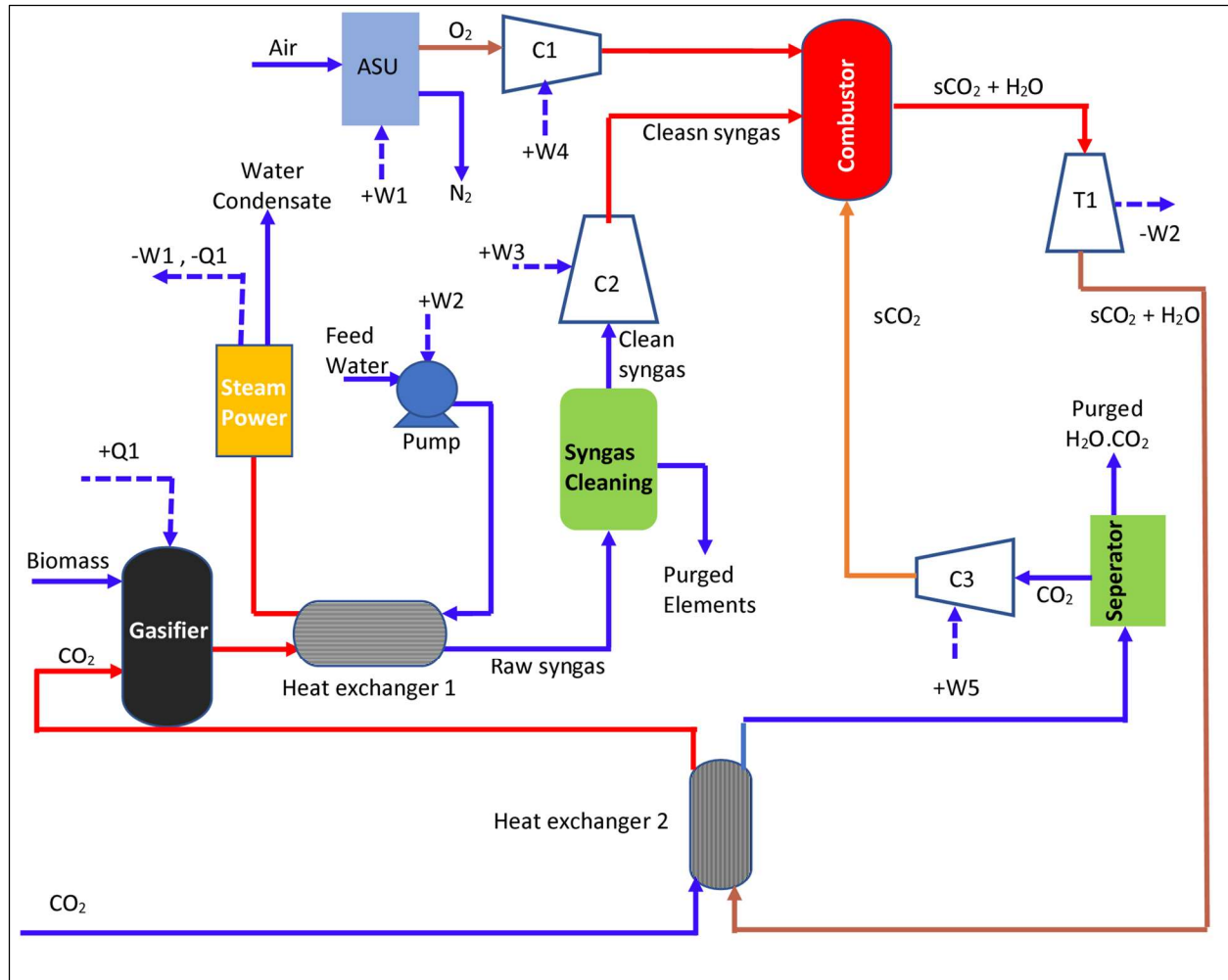* Cold gas efficiency is calculated as heat value of syngas versus biomass thermal energy input.

Figure 6.2.3: Schematic representation of the Allam cycle considered in this study. Solar thermal energy or heat from the combusted syngas meets the required heat input (+Q1) to the gasifier.

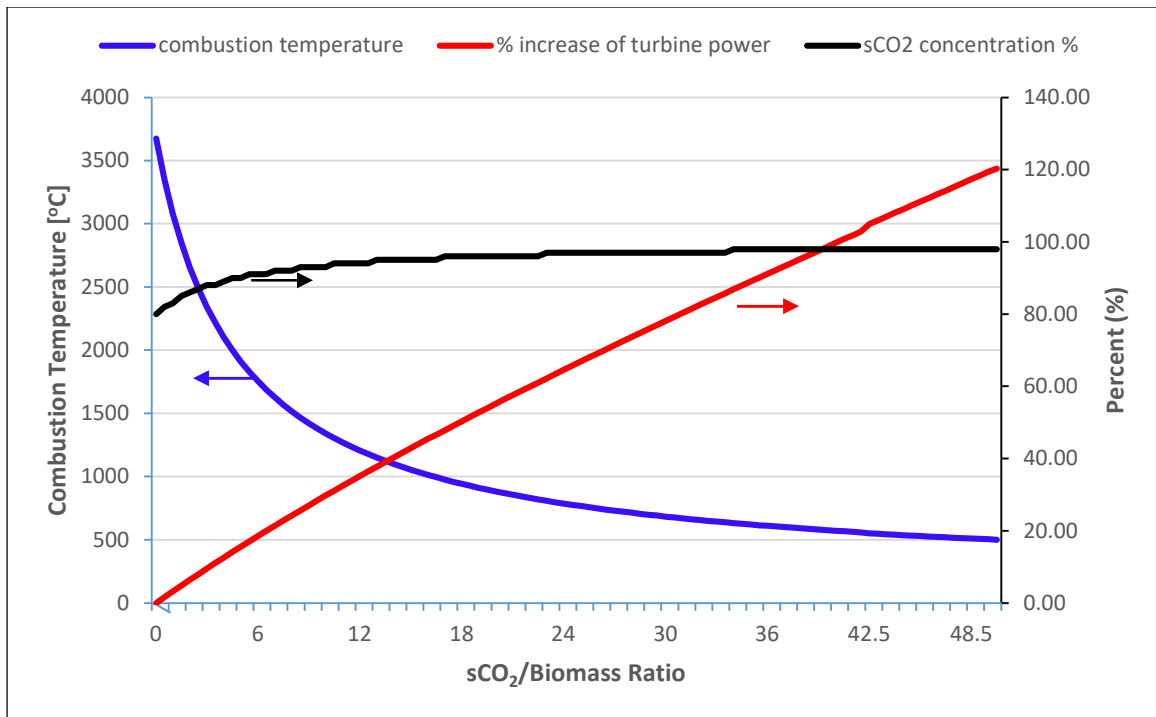| ASU	Air Separation Unit
C1, C2, C3	Compressors
+Q	Heat input
-Q	Heat rejected
sCO_2	Supercritical carbon dioxide
+W	Work input
-W	Work output

Figure 6.2.4(i): Effect if of recycled sCO$_2$ on combustion temperature, turbine power output, and sCO$_2$ concentration in the sCO$_2$ mixture leaving the combustor. sCO$_2$/Biomass ratio is the molar flow ratio of recycled sCO$_2$ to that of biomass feed; % increase of turbine power is the difference of turbine power outputs at 0 and sCO$_2$/Biomass ratio of interest, expressed as percentage; and sCO$_2$ concentration percentage is the percentage ratio of mass flow rates of sCO$_2$ and total sCO$_2$:H$_2$O mixture leaving the combustor.
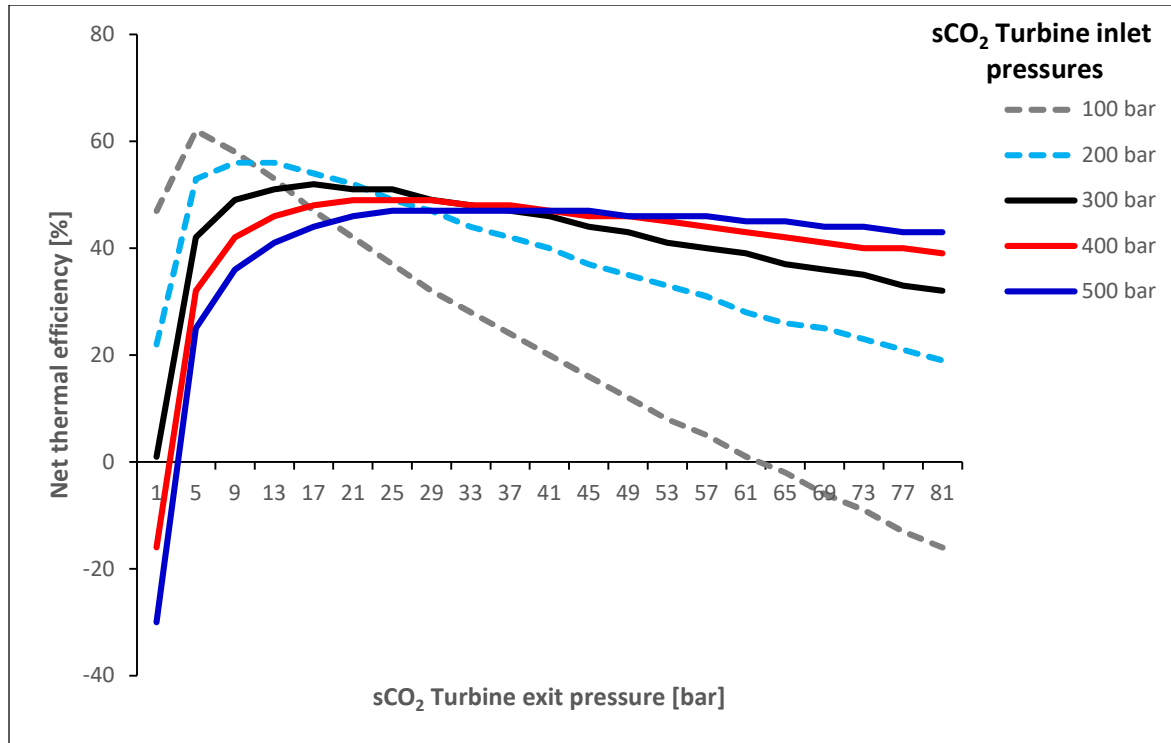
Figure 6.2.4(ii): Influence of sCO_2 turbine inlet and exit pressures on net thermal efficiency.
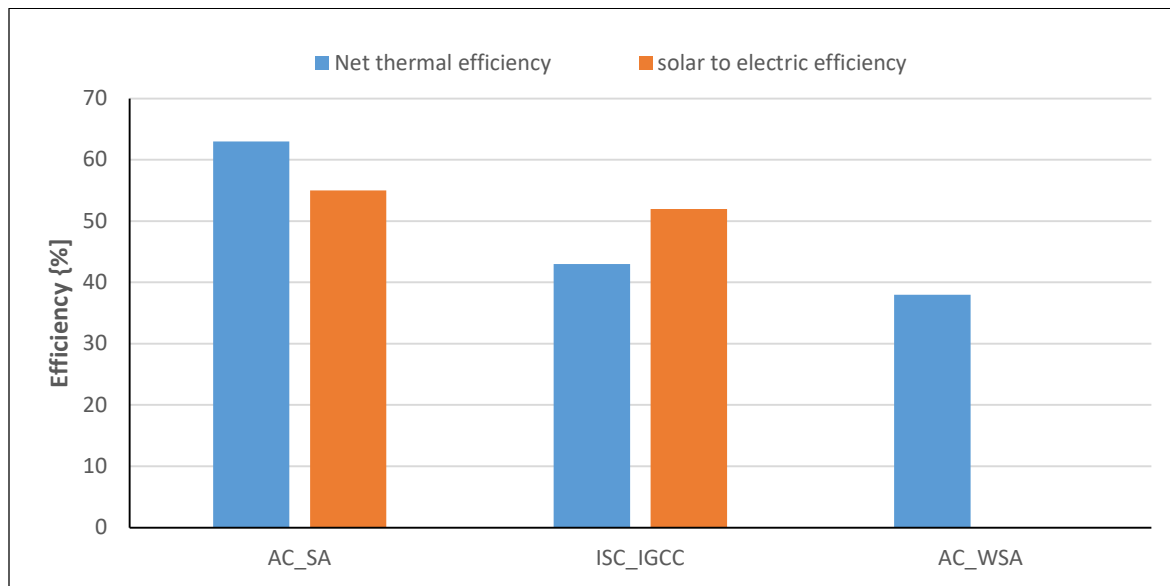

Figure 6.2.4(iii): Comparison of net thermal and solar to electric efficiency of: Allam cycle with solar assist (AC_SA); Integrated Gasification Combined Cycle with an indirect supercritical carbon dioxide Brayton cycle (ISC_IGCC); Allam Cycle without solar assist (AC_WSA).

References

[1]   R. S. Dhillon and G. von Wuehlisch, "Mitigation of global warming through renewable biomass," Biomass and Bioenergy, vol. 48, pp. 75–89, Jan. 2013

[2]   G. A. Florides and P. Christodoulides, "Global warming and carbon dioxide through sciences," Environ. Int., vol. 35, no. 2, pp. 390–401, Feb. 2009

[3]   H. C. Butterman and M. J. Castaldi, "Influence of CO2 Injection on biomass gasification," Ind. Eng. Chem. Res., no. 46, pp. 8875–8886, 2007

[4]   T. Renganathan, M. V. Yadav, S. Pushpavanam, R. K. Voolapalli, and Y. S. Cho, "CO2 utilization for gasification of carbonaceous feedstocks: A thermodynamic analysis," Chem. Eng. Sci., vol. 83, pp. 159–170, Dec. 2012

[5]   M. J. Castaldi and J. P. Dooher, "Investigation into a catalytically controlled reaction gasifier (CCRG) for coal to hydrogen," Int. J. Hydrogen Energy, vol. 32, no. 17, pp. 4170–4179, Dec. 2007

[6]   S. H. A. and X. Liu, "Aspen Plus simulation study of concentrated solar power and biomass gasification for co-production of power and liquid fuel," in SolarPACES-2018

[7]   S. A. Channiwala and P. P. Parikh, "A unified correlation for estimating HHV of solid, liquid and gaseous fuels," Fuel, vol. 81, pp. 1051–1063, 2002

[8]   R. Wang et al., "Comparative analysis of small-scale organic Rankine cycle systems for solar energy utilisation," Energies, vol. 12, no. 5, p. 829, Mar. 2019

[9]   E. Bellos and C. Tzivanidis, "Parametric analysis and optimization of an organic Rankine cycle with nanofluid based solar parabolic trough collectors," Renew. Energy, vol. 114, pp. 1376–1393, Dec. 2017

[10]   Y. Tanaka, S. Mesfun, K. Umeki, A. Toffolo, Y. Tamaura, and K. Yoshikawa, "Thermodynamic performance of a hybrid power generation system using biomass gasification and concentrated solar thermal processes," Appl. Energy, vol. 160, pp. 664–672, Dec. 2015

[11]   U. Pelay, L. Luo, Y. Fan, D. Stitou, and C. Castelain, "Integration of a thermochemical energy storage system in a Rankine cycle driven by concentrating solar power: Energy and exergy analyses," Energy, vol. 167, pp. 498–510, Jan. 2019

[12]   V. T. Cheang, R. A. Hedderwick, and C. McGregor, "Benchmarking supercritical carbon dioxide cycles against steam Rankine cycles for concentrated solar power," Sol. Energy, vol. 113, pp. 199–211, Mar. 2015

[13]   C. Xu et al., "A thermodynamic analysis of a solar hybrid coal-based direct-fired supercritical carbon dioxide power cycle," Energy Convers. Manag., vol. 196, pp. 77–91, Sep. 2019

[14]   A. C. Ferreira, M. L. Nunes, J. C. F. Teixeira, L. A. S. B. Martins, and S. F. C. F. Teixeira, "Thermodynamic

and economic optimization of a solar-powered Stirling engine for micro-cogeneration purposes," Energy, vol. 111, pp. 1–17, Sep. 2016

[15]   O. Aboelwafa, S-E. K. Fateen, A. Soliman, and I. M. Ismail, "A review on solar Rankine cycles: Working fluids, applications, and cycle modifications," Renew. Sustain. Energy Rev., vol. 82, pp. 868–885, Feb. 2018

[16]   A. J. Schrader, A. P. Muroyama, and P. G. Loutzenhiser, "Solar electricity via an Air Brayton cycle with an integrated two-step thermochemical cycle for heat storage based on Co3O4/CoO redox reactions: Thermodynamic analysis," Sol. Energy, vol. 118, pp. 485–495, Aug. 2015

[17]   Siddiqui M, Almitani KJP. Energy analysis of the S-CO2 Brayton Cycle with Improved Heat Regeneration. 2019;7:3

[18]   Lan W, Chen G, Zhu X, Wang X, Liu C, Xu BJSotTE. Biomass gasification-gas turbine combustion for power generation system model based on Aspen Plus. 2018;628:1278-86

[19]   Tavares R, Monteiro E, Tabet F, Rouboa AJRE. Numerical investigation of optimum operating conditions for syngas and hydrogen production from biomass gasification using Aspen Plus. 2020;146:1309-14

[20]   Ansari S, Liu X. Aspen Plus simulation study of concentrated solar power and biomass gasification for co-production of power and liquid fuel. SolarPACES-2018

[21]   McClung A, Brun K, Chordia L. Technical and economic evaluation of supercritical oxy-combustion for power generation. Fourth Supercritical CO 2 Power Cycles Symposium, Pittsburgh, PA, Sept. 2014. p. 9-10

[22]   Milani D, Luu MT, McNaughton R, Abbas AJEC, Management. Optimizing an advanced hybrid of solar-assisted supercritical CO2 Brayton cycle: A vital transition for low-carbon power generation industry. 2017;148:1317-31

[23]   Parraga J, Khalilpour KR, Vassallo AJR, Reviews SE. Polygeneration with biomass-integrated gasification combined cycle process: Review and prospective. 2018;92:219-34

Chapter 7: Biomass Gasification Process to Power and Liquid Fuel

7.1: Biomass Gasification for Co-production of Power and Liquid Fuel

Concentrated solar power (CSP) as external energy input for biomass gasification can be regarded as an alternative process to convert solar energy into power or liquid fuel. In this study, Aspen Plus was used to develop a simple model for CSP-assisted biomass gasification to produce synthetic gas (syngas). This was followed by an integrated gasification combined cycle (IGCC) system for power production or Fischer Tropsch synthesis for liquid fuel production. The effect of operating temperature of the gasification system was studied to determine the optimum temperature. It was found that gasification temperature of about 800°C is good enough to achieve maximum energy efficiency. The peak net efficiency of the hybrid process is 45% higher than any hybrid options found in the literature: a solar to power efficiency of 58% is achieved. In terms of the liquid fuel production option, 17-18 kg of liquid fuel can be produced per GJ of solar energy injected into the process.

7.1.1: Introduction

Concentrating solar power–biomass hybrid gasification for power generation is a promising option as a low cost dispatchable renewable power supply. Because of its flexibility, it could help to tackle the timing imbalance between peak demand and renewable energy production, and thus increase the contribution of renewable energy to the grid. It can also be supplied off-grid as the only power supply with the ability to provide base load power supply and the ability to quickly adjust the power output according to the demand, which has the potential to supply remote rural areas that are not connected to the grid. The addition of liquid fuel production to the CSP-IGCC process could increase the power output flexibility further, i.e. when the power demand is low, liquid fuel can be produced without lowering the biomass gasification capacity, which results in greater stability of the complicated biomass gasification process. Liquid fuel and chemicals produced from this process could also be sold as high-value chemicals, which adds additional value to the process.

Many researchers have conducted simulation studies on hybrid biomass-based energy systems for various industrial applications. There are many ways to use solar energy, but solar thermal conversion - especially CSP - is a good option to inject heat into the biomass gasification process [1-8]. The injection of solar energy will increase the net energy efficiency, save biomass feedstock and improve the carbon efficiency of the process. The incorporation of CSP to biomass gasification can provide energy continuously to the gasifier unit with intermittent combustion of syngas or CSP, either with or without energy storage [9]. The system block diagram of CSP-assisted biomass gasification that was studied for the present paper is indicated in Figure 7.1.1(i).

In this simulation study, a hybrid process is proposed to incorporate CSP into a biomass gasification unit for power generation with an IGCC system or liquid fuel production with Fischer Tropsch synthesis (FTS). A dual bed biomass gasification process was selected to cope with the need for flexibility in using external heat needed for biomass gasification process. Sand was chosen as the heat carrier between the two beds. Sand was heated in the heating bed by concentrated solar power. Hot sand was injected into the gasifier with steam to balance the heat load of the gasifier. When there was no solar, the heat load of the gasifier was met by combustion of produced syngas or recycled tail gas from FTS. Cold sand was then separated from the syngas and ash, before it was heated up again in the heating bed.

7.1.2: Methodology

Aspen Plus® is a tool used in process design. An integrated system model was developed for power generation using a biomass gasifier and syngas combustion turbine. The heat recovery steam generation system for power generation by steam turbine was also introduced. The developed model was studied to predict gasifier performance, energy efficiency of IGCC system, with or without CSP, and liquid fuel production, with or without CSP. The process was modeled for a plant with a capacity of 10 tons/day of wet biomass feedstock. The biomass was gasified into syngas, followed by IGCC or FTS process. The solar energy contribution of the CSP system was modeled in terms of solar-thermal heat injection into the gasifier unit. When there was no CSP, combustion of syngas was introduced to balance the heat load of the gasifier.

The share of solar thermal energy into the gasification system results in more syngas per unit of biomass.

A thermodynamic equilibrium-based RGibbs model was used to simulate the biomass gasification process. Wheat straw was selected as the biomass feedstock [10]. The biomass was gasified at a temperature of 600-1000 °C @ 1 bar_a with a controlled amount of water, so that no solid carbon formed. Water was fed at ambient temperature and pressure. The proximate analysis as fixed carbon (FC), volatile matter (VM), ash (ASH) and ultimate analysis as carbon (C), hydrogen (H), oxygen (O), nitrogen (N) and lower heating value (LHV) of the investigated biomass is given in the Table 7.1.2(i). The contents of chlorine and sulfur were ignored, because of the small amounts, which have little effect on the simulation results. The syngas cleanup was not included in the model. The IGGC model was based on a combined cycle using a syngas combustion turbine (Brayton cycle) and steam turbine (Rankine cycle). The combustion turbine was operated at 1200 °C and 15 bar_a with exit at 580 °C @ 1 bar_a. The super-heated steam was generated using a heat recovery steam generation (HRSG) system to recover heat from hot syngas in the gasifier and hot flue gases in the combustion turbine. The steam turbine was operated at 125 bar_a and 570 °C with exit at 20 °C @ 0.02 bar_a. In the Fischer Tropsch process for liquid fuel production, a once-through process was chosen, with syngas conversion set at 0.95 and the products distribution factor set at 0.90. All the hydrocarbons with C_{3+} were considered to be liquid fuel, while lighter C_1-C_2 hydrocarbons and unconverted syngas was considered to be tail gas. The tail gas was combusted to obtain the energy needed for the gasification process.

7.1.3: Results and Discussions

Figure 7.1.3(i) (a,b) indicates the effect of: temperature on composition of syngas; solar energy efficiency through the IGCC system; the net energy efficiency of the IGCC system, with or without solar. The simulation results for biomass gasification showed a molar ratio of H_2, and CO of about 2 at temperature 600 °C @ 1 bar_a. At higher temperatures, more syngas was produced, while the concentration of hydrogen decreased. It was also seen that when a higher temperature was used for gasification, it resulted in higher net energy efficiency, but this was not significant when the gasification temperature was higher than 800 °C. If the temperature

difference between the hot and cold sand is about 100 °C, the CSP system only needs to heat the sand to 900 °C. The simulation results show that energy efficiency for direct combustion is about 30%, while energy efficiency for the IGCC system without CSP varies between 38% and 42%. The energy efficiency for the IGGC system that was integrated with CSP is in the 48-58% range. This shows that when there is no solar input, the process can still be operated with a loss capacity of about only 30% compared to peak output. This indicates that solar storage is not necessary for such process thus can lower the capital investment for this hybrid process. When comparing the additional power output with the energy input from the solar system, it was found that power generation efficiency from solar is as high as 58%, which is higher than most of the other solar power generation processes, as per the comparison provided in Table 7.1.3(i). Figure 7.1.3(ii) indicates the liquid fuel production that is possible with and without CSP at various gasification temperatures. At gasification temperature of 700 °C, adding CSP can raise liquid fuel production from 1639 to 2226 kg/h: a 36% increase in liquid and improvement in carbon efficiency of about 60% was found. For every GJ of solar heat injected into the system, about 17-18 kg of hydrocarbons can be produced, as reported [12].

7.1.4: Conclusion

When CSP is combined into the proposed hybrid CSP-IGCC process, the energy efficiency of solar energy can be as high as 58% for power generation. For liquid fuel production, 17-18 kg of hydrocarbon can be produced from every GJ of solar energy input into the system. The capacity loss is less than 30% when no CSP input exists, which suggests that there is no need to store solar energy for smooth operation. Gasification at temperatures higher than 800 °C provides limited benefits, but may result in significant challenges for the solar receiver system. The results are promising, which makes the hybrid CSP-BTL process a good option for solar energy storage and transportation.

Note: This paper will be published in proceedings of the 24th International conference on concentrating solar power and chemical energy systems SolarPACES-2018.

7.2: Integrated Biomass Gasification Combined Cycle Process Facilitated with CSP

Concentrated solar power (CSP) hybrid with biomass power generation is a promising option to provide affordable dispatchable renewable energy supply in agricultural region with direct normal insolation (DNI) over 1500 kWh/m^2/h. Such hybridization can help to increase the renewable energy penetration into the grid by easing the 'duck-curve' challenge caused by other renewable energy such as CSP, PV and wind. A couple of hybrid CSP-biomass power plants are in operation in Europe and various hybridizations options covering Rankine cycle and biomass integrated gasification combine cycle have been proposed by various researchers. There is still room to improve the peak net efficiency and the thermal to power efficiency for further capital investment saving. The proposed hybrid CSP-biomass gasification approach resulted with improved thermal efficiency in comparison with direct biomass fired power plants, with less carbon dioxide (CO_2) emissions and improvement of renewable energy contribution to global energy mix.

A CSP-assisted biomass integrated gasification combine cycle process was simulated by using Aspen Plus$^®$. The requirement to the CSP system, and the biomass gasification conditions were studied to find out the optimum operating conditions to achieve the best solar thermal to power efficiency and the peak net efficiency. This study aims to propose a small and medium scale biomass-solar hybrid process to provide electricity in rural areas of Africa. The simulation results show that energy efficiency for the hybridization process was about 58% higher than seen with the Stirling engine, Rankine cycle and Brayton cycle. The gasifier at 800 °C @ 1bar$_a$ will produced 1.93 MW$_e$ per ton of wet biomass without CSP, which can be boost up to 2.597 MW$_e$ with CSP. This indicates that the plant's power production capacity can be boosted up to 35% by CSP.

7.2.1: Introduction

The fossil fuels are depleted rapidly and available in reserved geographical areas which are rich with the organic remnants while biomass and solar is frequently available energy resource to meet the energy demands of the society [13, 14]. The main objective of this study is to reduce the consumption of fossil fuels and increase the share of renewable energy to global energy mix. It is impossible to make direct use of the biomass for commuting purposes such as

aviation, marine, automobiles, long range travelling cannot compete with fossil fuels, due to certain physical characteristics such as energy density and ash content. Biomass feedstock can be converted through various chemical processes into gas, liquid and solid fuel, chemicals or energy products [15,16]. Solar energy can be injected into these processes. Conversion of biomass to energy is summarized in Figure 7.2.1(i).

Many hybrid power systems are thus being developed to maximize the application of renewables towards energy with higher energy efficiency and less greenhouse gases (GHG) [17]. It has been proven that biomass and solar hybrid power generation systems are already functional to meet the steadily growing demand of energy for sustainable development of the society [18,19]. Generally, unconventional types of feedstock, such as biomass, are combusted directly to meet energy demand or gasified to produce various chemicals, solid, gaseous or liquid fuel by the existing advanced technologies. Nowadays, the incorporation of solar/wind/geothermal energy in the aforementioned processes is increasing with addressing the issue of climate change and energy security [20].

Rapid urbanization with high living standards and commercial development is a major cause of global warming and uncertain price hike of fossil fuels. Hence, the demand of clean and green energy is increasing gradually. Between 2010 to 2035, global energy demand is expected to be increased by more than 31%, while renewable energy share would be increased up to 6% [21]. Therefore, it is essential to exploit cheap and cost-effective routes to utilize renewable energy resources, e.g. biomass, wind, solar and geothermal. Solar power and biomass are chosen to be good fuels for future energy needs. Globally, biomass is the fourth highest source of energy, contributing renewable heat of about 14.1% and 85.9% share by non-biomass sources. In 2015, the total share of all renewables in the global energy mix was 19.3% [22].

Among various methods for thermochemical conversion of biomass, gasification is one of the most promising way to produce syngas which can be easily converted into liquid fuel/energy/power. Because the gasification system is energy intensive process, energy needed for the gasifier can be provided by solar energy through concentrated solar power (CSP) or by combustion of syngas/natural gas/biomass. In the context of renewable share to energy mix,

hybridization of biomass gasification with CSP can play a significant role in transition towards clean and green energy [23]. The gasification assisted with CSP is good choice which can help to meet the heat load of a gasifier by the intermittency of solar power with combustion of biomass/syngas/natural gas.

The primary energy source for CSP is direct normal insolation (DNI) from the sun. The CSP is one of the most innovative technology for solar energy application towards thermal energy processes such as gasification, pyrolysis and combustion. The injection of solar heat by high temperature systems using solid particles to meet the heat load of the gasifier is one of the critical and most challenging part of this hybrid CSP-gasification technology [23]. The solid heat carrying medium can be heated to high temperature through the concentrated parabolic troughs or solar tower then it can be fed to the double bed fluidized gasifier for heat exchange with biomass feed. Therefore, after approaching the set temperature, this hot sand can be conveyed to the gasifier for indirect/direct heat exchange. Steam, nitrogen or flue gases can be used as a fluidizing agent during gasification. Usually sand mixed with biomass before gasification. The silica sand can be used as a heating media or a bed material in a fluidized bed gasifier [24]. Many researchers have done the modelling and simulation of gasification by the Aspen Plus process simulator to evaluate mass and energy balances and to optimize the process designs [17], [18].

Consequently, the key contribution of this study is the simulation of integrated biomass gasification combined cycle (IGCC) process facilitated with CSP. It is carbon neutral method towards clean and green energy pathway. The overall biomass gasification incorporated with CSP facility and the electric power generation through IGCC system can be summarized in the Figure 7.2.1(ii).

The advances in solar technology making ease to meet the heat load of biomass gasification with less air pollution. Many studies assessed optimum choice and application of CSP technologies in conventional and non-conventional power plants to produce power with considering a simple Rankine or Brayton cycle or combined cycle [25]. CSP-biomass integration for power production with Rankine cycle/Brayton cycle/combined cycle is already proven

sustainable technology, with its low cost base load and dispatchable renewable energy compared to stand-alone CSP power generation plants [26].

The present simulation study has been presented that hybrid CSP-biomass power plant has higher thermodynamic efficiency, higher electricity production, stable in operation, lower environmental impacts, lower water consumption and higher renewable output of the plant. The present study focused on following: to optimise sand to biomass ratio, controlled amount of steam, concentrate and transfer of solar energy to the gasification system by sand as a heating carrier and methodological performance of the gasification system. The silica sand has been considered as an inert and stable thermal energy carrier between CSP and gasification system.

The intermittency of syngas/biomass/natural gas combustion with CSP has been analysed with systematic flexibility for continuous operation of gasifier to produce power through IGCC system. There are some technical challenges to transfer solar heat through sand to the gasifier and actual run of this new option is still to be tested. This study evaluated the possible opportunity of CSP-biomass gasification process with IGCC system for power generation by considering maximum share of solar as energy source to the gasifier.

7.2.2: Modelling and Description of the Process

The modelling of overall gasification process along with integrated gasification combined cycle has been developed in process simulator Aspen Plus®. A simple model for gasification and IGCC system comprised of two distinct sections: biomass gasification and power generation system. The IGCC system based on two cycles: gas turbine (Brayton cycle) and steam turbine (Rankine cycle) with heat recovery steam generation (HRSG) system. For gas turbine, biomass was gasified at 600-1000 °C @ 1 bar_a to produce syngas then syngas was combusted in autothermal combustion turbine with controlled amount of air. For steam turbine, syngas from gasifier and flue gas from the gas turbine was used as a heat source to produce steam for Rankine cycle. The gas turbine was operated at 1200 °C and 15 bar_a. The steam turbine was operated at 780 °C and 125 bar_a to produce superheated steam from the flue gases of gas turbine and hot syngas from the gasifier.

The chemical reactions were based on Gibbs free energy minimization at equilibrium with some assumptions like uniform temperature, uniform mixing, steady state, no tar formation, ash is inert, nitrogen and sulphur are negligible. The wet biomass feed rate was 10 tons/hr to the gasifier. The biomass was gasified at temperature 600-1000 °C @ 1 bar$_a$ in the absence of air with controlled amount of steam so that no solid carbon will be produced in the syngas. The gasification system heat load was planned by the combustion of syngas or combustion of extra biomass or by solar energy through CSP. Approximately the heat load of the gasifier can be met by combustion of 30-40% extra biomass or by combustion of 30% produced syngas. We can save this biomass or syngas by suppling heat to the gasifier through the CSP system.

The heat injection to the gasifier can be done by suppling superheated steam or hot silica sand from CSP system. Commonly, sand can be used as a heat carrier to run endothermic gasification in dual fluidized bed gasifiers. The hot sand feed rate can be maintained with respect to biomass feed rate for appropriate mass and heat transfer to reach the required gasification temperature in a pilot scale dual fluidized bed (DFB) system. The heat injection through silica sand is still challenging, needed advanced technology and still under research and development phase to meet the higher heat load of the gasification system. The most challenging part is circulation and transportation of the sand through the biomass gasification and the CSP system.

Many researchers have developed dimensionless correlation at high density ratios to estimate the circulation rate of sand in a riser of a DFB high temperature gasifier [27]. The dual fluidized bed gasifier can be operated with air, CO_2, inert gas or flue gases from the same system. Many researchers have studied circulation of solid particles for heat transfer and integration of reactor with siphon [28]. This study has not considered on the circulation but focused on injection of heat to the gasifier by injection of desired amount of hot sand to the gasifier. The ratio of sand to biomass was in the range of 12-16 depending upon temperature of the gasification system. For this simulation study, temperature difference between sand and gasifier was 200 °C and atmospheric pressure. The hot sand from the CSP system can be feed to the fluidized bed gasifier at three points; top, middle or bottom. The sand-CSP hybrid

biomass DFB system consists of drying/pyrolysis reactor, char oxidation reactor, gas-solid separator and sand heating system as shown in the Figure 7.2.2(i).

It is already proven technology that the heat carrying medium (sand) can be injected to the gasifier through the pneumatic system or screw conveyors in all available technologies in this field. Recycled syngas captured carbon dioxide and nitrogen can also be used as a carrying gas for sand. But using recycled syngas, carbon dioxide or steam for biomass gasification is most promising and proven technology to produce high quality syngas.

Generally, the DFB gasification with circulation of hot fluidizing particles with simplified scheme and description is mentioned in Table 7.2.2(i) showing the possible three different technologies for dual fluidized bed gasification system [29].

The focus of this simulation study was not to consider the detailed chemical mechanisms and hydrodynamics of the fluidized bed gasifier but based on thermochemical equilibrium for wood biomass gasifier with assumptions of Gibbs free energy minimization. It was assumed that reactants should reach to chemical equilibrium to produce good quality syngas. The biomass gasification was demonstrated by the combination of the Aspen Plus$^{®}$ and dedicated Fortran files.

The modelling of IGCC system was done by two sub-systems; gas turbine and steam turbine. The produced syngas was combusted to run the gas turbine and steam from HRSG system was used to run steam turbine. Energy efficiency and solar efficiency was calculated for the biomass gasification and the IGCC system. The cogeneration gas-steam combined cycle is an environmentally friendly technology that produces high energy efficiency for power generation.

7.2.3: Results and Discussion

The simplest model to represent the biomass gasification system comprised of two subgroups. Firstly, biomass was decomposed into its elements in RYield reactor. Secondly, the

thermochemical equilibrium reactions in the RGibbs reactor that produce the syngas were considered. The equilibrium reactions in RGibbs carried out in the absence of air and minimum amount of steam so that no solid carbon detected in the syngas. The ultimate and proximate analysis of biomass, higher heating value of biomass on dry basis and steam to biomass ratio was considered to estimate the composition of syngas. The wheat straw and groundnut shell has been selected as the feedstock for gasification. The higher heating value (HHV) dry basis, proximate and ultimate analysis [30] used in the simulation study are given in the Table 7.2.3(i).

In the model, the produced syngas has to be conditioned so that syngas can be used for further application in the IGCC system. The separator block was used to separate out the ash from the syngas. The conditioned syngas can be combusted to meet the heat load of the gasifier or can be combusted to produced power in combustion steam turbine. The CSP was incorporated to meet the heat load of the gasifier to save syngas or biomass. The incorporation of CSP supports to produce more power and increase the energy efficiency of the IGCC system. The predicted composition of syngas with respect to temperature from wheat straw feedstock, as per simulation, is presented in Figure 7.2.3(i).

The simulation results showed that gasification at about 700-900 °C @ 1 bar_a is more favourable to get good quality syngas for power generation. The syngas was combusted in the combustion turbine at 1200 °C @ 15 bar_a to produce electrical power. The outlet conditions for combustion turbine was about 570 °C @ 1 bar_a. The contribution to power in the IGCC system was higher from the gas turbine as compared to steam turbine. The steam at 560 °C @ 125 bar_a produced from HRSG system was fed to vacuum steam turbine.

The operating conditions for steam turbine was 20 °C @ 0.02 bar_a. The effect of gasification temperature (T) and pressure (P) on predicted energy efficiency (E.E.), sand to biomass (S/B) ratio, hybrid process peak net efficiency, energy efficiency for solar input and capacity loss without CSP is presented in Table 7.2.3(ii).

The simulation results showed that higher gasification temperature resulted with higher net energy efficiency but not significantly, it also decreases the solar thermal efficiency slightly.

This indicates that it is not necessary to push for extreme high temperature, considering the challenges from the solar collector.

The IGCC system is more efficient, economical, sustainable and environment friendly process as compared to direct fired power plant to produce power or electricity. The comparison of energy efficiency for direct combustion with the energy efficiency for IGCC system with or without CSP, cold gas efficiency and solar energy efficiency with respect to temperature is presented in the Figure 7.2.3(ii).

The simulation results showed that energy efficiency for direct combustion is about 30%, while energy efficiency for IGCC system without CSP varies between 38% and 42%. The energy efficiency for IGGC system integrated with CSP is in the range of 48-58% depending upon the biomass feedstock and availability of solar energy. The results showed that the energy efficacy can be boost up to 30% by application of CSP into the gasification system. The net energy efficiency is 65% and solar energy efficiency is 58%. The available CSP power generation methods, solar collector temperature and energy efficiency is presented in Table 7.2.3(iii).

The energy efficiency observed by proposed IGCC system with CSP is 58% which is higher than any available CSP power generation method. The CSP biomass hybrid opportunities are summarized in Table 7.2.3(iv).

7.2.4: Conclusion

The simplest model for biomass gasification with CSP has remarkable prospective to inject solar energy at high temperature to biomass gasification process. The proposed process to produce power has extraordinary effects on mitigation of climate change and air pollution. Such hybridization can increase the share of renewable energy towards global energy mix. The energy efficiency for such hybridization biomass-CSP process is about 58% higher than Stirling engine, organic Rankine cycle and Brayton cycle. The capacity loss is less than 30% when no CSP input is available, which indicates that storage is not necessary, which means further capital cost reduction. Hot sand or syngas storage may be considered to meet the actual grid

demand. Higher steam gasification temperature increases the net efficiency but not significantly, it also decreases the solar thermal efficiency slightly. This indicates that it is not necessary to push for extreme high temperature, considering the challenges to achieve such higher temperature from the solar collector. The total power produced from each ton of wet biomass was 1.93 MW_e without CSP, which can be boosted up to 2.597 MW_e with CSP when the gasifier is operated at 800 °C @ 1bar. This indicates that the plant's power production capacity can be boosted up to 35% by CSP.

Note: This paper was published in proceedings of the 5th International Southern African Solar Energy Conference SASEC-2018.

Tables

Table 7.1.2(i): The ultimate and proximate analysis and lower heating value (LHV) of biomass [10] (* oxygen by difference)

Sr. No.	Material	Moisture content (%) by weight (wet basis)	Proximate analysis (%) by weight (dry basis)			Ultimate analysis (%) by weight (dry basis)				LHV MJ/kg (dry basis)
			FC	VM	ASH	C	H	O*	N	
1	Wheat straw	8.87	10.98	82.12	6.90	42.95	5.35	46.99	0.00	17.988

Table 7.1.3(i): The CSP power generation method, solar collector temperature and energy efficiency for various systems [11]

CSP power generation method	Solar collector temperature (°C)	Energy efficiency (%)
Organic Rankine cycle	300	~20%
Sub-critical steam Rankine cycle	400-450	35-40%
Supercritical CO₂	500-800	25-50%
Stirling engine	800-1000	~50%
Air Brayton cycle	1000-1100	50-55%
This study	800-1200	~58%

Table 7.2.2(i): Simplified process description of three technologies for DFB gasifier

Name of technology and duration	Simplified description	Process description
TNEE In the 1980's		Gasification: LVFB Char oxidation: HVPR Heat carrying medium: sand is injected at the top of the gasifier
FERCO In the 1970's		Gasification: HVPR Char oxidation: HVPR Heat carrier medium: sand is injected at the bottom.

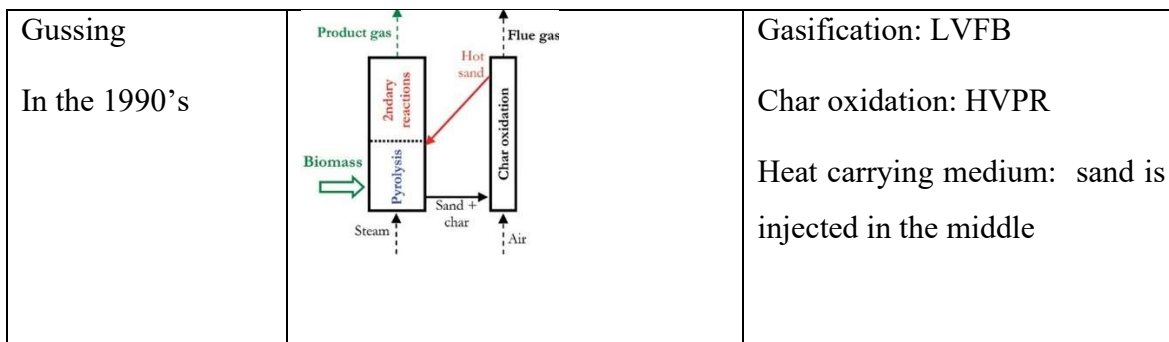| Gussing		Gasification: LVFB
In the 1990's		Char oxidation: HVPR
		Heat carrying medium: sand is injected in the middle

Table 7.2.3(i): Proximate analysis, ultimate analysis and HHV for locally available biomass feedstock

Analysis		Wheat straw	Groundnut shell
Moisture content % by weight (wet basis)		8.87	8.10
Proximate analysis % by weight (dry basis)	Fixed carbon (FC)	10.98	8.10
	Volatile matter (VM)	82.12	21.60
	Ash	6.90	72.70
Ultimate analysis % by weight (dry basis)	Carbon (C)	42.95	48.59
	Hydrogen (H)	5.35	5.64
	Oxygen (O)	46.99	39.49
	Nitrogen (N)	0.00	0.58
HHV (MJ/kg) dry basis		17.988	19.849

Table 7.2.3(ii). Effect of T and P on E.E., S/B ratio, peak net efficiency, E.E. for solar input and capacity loss without CSP

T (°C)	P (bar)	IGCC E.E. without CSP	S/B ratio (w/w)*	Hybrid process peak net	E.E. for solar input	Capacity loss without

		(%)		efficiency (%)**	(%)***	CSP (%)
600	1	38.0	17.1	42.6	58.1	28.1
700	1	41.5	17.7	44.8	57.7	27.8
800	1	43.0	18.2	45.9	57.5	27.2
	2.5	42.3	18.2	45.5	57.6	27.6
	5	41.6	18.0	44.9	57.7	27.9
	7.5	41.2	17.7	44.5	57.8	27.9
	10	40.9	17.4	44.2	57.9	27.8
900	1	43.2	20.2	46.2	57.4	27.9
1000	1	43.0	24.0	46.2	57.4	29.2

* Weight ratio of hot sand and biomass fed into the gasification system, T of hot sand was 200 °C higher than gasification T.

** Peak hybrid net efficiency is calculated as the peak power output versus total thermal input.

*** Energy efficiency for solar input is calculated as the addition of power output versus solar thermal input from CSP.

Table 7.2.3(iii): CSP power generation method, solar collector temperature and energy efficiency

CSP power generation method	Solar collector temperature (℃)	Energy efficiency (%)
Organic Rankine cycle	300	~20%
Sub-critical steam Rankine cycle	400-450	35-40%
Supercritical CO_2	500-800	25-50%
Stirling engine	800-1000	~50%

| Air Brayton cycle | 1000-1100 | 50-55% |
| This study | 800-1200 | ~58% |

Table 7.2.3(iv): CSP biomass hybrid options

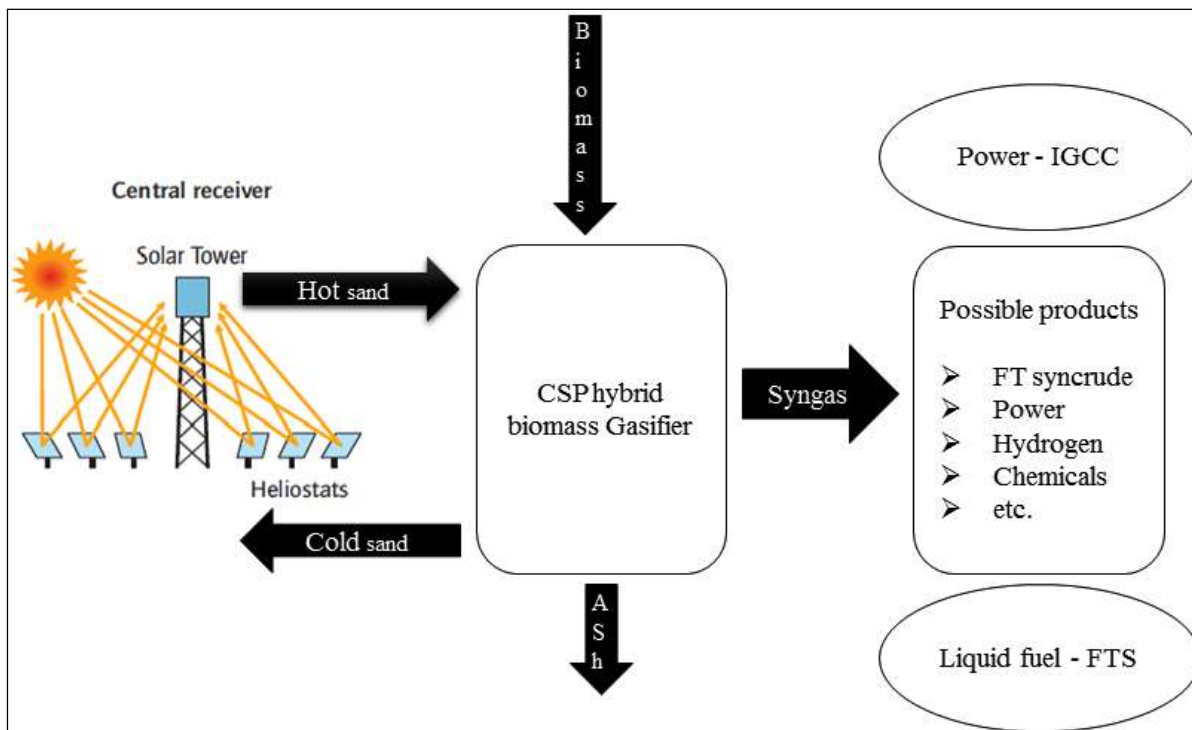| CSP-Biomass hybrid options	Peak net efficiency (%)
Biomass direct combustion + various CSP with Rankine cycle	29-33%
Independent indirect BIGCC + CSP with syngas storage	~30%

Figures

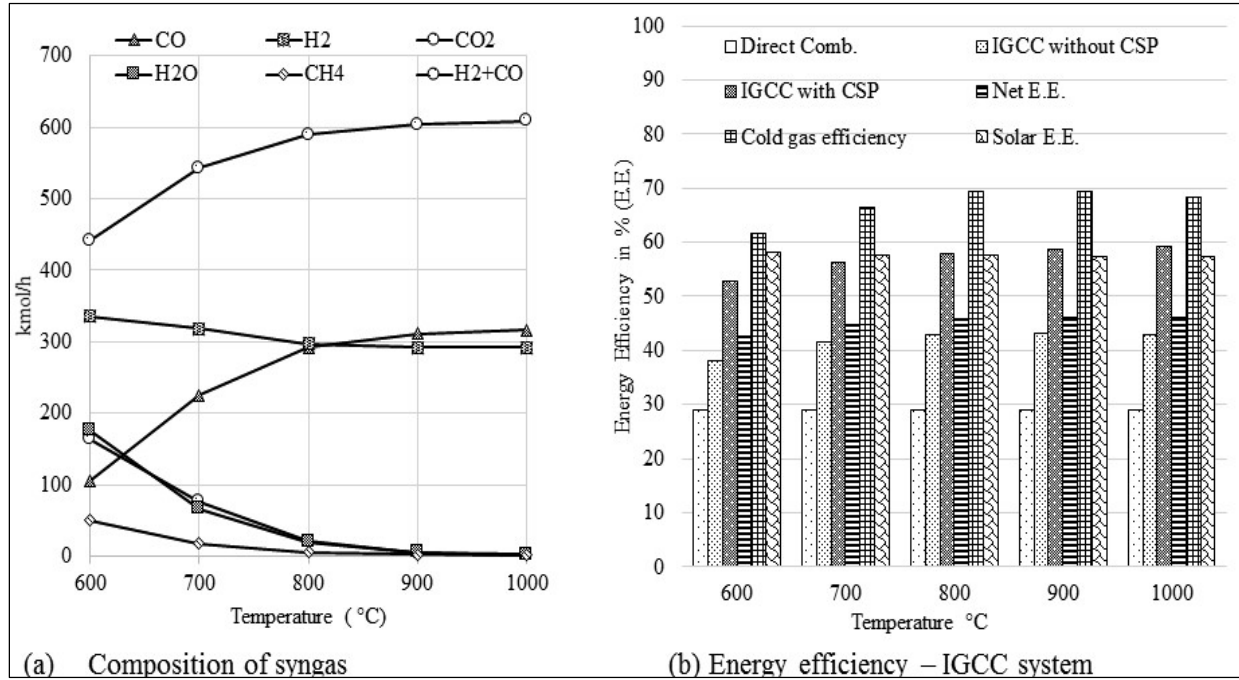Figure 7.1.1: System block diagram of CSP-assisted biomass gasification

Figure 7.1.3(i): (a) Effect of temperature on the composition of syngas. (b) Effect of temperature on energy efficiency through IGCC.

* E.E. for direct combustion is calculated as electricity output versus biomass thermal energy input in a direct fired plant. The steam condition for power generation is 570°C and 125 bar_a.

* E.E. for IGCC without CSP is calculated as electricity output versus biomass thermal energy input.

* E.E. for IGCC with CSP is calculated as the peak electricity output versus biomass thermal energy input.

* Net E.E. is calculated as the peak electricity output versus biomass plus peak solar thermal energy input.

* Solar E.E. is calculated as the addition peak electricity output with solar versus peak solar thermal input into the gasifier.

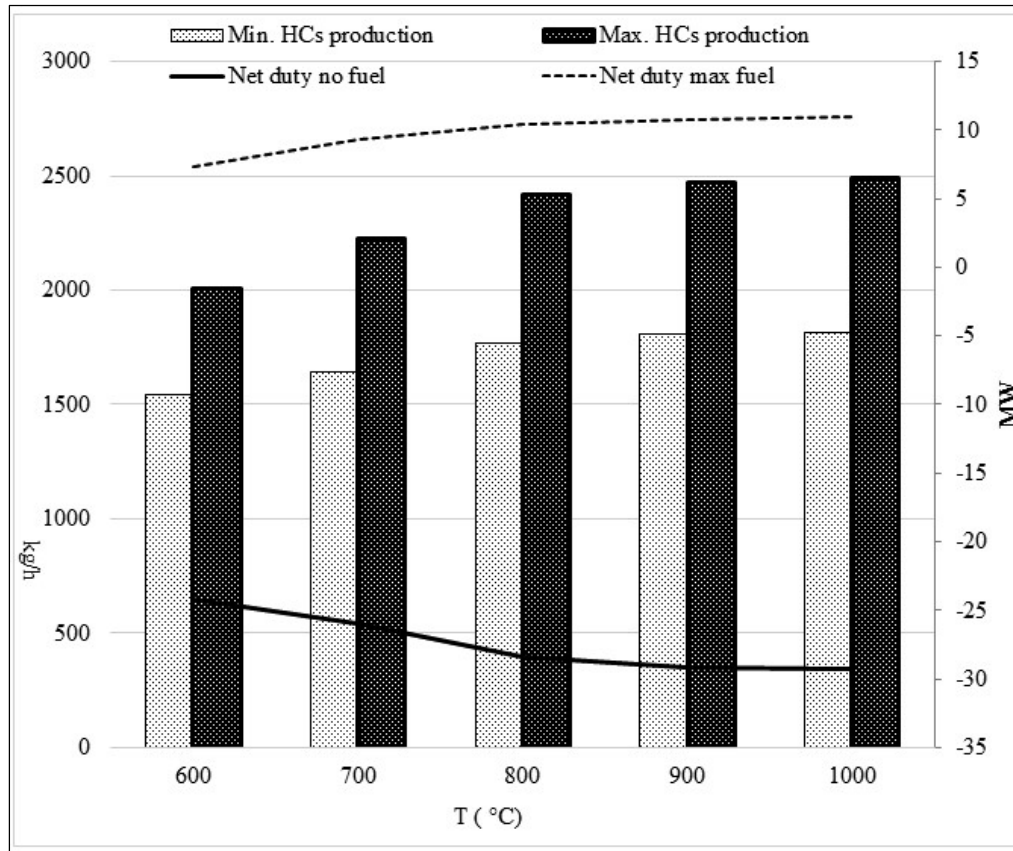* Cold gas efficiency is calculated as heat value of syngas versus biomass thermal energy input.

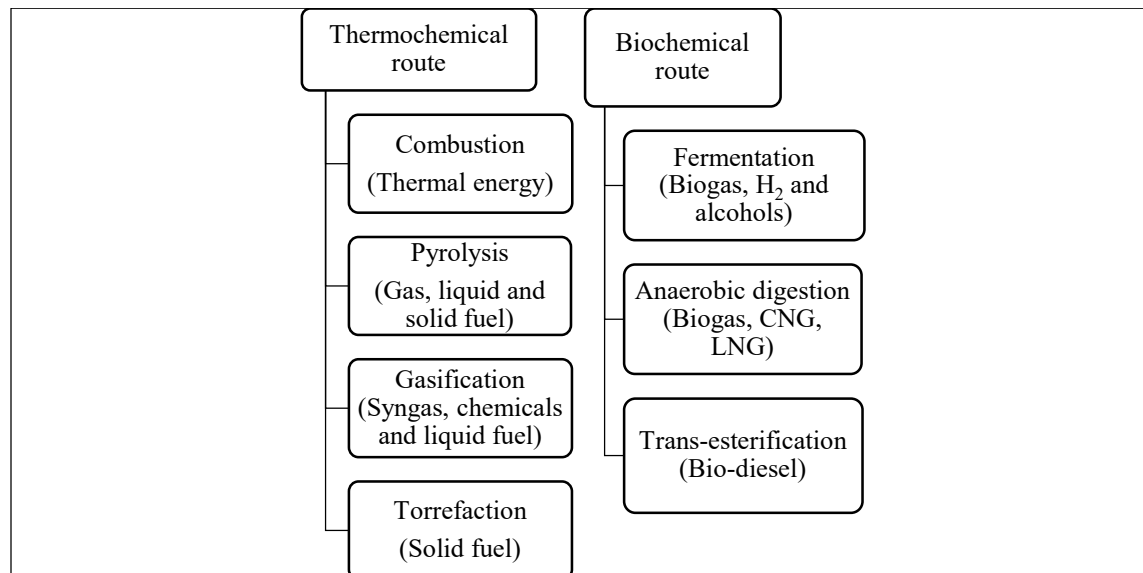Figure 7.1.3(ii): Effect of temperature on net heat duty and liquid fuel production

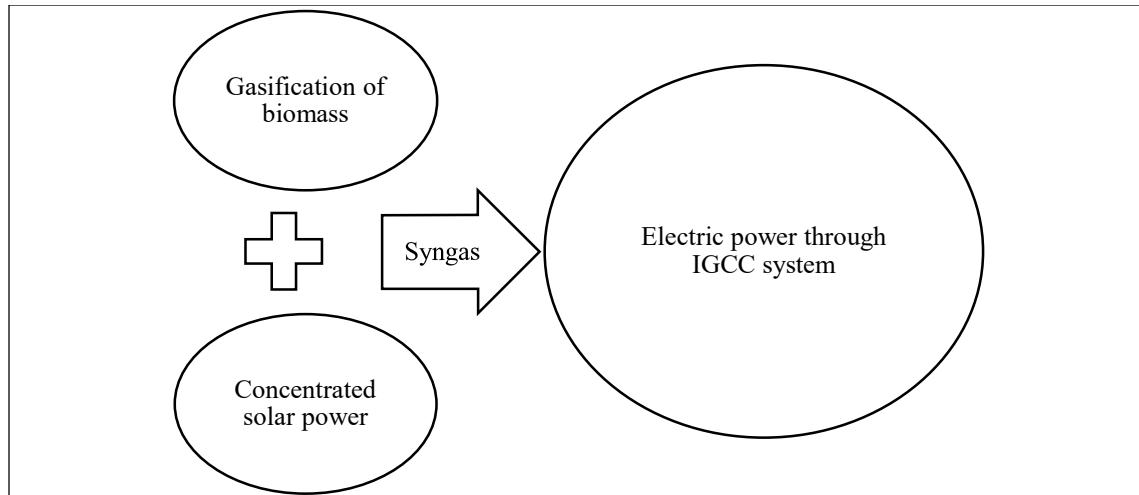Figure 7.2.1(i): Various technologies to convert biomass into energy and chemicals

Figure 7.2.1(ii): Overall biomass gasification incorporated with CSP and electric power generation through the IGCC system
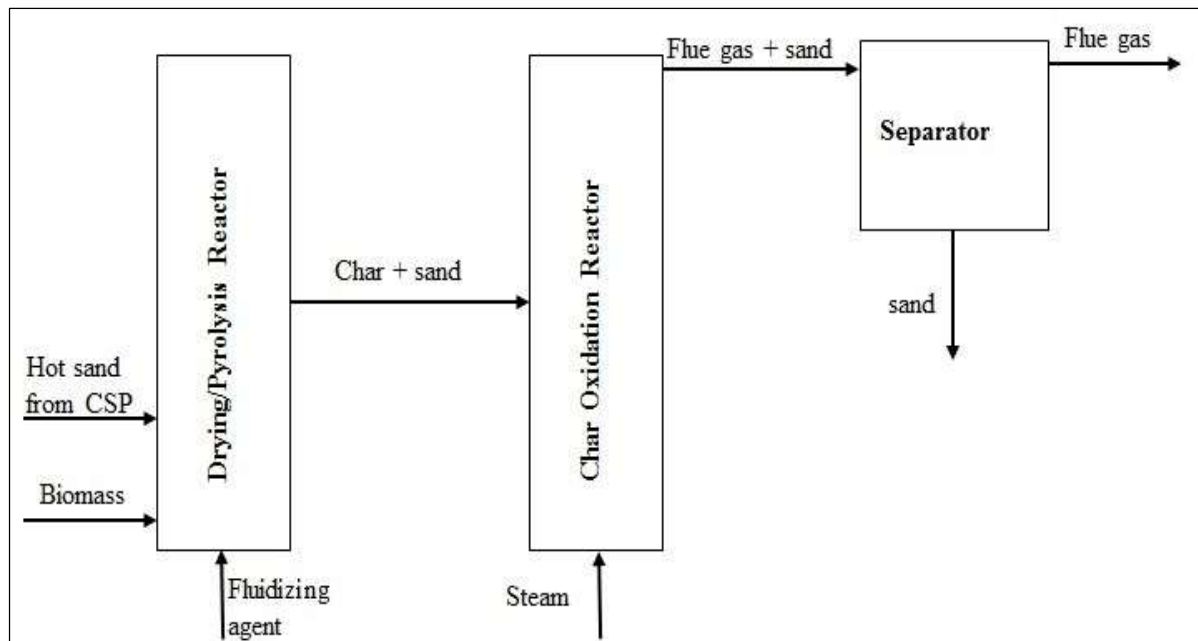

Figure 7.2.2(i): A general flow sheet for sand-CSP hybrid biomass DFB gasification system
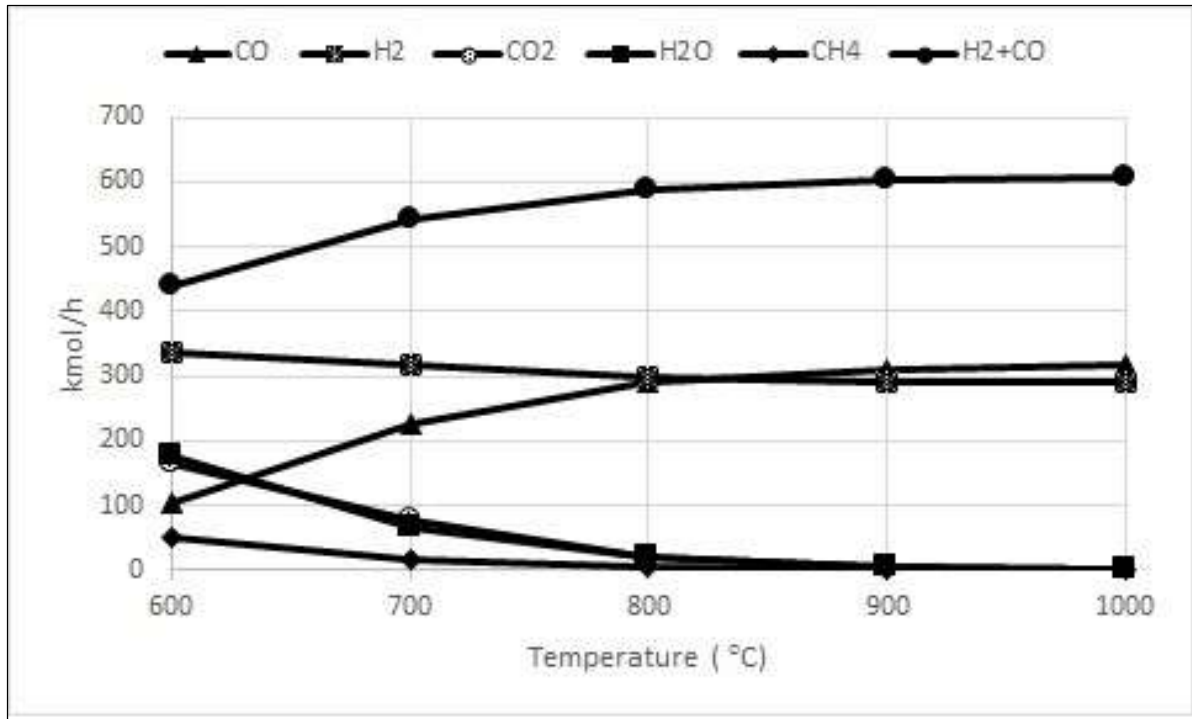
Figure 7.2.3(i). Effect of temperature in the gasifier on composition of syngas from wheat straw
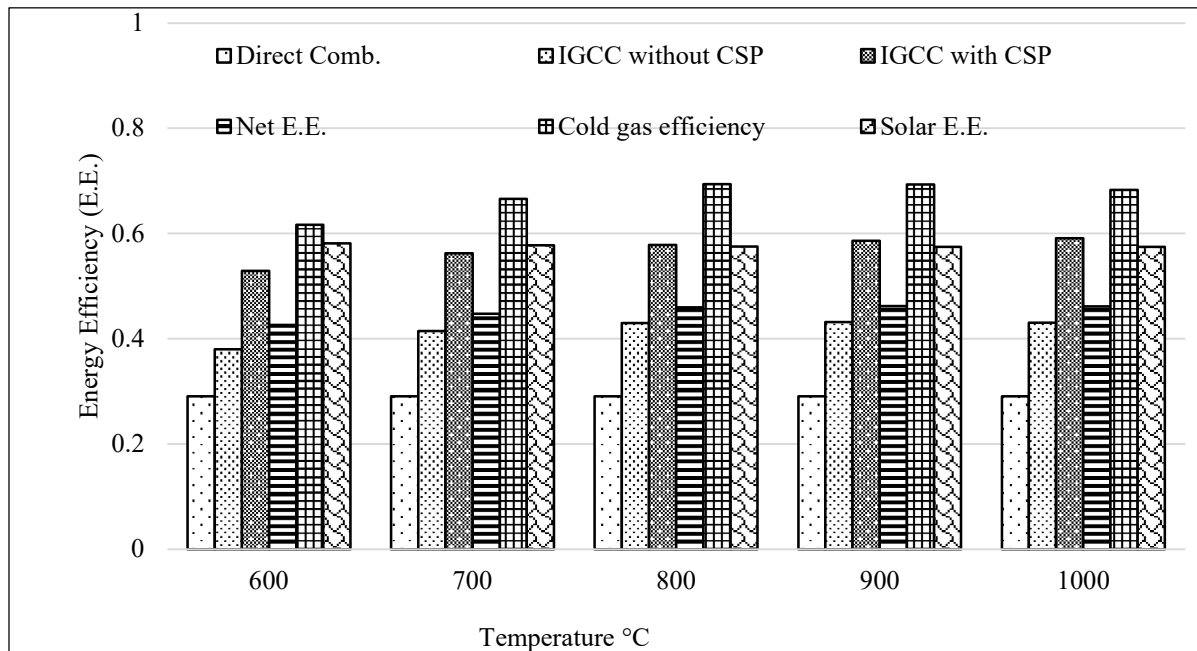

Figure 7.2.3(ii): Effect of temperature on energy efficiency for direct combustion and IGCC system with or without CSP

References

[1]   H. Rashidi and J. Khorshidi, "Exergy analysis and multiobjective optimization of a biomass gasification based multigeneration system" International Journal of Hydrogen Energy, 43 (2018) pp.2631–2644

[2]   F. Trieb, M. Moser, and J. Kern, "Liquid solar fuel – Liquid hydrocarbons from solar energy and biomass" Energy, 153 (2018) pp.1–11

[3]   A. M. Pantaleo, S. M. Camporeale, A. Miliozzi, V. Russo, N. Shah, and C. N. Markides, "Novel hybrid CSP-biomass CHP for flexible generation: Thermo-economic analysis and profitability assessment" Applied Energy, 204 (2017) pp.994–100

[4]   R. Milani, A. Szklo, and B. S. Hoffmann, "Hybridization of concentrated solar power with biomass gasification in Brazil's semi-arid region" Energy Conversion and Management, 143 (2017) pp.522–537

[5]   R. Soria, J. Portugal-Pereira, A. Szklo, R. Milani, and R. Schaeffer, "Hybrid concentrated solar power (CSP) – biomass plants in a semi-arid region: A strategy for CSP deployment in Brazil" Energy Policy, 86 (2015) pp.57–72

[6]   W. Qu, H. Hong, Q. Li, and Y. Xuan, "Co-producing electricity and solar syngas by transmitting photovoltaics and solar thermochemical process" Applied Energy, 217 (2018) pp.303–313

[7]   X Liu, B Patel, D Hildebrandt, "Analysis of the carbon efficiency of a hybrid XTL-CSP process" Computer Aided Chemical Engineering, 38 (2016) pp.835-840.

[8]   X Liu, B Patel, "Carbon efficiency targets for methanol production from a hybrid solar carbonaceous feedstock process" in SolarPACES 2016, AIP Conference Proceedings 1850, 100014 (2017).

[9]   T. Srinivas and B. V. Reddy, "Hybrid solar–biomass power plant without energy storage" Case Study, Thermal Engineering, 2 (2014) pp.75–81.

[10]   S. A. Channiwala and P. P. Parikh, "A unified correlation for estimating HHV of solid, liquid and gaseous fuels" Fuel, 81 (2002) pp.1051–1063

[11]   M. F. Demirbas, M. Balat and H. Balat, "Potential contribution of biomass to the sustainable energy development" Energy Conversion and Management 50 (2009) pp.1746-1760.

[12]   S. Ansari, X. Liu, "Using CSP to boost liquid fuel production in a BTL process" in SolarPACES-2017, AIP Conference Proceedings 2033, 130001 (2018)

[13]   S. Proskurina, J. Heinim, and O, F. Schipfer, and E. Vakkilainen, "Biomass for industrial applications: The role of torrefaction," Renew. Energy, vol. 111, pp. 265–274, 2017.

[14]   F. Trieb, M. Moser, and J. Kern, "Liquid solar fuel – Liquid hydrocarbons from solar energy and biomass,"

Energy, vol. 153, pp. 1–11, 2018.

[15] Y. Shen, L. Jarboe, R. Brown, and Z. Wen, "A thermochemical-biochemical hybrid processing of lignocellulosic biomass for producing fuels and chemicals," Biotechnol. Adv., vol. 33, no. 8, pp. 1799–1813, 2015.

[16] A. A. Boateng, P. J. Weimer, H. G. Jung, and J. F. S. Lamb, "Response of thermochemical and biochemical conversion processes to lignin concentration in alfalfa stems," Energy and Fuels, vol. 22, no. 4, pp. 2810–2815, 2008.

[17] J-Y. Lee, K. B. Aviso, and R. R. Tan, "Optimal sizing and design of hybrid power systems," ACS Sustain. Chem. Eng., vol. 6, pp. 2482–2490, 2018.

[18] N. Muradov, A. Gujar, J. Baik, and A. T-Raissi, "Production of Fischer-Tropsch hydrocarbons via oxygen-blown gasification of charred pinewood pellets," Fuel Process. Technol., vol. 140, pp. 236–244, 2015.

[19] W. Qu, H. Hong, Q. Li, and Y. Xuan, "Co-producing electricity and solar syngas by transmitting photovoltaics and solar thermochemical process," Appl. Energy, vol. 217, pp. 303–313, 2018.

[20] P. Kaushal and R. Tyagi, "Advanced simulation of biomass gasification in a fluidized bed reactor using Aspen Plus," Renew. Energy, vol. 101, pp. 629–636, 2017.

[21] K. Im-Orb, W. Wiyaratn, and A. Arpornwichanop, "Technical and economic assessment of the pyrolysis and gasification integrated process for biomass conversion," Energy, vol. EGY 12688, 2018.

[22] REN21, Renewables 2017: global status report, vol. 72, no. October 2016. 2017.

[23] S. Sahitya, H. Baig, R. Jani, N. Gadhiya, P. Das, T. K. Mallick, and S. Maiti, "Hydrogen-rich syngas from jatropha curcas shell biomass char in Fresnel Lens Solar Concentrator Assembly," Energy and Fuels, vol. 31. pp. 8335–8347, 2017.

[24] C. Wieckert, A. Obrist, P. von Zedtwitz, G. Maag, and A. Steinfeld, "Syngas production by thermochemical gasification of carbonaceous waste materials in a 150 kW th Packed-Bed Solar Reactor," Energy and Fuels, vol. 27, pp. 4770–4776, 2013.

[25] R. Milani, A. Szklo, and B. S. Hoffmann, "Hybridization of concentrated solar power with biomass gasification in Brazil's semi-arid region," Energy Convers. Manag., vol. 143, pp. 522–537, 2017.

[26] J. H. Peterseim, S. White, A. Tadros, and U. Hellwig, "Concentrated solar power hybrid plants: Which technologies are best suited for hybridisation?," Renew. Energy, vol. 57, pp. 520–532, 2013.

[27] A. Calderón, A. Palacios, C. Barreneche, M. Segarra, C. Prieto, A. Rodriguez-Sanchez, and A. I. Fernández, "High temperature systems using solid particles as TES and HTF material: A review," Appl. Energy, vol. 213, no. June 2017, pp. 100–111, 2018.

[28]   S. Koppatz, C. Pfeifer, and H. Hofbauer, "Comparison of the performance behaviour of silica sand and olivine in a dual fluidised bed reactor system for steam gasification of biomass at pilot plant scale," Chem. Eng. J., vol. 175, no. 1, pp. 468–483, 2011.

[29]   L. Abdelouahed, O. Authier, G. Mauviel, J. P. Corriou, G. Verdier, and A. Dufour, "Detailed modeling of biomass gasification in dual fluidized bed reactors under Aspen Plus," Energy and Fuels, vol. 26, no. 6, pp. 3840–3855, 2012.

[30]   S. A. Channiwala and P. P. Parikh, "A unified correlation for estimating HHV of solid, liquid and gaseous fuels," Fuel, vol. 81, pp. 1051–1063, 2002.

Chapter 8: Conclusion

8.1: Concluding Remarks and Perspectives

The aim of this study was to investigate systematic issues related to the injection of CSP-thermal energy into an endothermic biomass gasification process without energy storage, in order to produce electricity, FT-liquid fuel and other chemicals. The major objective was to provide technical insight into hybridization of CSP and biomass gasification, with a view to implementing this pathway as an alternative process for supplying energy on a continuous basis. The polygeneration approach from hybrid biomass gasification showed that it provides an opportunity to utilize the resources in an efficient way. It will enhance the energy efficiency and operational flexibility. This approach will reduce uncertainty and grid connection issues in the case of power generation.

This study considered a combination of various renewable technologies in a unique platform to explore the long-term potential of renewables. CSP could be a reliable resource to dispatch thermal energy into an endothermic gasification process. CSP hybridization with biomass gasification was assessed through case studies. The case studies showed that it will increase the share of renewables to the energy mix.

On the solar side, CSP thermal heat was considered as an equivalent to the heat duty of the gasifier or it can be used to preheat various feed streams where it is required. The wheat straw, corn cobs, coconut shells, groundnut shells, pinewood sawdust and municipal solid waste were considered as the unconventional feedstock. On the power production side, IGCC cycle (either conventional Rankine or organic Rankine cycle) was investigated. Assessment of the CSP-hybrid polygeneration system was done using target analysis and process simulation techniques. The simulation results were compared with the experimental data in the literature to optimize the utilization of CSP-thermal energy and biomass resources.

Three basic tools of material, energy and work balance were used to determine the feasible regions for syngas production when using the specified molar ratio of H_2 and CO from various types of unconventional feedstock then syngas to other energy products. The performance of the gasification system was investigated through the net energy requirement of the process which is represented by change in enthalpy of the process and the net-work requirement of the process which is represented by change in Gibbs free energy of the process. The feasibility of ultimate process targets was tested by process simulation in Aspen Plus® and validated with experimental data to conclude that how far the real process is placed as compared to the actual process.

In this study, many case studies were examined with ultimate targets to determine mass, energy and work flow, and operating conditions. The results of these case studies provide design guidelines and future recommendations regarding commercial deployment and regarding the technical advantages of using a CSP hybrid polygeneration system.

8.2: Conclusion from the Case Studies

In terms of energy and work, the enthalpy change (ΔH) and Gibbs free energy change (ΔG) should both be zero for all the cases, in order to achieve the target ratios. With a fully integrated energy process, at $\Delta G = 0$ the process does not require any external heat for the process to proceed. Therefore, at this point, any source of external heat at a temperature high enough to enable heat flow at any point in the process will be sufficient to drive the process. We consider this to be the ultimate target for biomass gasification to produce more syngas. If ΔH of the process is positive then it will tell us that there is an opportunity to conserve additional external energy in the form of electricity, power, liquid fuel, H_2, dimethyl ether, methanol, ethanol and other chemicals.

In conclusion from the case study of biomass to dimethyl ether (DME), it shows that a 91% carbon efficiency is possible by co-feeding biomass and methane at a ratio of 1:0.83 resulting in no energy cost and zero chemical potential loss. This is the ultimate target for the conversion of biomass to DME. We have also shown that co-feeding biomass with CH_4 can

improve the performance by reducing the C/H imbalance without the additional of excess oxygen, which leads to more CO_2 emission, and thus leading to highly energy and work efficient process. Co-feeding CH_4 can increase the carbon efficiency to 100% with no CO_2 production and ultimately can allow feeding CO_2, which could lead to a carbon negative process.

By conducting work balance target analysis, we found that hydrogen production of the ethanol to hydrogen process can be increased up to 87% compared to ethanol partial oxidation process and 17% more compared to the target of the ΔH neutral process, with less oxygen required and more water can be tolerated. We consider this to be the ultimate target for ethanol reforming, which enables the chemical potential of ethanol to be conserved and also provides an opportunity to store additional external energy in the form of H_2 fuel.

It is concluded from the case study of solar to H_2 that the H_2 production efficiency is about 13 kmol per MW_{th} solar thermal energy. This number represents that there is a good potential to convert solar into H_2 fuel. It is concluded that when CSP thermal energy is available, H_2 production can be boost up to 60%. The concentration of H_2 can be increased from 73.0 to 112.0 kmol/h. The results are promising, which makes the hybrid CSP steam gasification process a good option to convert renewables resources into H_2 fuel. This study provides a parametric analysis to transform biomass and solar into valuable and carbon-neutral alternative fuels.

In another case study, gasification was simulated with air, O_2, CO_2 and steam as gasification agents to produce syngas. The syngas was passed through the methanation reactor to maximise CH_4 content before it is sent for power generation in a normal gas turbine. However, the steam case proves as the best case. As for the case with no gasification agent, the molar amount of CH_4 produced was lower due to the formation of C in the gasification stage. When O_2 is used, the CH_4 fraction in the stream sent to the power generation is still much low despite the absence of N_2 from the feed. All processes studied produce a high CO_2 content after methanation and further detailed analysis to boost H_2 and CH_4 by adding water to the methanator should be considered in future studies. The ability to use heat generated in the

methanation process for gasification (heat integration) offers an advantage in this system when trying to generate CH_4 for power production via a normal gas turbine. An application of CSP to the system increases the amount of CH_4 produced by about 20% for all cases thus increasing the efficiency of the processes.

Case study of CO_2-gasification of biomass shows the potential benefit on slightly higher energy efficiency with less GHG emissions to the environment. The increase in energy efficiency is a good indicator to meet power demand. However, the study reveals that solar thermal to power efficiency for CO_2-gasification system is slightly less than steam-IGCC system. The results are promising, which makes the hybrid CSP-CO_2-gasification process a good option to convert renewables resources (biomass and solar) into electricity. Recycling sCO_2 back to the combustor dilutes the syngas in the combustor and thus oxy-combustion at lower temperatures are attainable. This points to a potential highly efficient Allam cycles operating at a practical condition for the current IGCC equipment technology. Higher inlet turbine pressure safeguards stable efficient operation of the Allam cycle for a wider range of exit pressures. The solar-assisted Allam cycle affords higher net thermal efficiencies because of the extra power which is attained by avoiding combustion of syngas to provide heat for gasification.

The case study of solar to electricity or liquid fuel achieves higher net electricity output per unit of biomass of approximately 53%. When CSP is combined into the proposed hybrid CSP-IGCC process, the energy efficiency of solar energy can be as high as 58% for power generation. For liquid fuel production, 17-18 kg of hydrocarbon can be produced from every GJ of solar energy input into the system. The capacity loss is less than 30% when no CSP input exists, which suggests that there is no need to store solar energy for smooth operation. Gasification at temperatures higher than 800 °C provides limited benefits but may result in significant challenges for the solar receiver system. The results are promising, which makes the hybrid CSP-BTL process a good option for solar energy storage and transportation.

In conclusion, the outcomes from case studies by target analysis and simulation model are promising, which makes the renewable hybrid polygeneration system as an attractive option

to convert renewables resources (biomass and solar) into clean power, liquid fuel, green H_2 fuel and chemicals. We concluded that additional research work should be performed considering a more extensive range of unconventional feedstock, CSP-thermal energy, CSP steam generation system and power production technologies to utilize the full potential of renewable resources.

8.3: Future Work and Recommendations

This study has examined case studies with a wide range of unconventional feedstock to provide a fundamental base for new assessments. For CSP hybridization with biomass gasification, instead of conventional steam generation system, it was assessed that using solid heat transfer medium will be reliable and economical to improve solar to electricity efficiency. It will result with higher energy stability, reliability and dispatchability.

The key findings of this study lead to a conclusion that there is a need to analysis further to increase the incorporation of CSP-thermal energy to the gasification system. Further challenges are to utilizer solid heat transfer medium and CO_2 as a heat transfer medium. There is ongoing research and development on CSP technologies. To use CSP for high temperature gasification is still challenging. Concerning to store solar thermal energy, new approaches are being tested to overcome thermochemical storage challenges and corrosion challenges. It would be a promising system as an emerging technology in the field of hybrid biomass gasification technology.